Thesis for Doctor of Engineering

Effects of Cold Atmospheric Pressure Plasma Jet on the Viability of *Bacillus subtilis* Endospores

Vinita Sharma

2013

Department of Production and Science and Technology,
Graduate school of Engineering, Gunma University

29-1 Hon-cho, Ota, Gunma 373-0057, Japan

Table of Contents

Chapter 1 - General Introduction

1.1 Background Research

Bacteria are ubiquitous and inevitable part of our existence. They are the most abundant and ancient form of the life. They immensely support the existence of the life but on the other hand they put our lives and money at stake. They often make the base of the food webs as they break down dead organic matter into simpler consumable forms for the producers or other microorganisms. They help certain plants (*legumes*) to convert N_2 gas into proteins (nitrogen fixation). They have symbiotic relationships with lots of animals including human beings. They are indispensable in our food industry. Sometimes, they are used in combination with yeasts and molds, particularly for fermentation based processes. They are used to make therapeutic drugs like insulin, vitamins etc.. Certain *actinomycetes (*a group of bacteria), make antibiotics like streptomycin and *nocardicin* but some pathogenic bacteria like *Streptococcus, Staphylococcus, E. coli, Leptospira, Erwinia amylovora etc.* cause some life threatening diseases to human beings, livestock and plants. They are used for industrial waste processing and for bioremediation. The ability of bacteria to digest hydrocarbons in petroleum is used to clean up oil spills. Researchers believe 48,000 deaths could have been prevented and $8.1 billion dollars could have been saved in the United States, if patients hadn't gotten infections after being admitted to a hospital [1] and most of the infections are caused by bacteria (endospores). To ensure the safety of our heath, food products, medical equipment, packaging or aseptic conditions in the laboratories, we need to eradicate bacteria from that particular environment. To do so, we need to sterilize things. Sterilization is a little bit more than just removing bacteria. Sterilization is the process by which all living cells, viable spores, viruses or viroids and even prions are either destroyed or removed from an object or a habitat.

There are several methods to achieve a high level of sterilization. According to FDA (U.S. Food and Drug Administration), 1997, a sterilization device or method should meet the acceptable sterility assurance level (SAL) which is 10^6 i.e. one chance in a million to be contaminated. There are several physical and chemical methods of sterilization. Physical methods are like thermal inactivation, filtration, and radiation. The chemical methods, achieve sterilization with the help of chemicals like H_2O_2, ethylene oxide, peracetic acid, beta propiolactone, alcohol, chlorine and its oxides and aldehydes etc.. These methods have their own merits and demerits. Thermal methods are effective and economic but they need higher temperature which makes them unsuitable for heat liable substrates. Filtration just filters out microorganisms but doesn't kill them. Radiation methods are expensive, need special operating conditions. Gamma radiation affects the bulk properties of the polymers being treated, as it breaks bonds and cross-linked chains within the volume of the material [3]. In late 1980s, there were strict regulations on the ethylene oxide and radiation sterilization in Japan [2]. Chemical methods are effective but they are not environment or people friendly. They require long sterilization time and sometimes, much longer venting time after sterilization. Most widely used ethylene oxide, is carcinogenic and its residues get absorbed on the materials [4, 5]. To overcome these problems, some new methods like high pressure sterilization, pressure assisted thermal sterilization, supercritical fluid sterilization; pulsed electric field sterilization etc. came into existence. Although they are better than the traditional sterilization methods in some ways but still they have their own limitations like in some cases, still, the working temperature is too high for heat sensitive materials. The main problem with these methods is their effectiveness against endospores. They are very effective against vegetative cells. Efforts are being made to make them more effective but still they are not the perfect solutions for perfect sterilization.

1.2 **Requirements for a Good Sterilization Process**

A good sterilization process should have rapid microbicidal activity, compatibility with surfaces being treated, noncorrosive, easily removable from the surface with the least residue, presents no health hazards to consumers and operational personnel, compatibility with environment,

reliable, economical and no adverse effects on the quality of the product. So, far no method fulfills all of these mentioned requirements. So, we are in an urgent need to have a sophisticated method of sterilization that fulfills all of the mentioned requirements.

Cold atmospheric pressure plasma could be a solution of this problem. As it works at low temperature, no chemical residues, safe and highly energetic to attain a higher level of sterilization in a shorter period of time, very low penetration power so it doesn't affect the bulk properties of the substrate. There is absolutely no need of post sterilization venting time. It works at atmospheric pressure so it's comparatively less expensive and easy to operate.

1.3 Objective of this Study

First of all, we would like to characterize our own designed plasma jet generating device, electrically and optically. We call this device "Cold Atmospheric Pressure Plasma Torch – 9 Ne" (CAPPLAT- 9Ne). This device is a commercial unit. We would like to compare it with CAPPLAT the basic unit. We would like to figure out the mechanism of plasma generation.

Then we would like to use the plasma jet generated by CAPPLAT- 9Ne to inactivate a *Bacillus subtilis* endospore population of $1.0X10^7$ to $1.4X10^7$ endospores/ml. We decided to work on $1.0X10^7$ to$1.4X10^7$ endospores/ml because it is slightly higher than the acceptable sterility assurance level or SAL (10^6). We would like to figure out the mechanism of endospore inactivation.

We would repeat the same experiment with the CAPPLAT the basic unit to compare the effectiveness of our commercial unit (CAPPLAT- 9Ne) as a sterilization tool. We would add some oxidants to the plasma jet to see if we could enhance the sterilization efficacy.

1.4 Novelty of this Research

CAPPLAT- 9 Ne the commercial unit is our own designed plasma generating device. Nobody has ever used it before for any research purposes. CAPPLAT the basic unit was also never used for

any bio-applications. There is not enough work on cold atmospheric pressure plasma to propose a well explained mechanism of bacterial inactivation. More work has been done on cold plasma at reduced pressure. The respective roles of UV photons and radicals at reduced pressure are already well understood [6–9], which is not the case yet at atmospheric pressure [10, 11].

1.5. Structure of the thesis

This thesis will have five chapters. Chapter 1 will be a general introduction. Chapter 2 will be discussing about CAPPLAT- 9Ne in detail. Chapter 3 will have information about CAPPLAT the basic unit and addition of oxidants (O_2 and H_2O_2) to the plasma jet. Chapter 4 will cover all of the aspects of our experiments about endospores. Chapter 5 will be devoted to the see the effect of CAPPLAT the basic unit on *Bacillus subtilis* endospores. We will also see the effect of the plasma on the viability of the endospores after the addition of oxidants (O_2 and H_2O_2) and finally, Chapter 6 will summarize the whole work.

Figure 1.1Research Outline

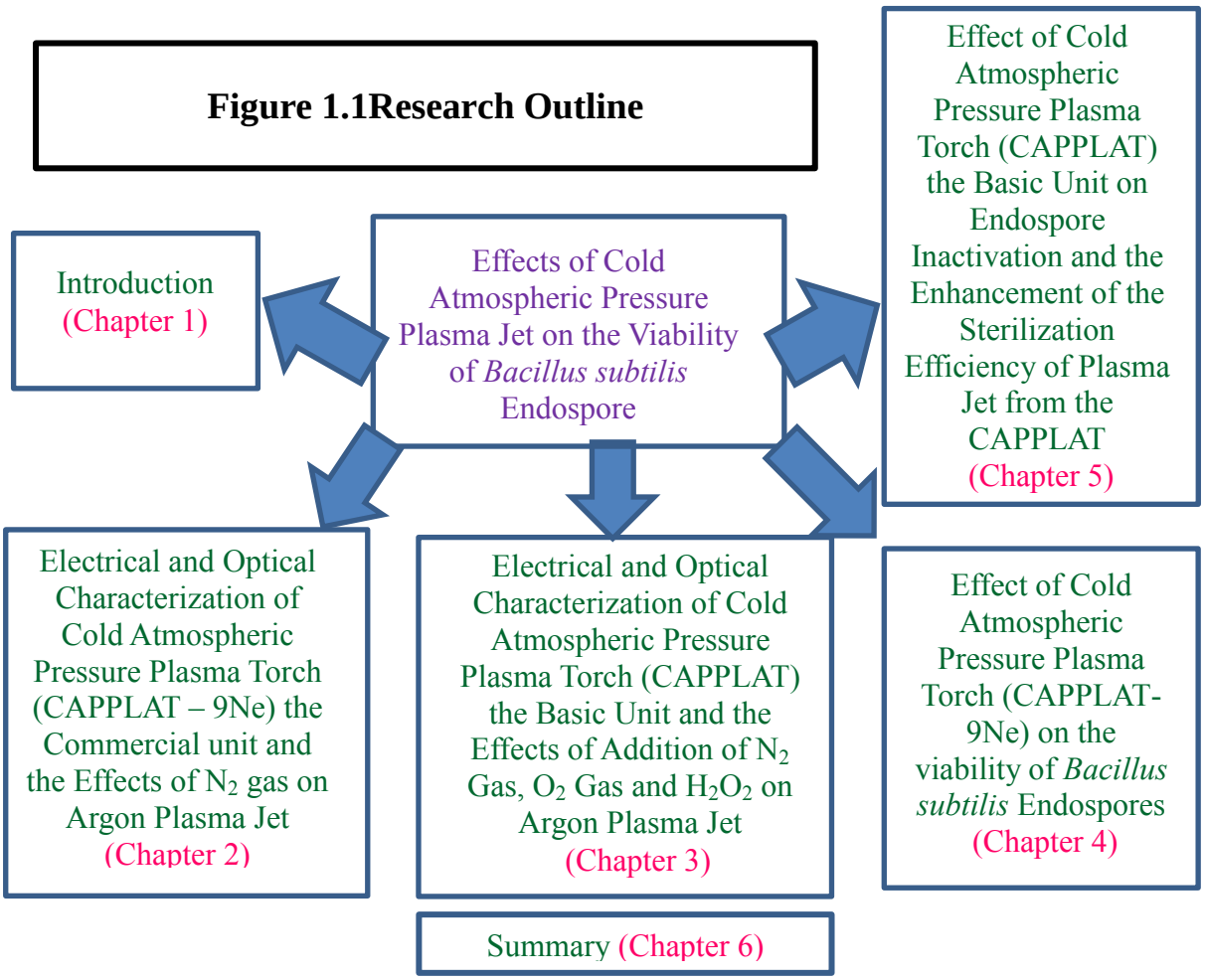

1.6 References

[1] Miriam Falco. CNN Medical News Managing Editor. 2010.

[2] Taniguchi M., Suzuki H, Sato M, and Kobayashi T. Sterilization of plasma powder by treatment with supercritical carbon dioxide. Agric. Biol. Chem., 51 – 3425, 1987.

[3] Henn GG, Birkinshaw C, Buggy M, and Jones E. A comparison study of the effects of gamma-irradiation and ethylene oxide sterilization on the properties of compression moulded poly-D-L-lactide. J. Mat. Sci.—Mater. Med. 7, 591–595, 1996

[4] Holyoak GR, Wang S, Liu Y, and Bunch TD. Toxic effects of ethylene oxide residues on bovine embryos in vitro. Toxicology, 108, 33–38, 1996.

[5] Zhang YZ, Bjursten LM, Freij-Larson C, Kober M, and Wessle´n B. Tissue response to commercial silicone and polyurethane elastomers after different sterilization procedures. Biomaterials, 17, 2265–2272, 1996

[6] Moisan M, Barbeau J, and Pelletier J. Le vide: Sci. Tech. Appl., 299, 15–28, 2001

[7] Moisan M, Barbeau J, Moreau S, Pelletier J, Tabrizian M, and Yahia, L.H. Int. J. Pharm., 226, 1–21, 2001.

[8] Moisan M, Barbeau J, Pelletier J, Philip N, and Saoudi B. 13th Int. Coll. Plasma Processes (SFV), Antibes; (Mai 2001). Le vide: Sci. Tech. Appl. Numéro spécial: Actes de Colloque, pp. 12–18, 2001.

[9] Philip N, Saoudi B, Barbeau J, Moisan M, and Pelletier J. 13th Int. Coll. Plasma Processes (SFV), Antibes; (Mai 2001). Le vide: Sci. Tech. Appl. Numéro spécial: Actes de Colloque, pp. 245–247, 2001.

[10] Laroussi M. IEEE Trans. Plasma Sci. 24, 1188–1191, 1996.

[11] Hermann H W, Henins I, Park J and Selwyn G S. Physics Plasmas 6, 2284–2289, 1999.

1.2 Plasma

Plasma is an ionized gas which contains free electrons, ions, radicals and highly excited neutral and charged species. The term plasma was introduced by Irving Langmuir. Plasma can be

created by providing energy to a neutral gas in order to ionize it. The source of energy could be thermal, electric and electromagnetic radiations. Plasmas are chemically and physically very active media in spite of their quasi neutral status. Basic idea of plasma production, composition, types is summarized in Figure 1.2.1.

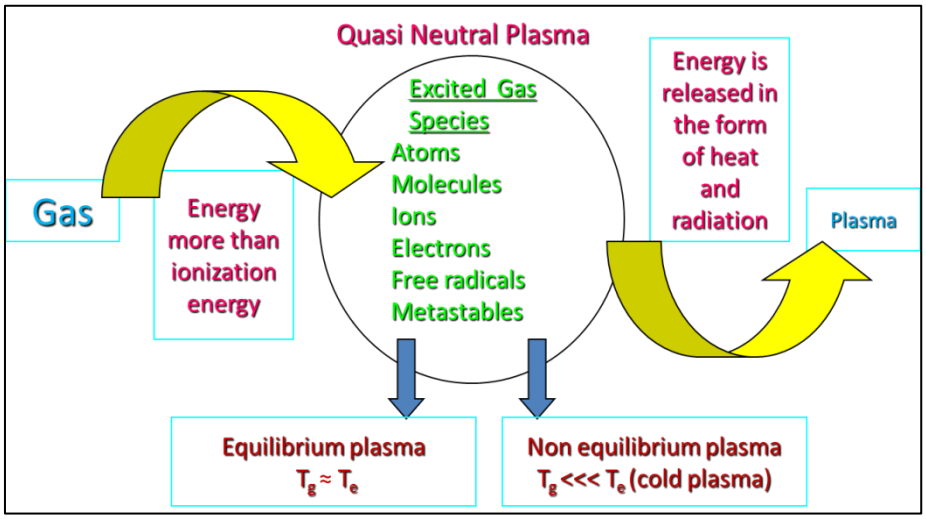

Figure1.2.1 - Summery of Plasma Production

David A. Frank-Kamenezki used the term "the fourth state of matter" for the plasma. 99% of our Universe including stars, nebulae, interstellar space are consists of plasma [1]. Our Solar System is also filled with plasma in the form of the solar winds. On the earth besides laboratories we can see plasma in our daily lives as lightning, fluorescent lamps, plasma TV etc.. In advanced engineering and technology, we use plasmas in welding, switching, surface activation, chemical conversion, environment protection, melting, incineration and partial discharges in electrical engineering etc..

1.2.1 Classification of Plasma

Depending on the type of energy supply and the amount of energy transferred to the plasma, the properties of plasma change in terms of temperature and electron density [1, 2]. Atmospheric plasmas can be divided into two categories – local thermodynamic equilibrium plasma (*LTE plasma*) or thermal plasma and non- local thermodynamic equilibrium plasma (Non *LTE plasma*) or cold plasma [2, 3].

1.2.1.1 Local Thermodynamic Equilibrium Plasma or Thermal Plasma (LTE plasmas)

In LTE plasmas, transitions and chemical reactions are controlled by collisions and radiative processes [4]. Collisions are micro-reversible i.e. excitations is accompanied with de-excitation; Ionization is accompanied with recombination and vice versa to maintain the kinetic balance [5]. To have LTE, it is required that the local gradients of plasma properties like temperature, electron density, and thermal conductivity should be low enough to let a particle in the plasma reach the equilibrium: diffusion time must be similar or higher than the time, the particle needs to reach the equilibrium [2]. Inelastic collisions between electrons and heavy particles create active species in plasma whereas elastic collisions heat up the heavy particles and electrons lose their energy. That is why for local thermodynamic equilibrium plasma or thermal plasma the temperature of electrons (T_e), temperature of heavy particles (T_h) and the overall temperature of the gas (T_g) are almost the same i.e. $T_e \approx T_h \approx T_g \approx 10{,}000K$, as we see in arc discharges [1].

1.2.1.2 Non Local Thermodynamic Equilibrium Plasma or Thermal Plasma (Non LTE plasmas)

In LTE plasma, the temperature of gas, heavy particles and electrons are the same but in Non LTE plasmas the temperature of electrons (T_e) is much higher than the temperature of heavy particles (T_h) but because of huge mass difference between heavy particles and electrons, the temperature of plasma or the temperature of the gas (T_g) is governed by the temperature of heavy particles i.e. $T_e >> T_h \approx T_g$. The deviation of Non-LTE plasmas from Boltzman distribution for the density of electrons could be explained by the fact that the electron induced de-excitation rate of atoms is lower than the corresponding electron induced excitation rate because of significant radiative de-excitation rate [5]. Electrons move very fast whereas heavy particles are almost static in comparison to the electrons so unlike LTE plasmas, non LTE plasmas have local gradients of plasma properties like temperature, electron density, and thermal conductivity should be high enough and diffusion time should be less than the time, the particles need to reach the equilibrium. In this scenario, we will have non-equilibrium plasma. Inelastic collisions between electrons and

heavy particles are responsible for plasma chemistry whereas only a few elastic collisions heat up the heavy particles slightly ($T_h \approx$ 300 - 1000 K) that is why electrons remain highly energetic ($Te \approx$ 10,000- 100,000 K), as we see in glow discharges [1]. That is why overall temperature of the plasma remains low (cold plasma).

1.2.2 Atmospheric Pressure Plasmas

Figure1.2.2 shows the relationship between the temperature and the pressure and their effects on the nature of the plasma [7]. As we increase the pressure, temperatures of electrons and heavy particles also change and the whole plasma system moves from non-local thermodynamic equilibrium (cold plasma) to Local thermodynamic equilibrium (thermal plasma) or we can say the transition from glow discharge to arc discharge. In the low pressure zone (10^{-3} to 10^{-1} Torr), gas temperature (T_g is much lower than the electron temperature (T_e) (Figure1.2.2).

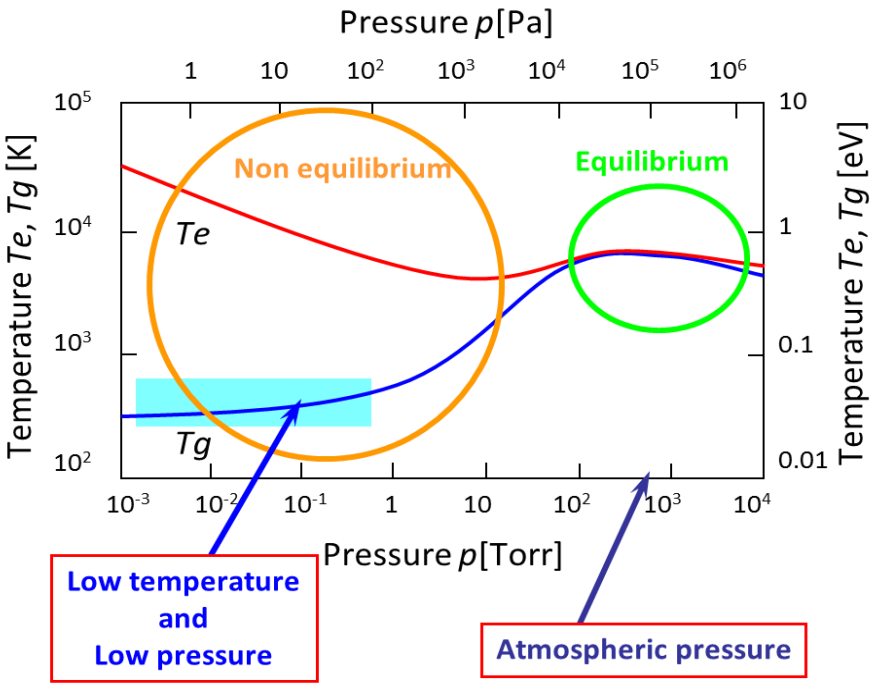

Figure1.2.2 Relationship between the temperature and the pressure, for equilibrium and non-equilibrium plasmas (Taken from the reference 7)

In low pressure zone, only inelastic collisions between electrons and heavy particles are responsible for the plasma chemistry which cannot increase the temperature of heavy particles or

the plasmas. As the pressure keeps increasing, difference between the temperature of electrons and heavy particles keeps decreasing and finally, both processes inelastic collisions for plasma chemistry and elastic collisions to increase the temperature of heavy particles get intensified and plasma approaches close to the thermodynamic equilibrium. At atmospheric pressure plasma is almost LTE plasma.

High power density induces LTE plasma (arc plasmas) and low density feeding power or pulsed power supply induces Non-LTE plasmas (homogeneous plasmas) as short pulse durations prevent from attaining equilibrium [1, 4]. In an atmospheric plasma jet, plasma core is in thermodynamic equilibrium whereas peripheral one is in non-thermodynamic equilibrium [1, 4].

1.2.3 Sources and the Mode of Atmospheric Pressure Plasma Discharges

To produce atmospheric plasma, different types of sources with different types of frequencies can be used. These sources can mainly be divided into three types of sources namely DC (direct current) discharges, low frequency discharges in continuous or pulsed mode, RF (radio wave frequency) discharges and microwave discharges. In DC low frequency discharges with continuous working mode, we can have arc plasma torches [24] but if we have pulsed working mode we can have dielectric barrier discharges. Depending on other parameters, these discharges can be filamentary or glow [25, 26]. RF discharges can also work with low and high power supply [27, 28 & 29]. Among these different types of discharges, DBD discharges are most widely used.

1.2.3.1 Dielectric Barrier Discharges

Dielectric barrier discharge or silent discharge works on higher pressure [8, 9] about 10-1000 kPa. Dielectric barrier discharge is a special type of AC or RF discharge with the frequency in the range of 1 to 20 kHz. The discharge can be ignited by sinusoidal power source [10] or pulsed power source [11]. The dielectric barrier is placed between two electrodes. The electrodes can be planner or concentric, as shown in Figure1.2.3.

Dielectric barriers can touch one or both or not any electrodes (Figure1.2.3). Normally there is a distance of few millimeters in case of dielectric barrier discharges but there is no gap in case of surface discharges. Sometimes, all of the space between electrodes is packed with dielectric substances (Figure1.2.4).

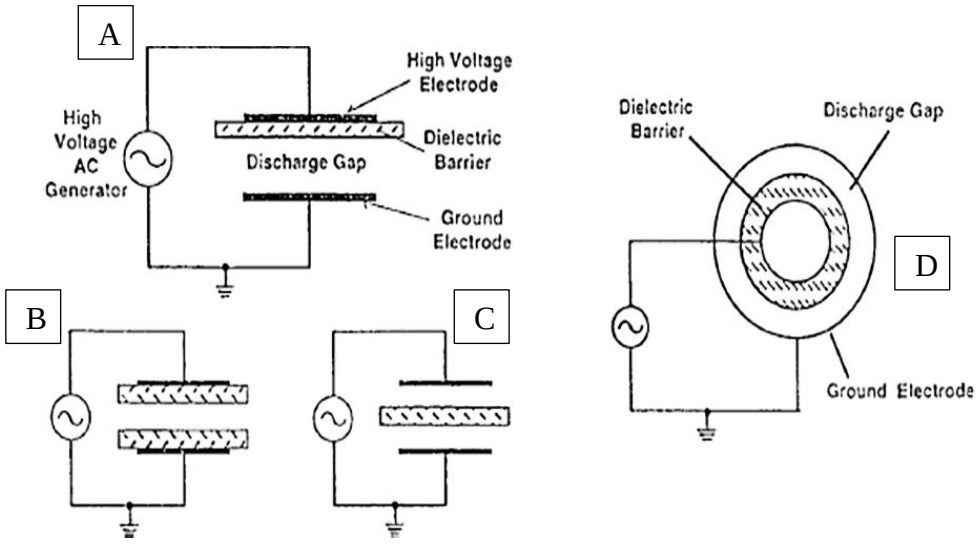

Figure1.2.3 Parallel and concentric configurations of dielectric barrier discharge; A, B, C show the arrangement for parallel electrodes; D shows the arrangement for concentric electrodes (Taken from references 30)

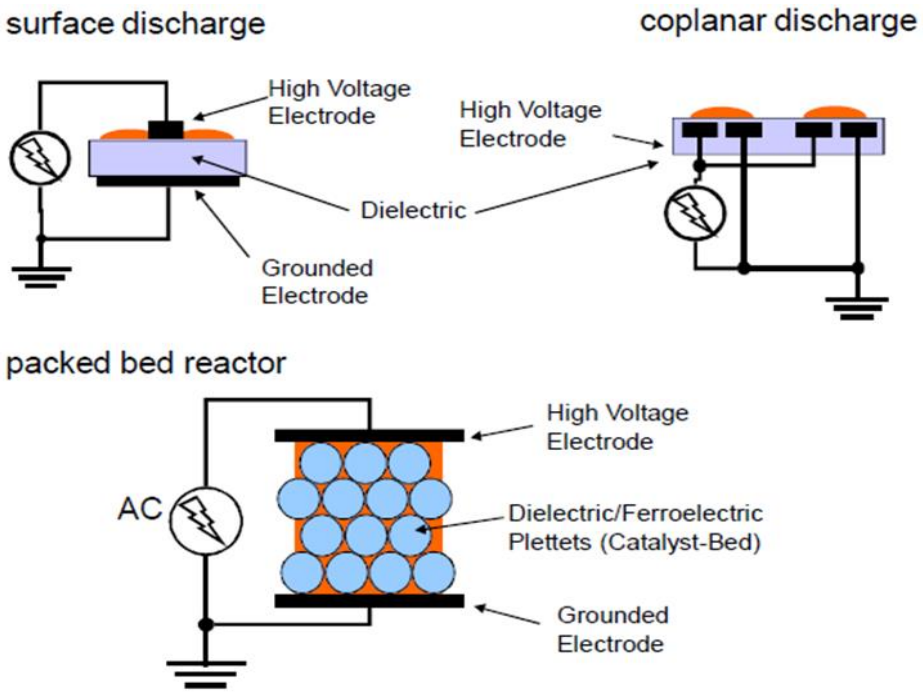

Figure1.2.4 showing different types of configurations of electrodes without spaces between electrodes (Taken from reference 6)

Both filamentary and glow discharge modes are observed at atmospheric pressure. The nature of discharge depends on the working gas or the mixture of gases, dielectric barrier and the operating conditions [14].

1.2.3.2 Filamentary Dielectric Barrier Discharges.

In most of the cases, DBD has multi-steamer mode of operation with the formation of microdischarges [13] which subsequently change into visible filaments. They strike at the same place when the polarity changes because of the memory effect and these microdischarges look like continuous filaments.

When a high voltage is applied across the electrodes, the background electrons or knocked out electrons from the heavy particles, start multiple avalanches which are governed by Townsend ionization coefficient α which is the function of reduced electric field *E/n* where *E* is electric field and *n* is the gas density. The charge accumulation in avalanches because of strong applied electric field creates local electric fields which allow streamers grow. There is a transition from avalanches to streamers and then streamers propagate within 10 ns from the anode to the cathode in the direction, opposite to the avalanches, with a very high speed (about 10^8 cm/s, an order of magnitude faster than the avalanches) to cover the distance between electrodes in nanoseconds [15]. Streamers are local ionization waves usually move from the anode to the cathode (Figure1.2.5).

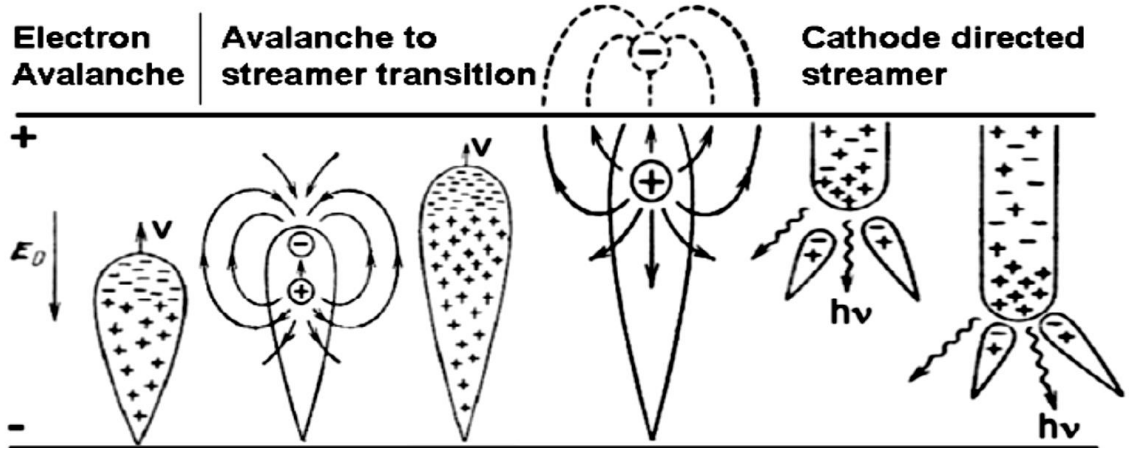

Figure1.2.5 Evolution of electron avalanche in discharge gap, showing avalanche development, avalanche-to-streamer transition, and streamer propagation (Taken from reference 15)

Streamers are formed at the same place because of the memory effect of the charge deposition on the dielectric surface and the residual charges from the previous cycle. The electrons in conducting channels dissipate rapidly while the heavy ions stay for several microseconds [15]. The electron accumulation on dielectric barrier prevents further avalanches and streamer formation until the change in polarity.

1.2.3.3 Diffuse Dielectric-Barrier Discharges (Glow Discharge)

The glow mode of DBD could be uniform or filamentary. In case of DBD glow discharge, the filaments are formed because of avalanches rather than streamers. In glow discharge, filaments are initiated by Townsend ionization whereas filamentary dielectric barrier discharge is because of streamer breakdown [16, 17]. S. Okazaki introduced the term APGD (atmospheric pressure glow discharge). Okazaki and her co-workers obtained glow barrier discharge at 50 Hz sinusoidal feeding voltage with pure He, N_2 and air without any additive gas. They used ceramic dielectric [18, 19, and 20]. Plasma density in micro discharges is much higher than the surroundings. The locations of microdischarge formations can be considered as active locations on whole DBD. As a result of microdischarges, lots of energy dissipates which decreases the temperature but surrounding local temperature still stays high. Microdischarges or filaments strike at the same place. Although these areas and discharge volumes are small but if the temperature difference persists for a long time at the same place, it will make the effect of the plasma non-uniform on the substrate. So, it is very necessary to have uniform glow discharge to have a uniform effect on the surface of the substrate. To have glow discharge or to prevent filamentation, we should have enough pre-ionization electron density, which can be achieved by sufficient pre-ionization by x-rays, electron beams or by double-discharge techniques, [21].The higher pre-ionization electron density helps to overlap and coalesce the primary avalanche heads to smooth out the space charge field gradient which will otherwise make streamers. Brenning et al. [22] pointed out the importance of an additional minimum pre-ionization rate just prior to and during breakdown. Impurities, gas additives, the presence of metastables and residual ions also affect glow discharges. The densities of residual species from the

previous half period that can initiate the diffuse discharge in the next half cycle depend on the repetition frequency. Therefore, the feeding voltage frequency plays an important role in the transition to the diffuse mode. Some dielectric materials can trap considerable amounts of charges uniformly on the surface. When the electric field changes its polarity, the charge carriers are expelled from the surface and initiate a diffuse discharge [23]. By feeding additive gas into working gas can also help to attain glow discharge by the process of quenching.

1.2.4 Electrical and Optical Characterization

To understand DBD discharges and to ascertain that the discharges are filamentary or glow discharges, electrical characterization of plasma is indispensable. It helps us to understand the discharge voltage, discharge current, and the impedance of the entire load not just the plasma discharge. Nature of the current waveform and pulse width can give clues about the nature of the discharge as the spikey current waveform shows filamentary discharge whereas a smooth waveform is the representation of glow discharge besides that filamentary current has narrower pulse width than the glow discharge current. In dielectric barrier discharges, it actually acts like a combination of two capacitors, one is the dielectric barrier and the other one is the gap between electrodes which also acts like a capacitor but in case of surface discharge there is no gap between electrodes and DBD. So, an equivalent R-C parallel circuit (Figure1.2.6) can be used for electrical characterization where *C* represents capacitance of silicon dielectric substance used between two concentric electrodes and *R* represents resistance of the discharge.

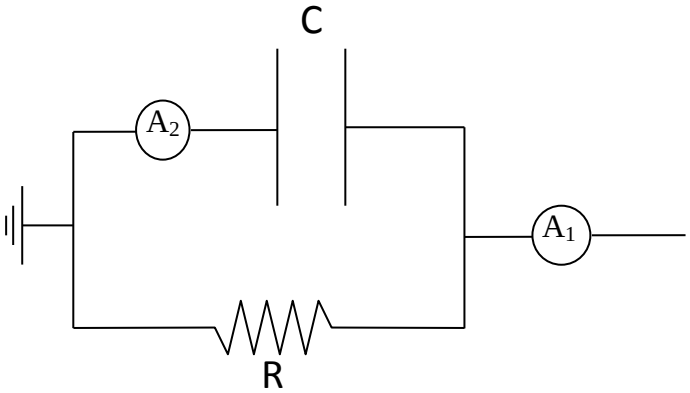

Figure1.2.6 An equivalent circuit model for surface dielectric barrier discharge

To record waveforms, we used oscilloscope. Changes in nominal applied voltage on current can also give us the idea about changes in electron density in current. The quantity of charge transfer is mainly determined by the categories of dielectric and the width of gap spacing [30]. According to the above circuit total current (A_1) will be the sum of capacitive current (A_2) and discharge current. We can measure total current and capacitive current then using the above circuit discharge current (A_1- A2) can be calculated.

Plasma is quasi-neutral in nature. It is the mixture of highly active species which are responsible for the effects of plasma on substrates. To confirm the presence of different active species and to understand the mechanism of the formation of the active species, optical characterization of plasma is necessary. Optical emission spectroscopy (OES) is well known as non-invasive and non-disturbing technique for plasma diagnostics [32-36]. In plasmas, excitation and de-excitation processes keep going on. When excited molecules de-excite they emit radiations and the optic fiber probe of optical emission spectroscopy captures these emission radiations of active species which are analyzed and the intensity of emission radiation is measured as the function of the wavelength. As all of the transitions take place at very specific wavelengths, so, these spectrum help us to identify different active species. Using a special OES simulation program the rotational and vibrational temperature of excited molecules can be measured [37]. For equilibrium plasmas, the electron temperature can be derived whereas for non-equilibrium plasmas excitation temperature can be measured [37].

1.2.5 Mechanism and Applications of Atmospheric Pressure Cold Plasma Jet

Plasma jet producing devices consist of two concentric electrodes. There are several possible configurations for electrodes like one powered and one grounded electrode, without grounded electrode, combination of two tubes where inner tube is streamed with an inert gas for charge ignition and outer for precursor, with two coaxial electrodes with dielectric in between and plasma jets with an inner RF driven needle electrode, with and without grounded ring electrode [38]. The

gas discharge can be ignited by RF power or by high voltage pulsed power. The plasma produced between the electrodes is expanded outside of the electrode configuration in the form of plasma jet because of the pressure of the air flow from the above as shown in Figure 1.2.7. Between the electrodes, we have active plasma which is rich in active species. In plasma effluents (Jet) as shown in Figure 1.2.8, the density of charged species is lower. It has mainly long lived species and free electrons which are responsible for the plasma chemistry on substrates.

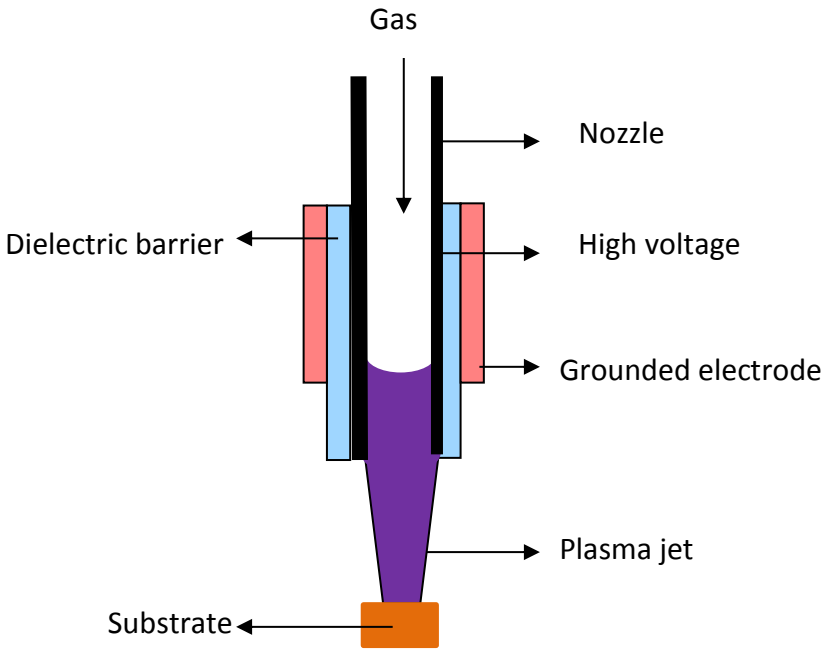

Figure1.2.7 – Schematic representation of plasma jet

Figure1.2.8 – Plasma Jet

Plasma jets are widely used in plasma processing applications. It is particularly useful to complex shaped substrates. They are used for surface treatments like surface cleaning, surface etching, and surface activation. They are also used for surface coating. It is really important, because the surface coating happens without any changes in the intrinsic bulk properties. There are two types of surface coating – air plasma spray (APS) coating and plasma enhanced chemical vapor deposition. Although the mechanism for lots of processes is not clear yet, but in recent years lots of progress have been made and it seems like for surface cleaning metastable energetic species are responsible [38, 39]. For etching, lots of parameters besides plasma composition like substrate nature, power, and gas flow play an important role. For surface activation, active species in plasma

change the surface energy and make it ready for grafting. Plasma jets have also been used for sterilization or bacterial inactivation.

1.2.6 References

[1] Tendero C, Tixier C, and Tristant P. Spectrochimica Acta Part B 61, 2, 2006.

[2] Boulos MI, Fauchais P, and Pfender E. Thermal plasmas: Fundamental and Applications. Volume 1, plenum Press, New York, ISBN: 0-306-44607-3, 452, 1994.

[3] Massines F, Ségur P, Gherardi N, Khamphan C, and Ricard A. Surf. and Coat Techn., 174-175:8, 2003.

[4] Fei Xiaomeng, Kuroda Shin-ichi, Kondo Yuki, Mori Tamio, and Hosoi Katsuhiko. Comparison of High-density Polyethylene Surface Treatment Using Two Types of Cold Atmospheric Pressure Ar Plasma Jets, 2010.

[5] Moisan M, Calzada MD, Gamero A, and Sola A. Experimental investigation and characterization of the departure from local thermodynamic equilibrium along a surface-wave-sustained discharge at atmospheric pressure, J. Appl. Phys. 80 (1) 46– 55, 1996.

[6] Wagner Hans-Erich and Brandenburg Ronny. Atmospheric Pressure Plasmas. Plasma Applications in Material Science PAMS-2011.

[7] Roth JR. Industrial Plasma Engineering. Vol.1: principles, IOP publishing Ltd. 1995.

[8] Eliasson B, and Kogelschatz U. IEEE Trans. Plasma Sci.19309, 1991.

[9] Kogelschatz U, Eliasson B, and Ehli W. J. PhysiqueIV7C4 47, 1995.

[10] Jimenez C, Martin S, Gherardi N, Durand J, Cot D, and Massines F. Etude de la formation de nano et micro particules dans une de´charge a` la pression atmosphe´rique, Mate´riaux 2002:

de la conception a` la mise en oeuvre, 21– 25 Octobre 2002, Tours, France, Tours VINCI, Tours , CD-ROM, 2002.

[11] Salge J. Plasma-assisted depositon at atmospheric pressure, Surf. Coat. Technol. 80, 1 –7, 1996.

[12] Kogelschatz U. Atmospheric pressure plasma technology. Plasma Phys. Control. Fusion 46 B63–B75, 2004.

[13] Kogelschatz U. Dielectric-barrier Discharges: Their History, Discharge Physics, and Industrial Applications. Plasma Chemistry and Plasma Processing, Vol. 23, No. 1, 2003.

[14] Kogelschatz U. For a recent review of the diverse phenomenon in barrier discharges, see: IEEE Trans. Plasma Sci. 30 (4), 1400–1408, 2002.

[15] Chirokov A, Gutsol A, and Fridman A. Atmospheric pressure plasma of dielectric barrier discharges. Pure and Applied Chemistry, 77(2), pp.487–495, 2005.

[16] Brauer I, Punset C, Purwins HG, and Boeuf JP. J. Appl. Phys. 85 (11), 7569–7572, 1999.

[17] Müller I, Punset C, Ammelt E, Purwins HG, and Boeuf JP. IEEE Trans. Plasma Sci. 27, 20, 1999.

[18] Kanazawa S, Kogoma M, Moriwaki T, and Okazaki S. International Symposium on Plasma Chemistry, Tokyo (Japan), 1987, 1844.

[19] Kanazawa S, Kogoma M, Moriwaki T, and Okazaki S. J. Phys. D: Appl. Phys. 21, 838, 1988.

[20] Okazaki S, Kogoma M, Uehara M, and Kimura Y. J. Phys. D: Appl. Phys. 26, 889, 1993.

[21] Kogelschatz U. Plasma Science, IEEE Transactions, 30 (4), pp. 1400 – 1408, 2002.

N. Brenning, I. Axnäs, J.O. Nilsson, J.E. Eninger, IEEE Trans. Plama Sci. 25 (1997) 83- 88.

[22] Tepper J, Lindmayer M, and Salge J. Proceedings of the Sixth International Symposium on High Pressure Low Temperature Plasma Chemistry, HAKONE VI, Cork, (Ireland), 123, 1998.

[23] Fauchais P. Plasmas thermiques: production et applications. Techniquesde l'Inge´nieur, Traite´ Ge´nie e´lectrique. D2 820, pp. 1 – 25.

[24] Massines F, and Gouda G. A comparison of polypropylene-surface treatment by filamentary, homogeneous and glow discharges in helium at atmospheric pressure, J. Phys. D: Appl. Phys. 31, 3411 – 3420, 1998.

[25] Yokoyama T, Kogoma M, Moriwaki T, and Okazaki S. The mechanism of the stabilisation of glow plasma at atmospheric

[26] Laimer J and Stŏri H. Plasma Process. Polym. 3, 573, 2006.

[27] Shi JJ and Kong MG. IEEE. Trans. Plasma Sci. 33, 624, 2005.

[28] Park J, Henins I, Herrmann HW, Selwyn GS. J. Appl. Phys. 89, 20, 2001.

[29] Wagner H E, Brandenburg R, Kozlov K V, Sonnenfeld A, Michel P, and Behnke JF.Vacuum 71, 417, 2003.

[30] Kogelschatz U, Eliasson B, and Ehli W. J. PhysiqueIV7C4 47, 1995.

[31] Ricard A and Czerwiec T. Thin Solid Films 341, 1, 1999.

[32] Fateev A and Leipold F. Plasma Process. Polym. 2, 193, 2005.

[33] Simon A, and Anghel SD. Nucl. Instr. Methods in Phys. Res. B 2009, 267, 438, 2005.

[34] Roberts R. J. Res. Natl. Inst. Stand. Technol. 100, 353, 1995.

[35] Jamroz P and Zyrnicki W. Vacuum 84, 940, 2010.

[36] Meiners A, Leck M, and Abel B. Multiple parameter optimization and spectroscopic characterization of a dielectric barrier discharge in N2, Plasma Sources Sci. Technol. 18-045015, 2009.

[37] Behnke JF, Lange H, Michel P, Opalinska T, Steffen H, Wagner HE. The cleaning process of metal surfaces in barrier discharge plasmas, International Symposium of High Pressure Low Temperature Plasma Chemistry. Milovy, Czech Republic, 1998, pp. 138– 142, 1996.

[38] Thiebaut JM, Belmonte T, Chaleix D, Choquet P, Baravian G, Puech V, and Michel H. Comparison of surface cleaning by two atmosphericpressure discharges, Surf. Coat. Technol. 169– 170, 181– 185, 2003.

1.3 Bacterial Endospores

1.3.1 Introduction of Bacteria and Endospores

Bacteria are unicellular microscopic, prokaryotic and ubiquitous organisms. They do not have membrane bound well defined nucleus or other cell organelles like eukaryotic cells. Bacteria are inevitable part of our lives. They are indispensable in our food-product industries and pharmaceuticals but on the other hand they cause a huge loss of money and lives too.

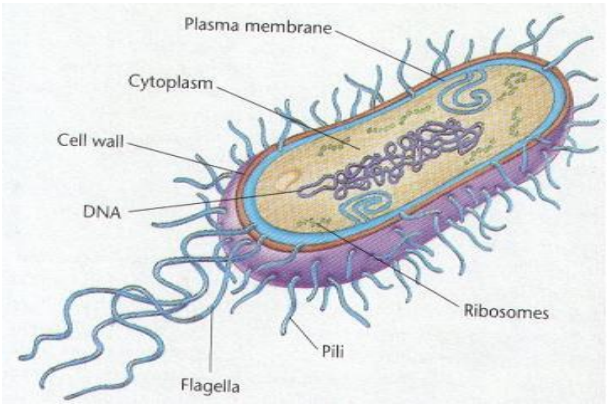

Figure 1.3.1 Schematic Representation of a Typical Bacterial Cell (Taken from reference 5)

In this study we used *Bacillus subtilis* which is a rod shaped (*Bacillus*), gram positive, aerobic and spore forming bacterium. Many gram positive bacteria like *Bacillus* and *Clostridium* form a distinct type of highly dormant cells, called endospores or spores. The endospores are highly resistant to environmental stresses like heat, desiccation, radiations, chemicals etc. Depletion of nutrients triggers a complex set of events that leads to the endospore formation [1]. These spores survive for an incredibly long period without any detectable metabolic activities.

1.3.2 Sporulation

The process of endospore formation is called sporulation. It completes in seven stages and requires about 8 hours [3]. In the first stage, the genetic material forms an axial filament and the inward folding starts, dividing mother cell into two unequal parts. In the second stage, the mother cell divides into two unequal parts by a septum, the smaller part becomes forespore and the bigger one mother spore.

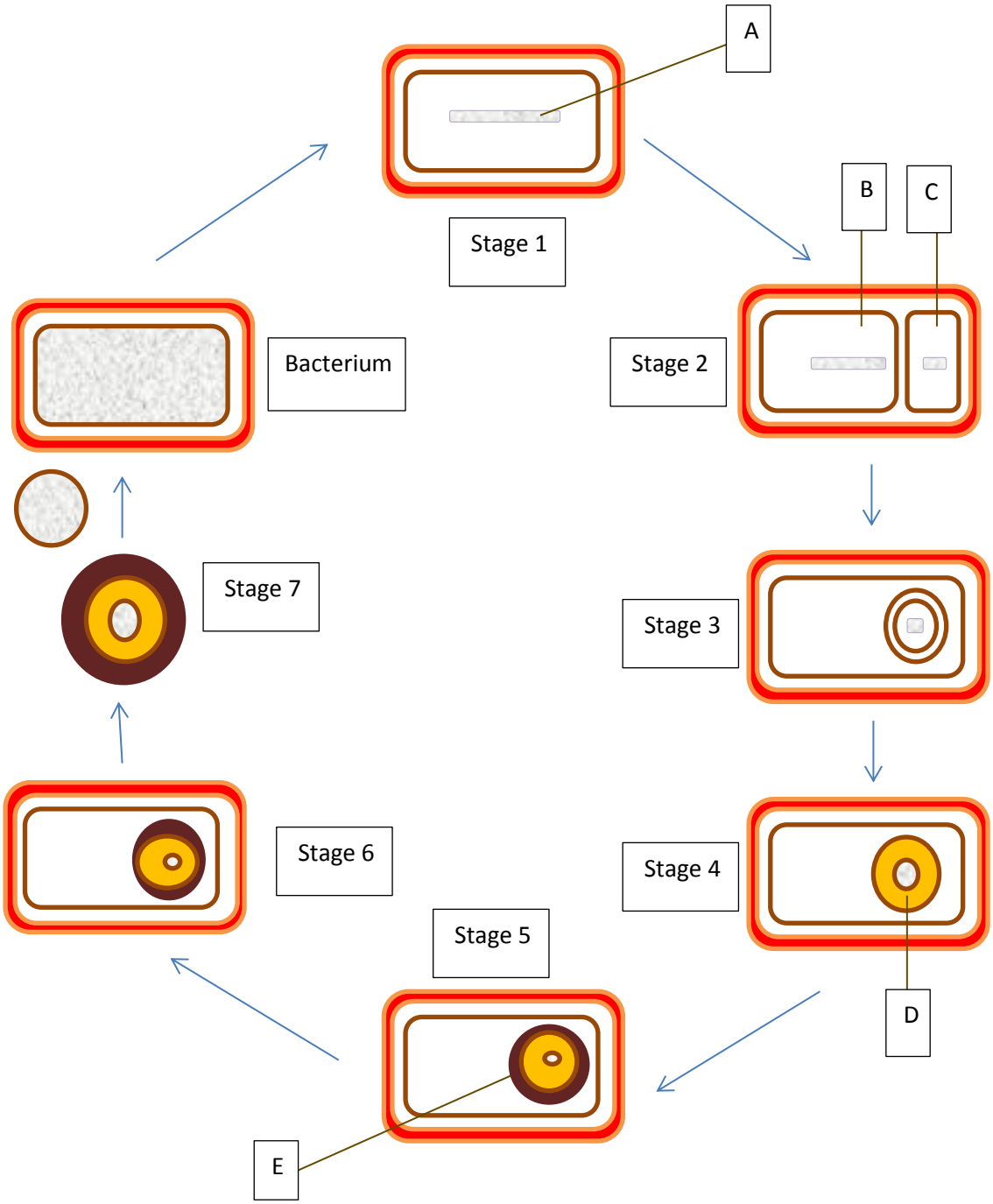

Figure 1.3.2 Schematic Representation of the Process of Sporulation: Stage 1: Axial Filament Formation; Stage 2: Forspore Formation; Stage 3: Engulfment of Forspore; Stage 4: Cortex Formation; stage 5: Spore wall Formation; Stage 6: Maturation of Spore; Stage 7: Autolysis of Mother Cell (Sporangium) to Release Mature Spore (Based on references 3 and 5)

A- Axial filament; B- mother cell; C- Forespore; D – Cortex; E – Spore Wall

Then the mother spore starts engulfing the forespore and in the third stage, mother spore engulfs the forspore completely and as a result, the forspore has one more layer on it. In the fourth stage,

cortex starts developing between these two layers. Dipicolinic acid also accumulates in dehydrating protoplast as calcium dipicolinate. In the fifth stage, multilayered protein coat starts developing around cortex. In stage sixth, newly formed spore matures and becomes refractile which is very resistant to environmental stresses. In the last stage, the seventh stage, with the help of some lytic enzymes the mature endospore is released by the autolysis of the mother cell [3, 5, and 6] (Figure 1.3.2). A mature endospore doesn't have any detectable metabolism. The dormant endospores can survive over hundreds of millions of years, [2] in the state of cryptobiosis. The whole process is highly specific and controlled by a specific set of genes. In appropriate condition for spore formation (nutrient depletion), pattern for vegetative gene expression is replaced by sporulation gene expression. A series of transcription factors called sigma factors bind to core polymerase and let it transcribe specific promoters to ensure sporulation [4].

1.3.3 Bacterial **Endospores or Spore**

A typical endospore is a concentric, multilayered structure. Normally, it has the following layers - exosporium, spore coats, outer membrane, cortex, germ cell wall, inner membrane, and central core [7]. In case of *Bacillus subtilis* (Figure 1.3.3 A) either it does not have exosporium or highly reduced in size [7]. *Bacillus anthracis (*Figure 1.3.3 B) has all of the layers.

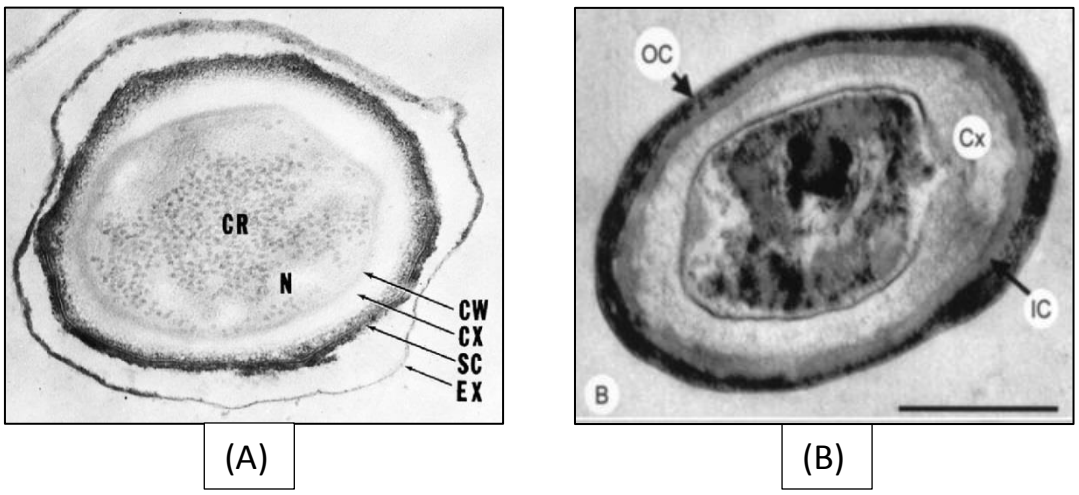

Figure 1.3.3 (A) *Bacillus anthracis* endospore (X 151,000); Exosporium (EX); SPORECOAT (SC); Cortex (CX); Core Wall (CW); Protoplast or Core (CR); Nucleoid and Ribosomes (N,) (Taken from reference 5)
(B) *Bacillus subtilis* Spore (Wild-type Spore): IC; Inner coat; OC: outer Coat; Cx: Cortex; Bar -500 nm (Taken from reference 3)

1.3.3.1. Spore coat

It is a tough proteinaceous multilayered shield which provides the mechanical integrity and excludes large molecules while allowing small molecules to access germination receptors beneath the coat and outer coat. It has about 50 proteins [17] and some of them are highly cross linked. Spore coat has two major layers; an inner coat and an outer coat [18]. The inner lamellar coat is composed of 2 to 5 layers and about 75 nm wide, the outer coat is wider which is about 70 to 200 nm wide [3]. Spore coat is important for the resistance to some chemicals, exogenous lytic enzymes and to predation to protozoa but has no role in spore resistance to heat, radiation and other chemicals [3, 8]. Most of the coat proteins function is not known yet .The coat also appears the house of enzymes with direct role in germination and perhaps in detoxification [15, 16]. Sometimes spores like *Bacillus anthracis* have exosporium (Figure 1.3.3 A) but *Bacillus subtilis* (Figure 1.3.3 B) doesn't have. Although it is considered that the spore coat doesn't have any active direct role in germination but it acts like a sieve and allows the entrance of certain molecules, very selectively, if it is true then removal of spore coat should accelerate the germination, not inhibit it [3] but the removal of spore coat inhibits the germination. There is a close connection between the integrity of the coat and the ability to germinate correctly, since defects in germination were found to be characteristics of coat mutants [18].

1.3.3.2 Cortex.

The cortex is composed of peptidoglycan with a structure similar to that of vegetative peptidoglycan with several spore specific modifications [10]. The germ cell wall lying under the cortex is also composed of peptidoglycan identical of the vegetative cell peptidoglycan [7]. The cortex is less cross linked than the vegetative cells [6]. Detailed structure of peptidoglycan of gram positive bacterial cell wall is shown in Figure 1.3.4 and Figure 1.3.5.

Formation of cortex is important for the reduction of water content and pH too which is essential for spore's enzymatic dormancy maintenance [19].

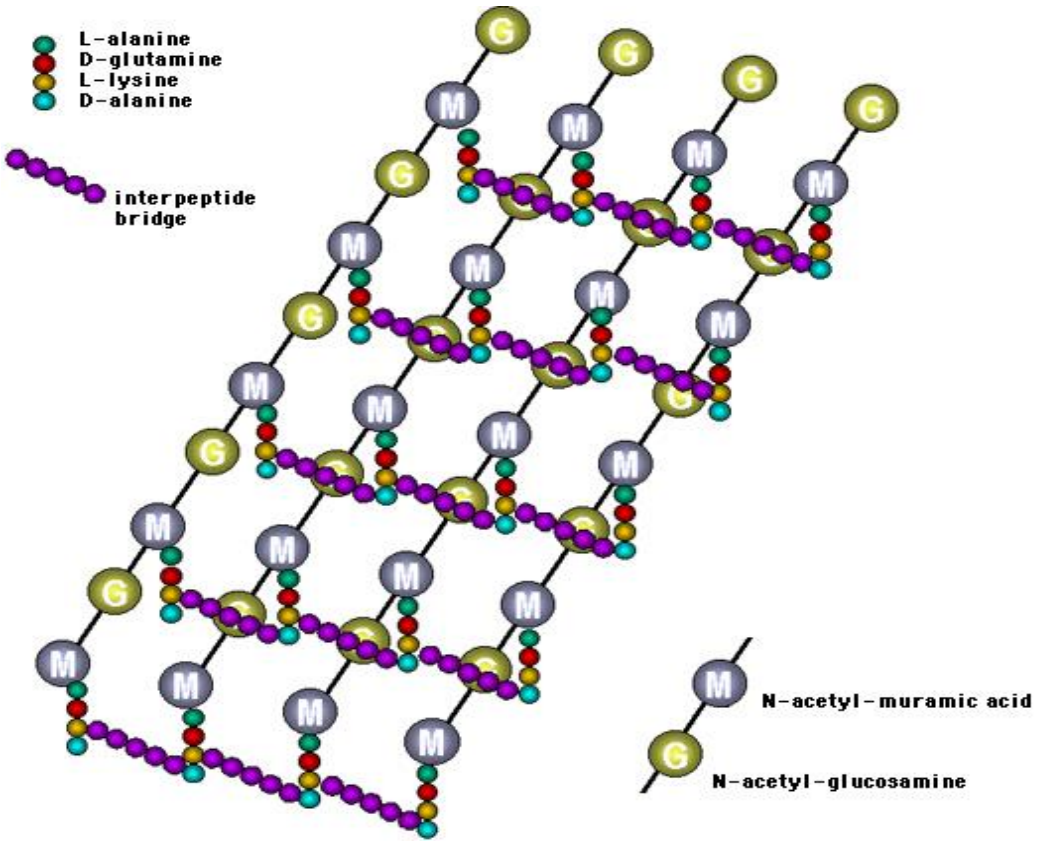

Figure 1.3.4 Showing thicker Glycan Backbone, Inter-Peptide Bridges that Joins Amino Acid Side Chains (Gram Positive Cell Wall)

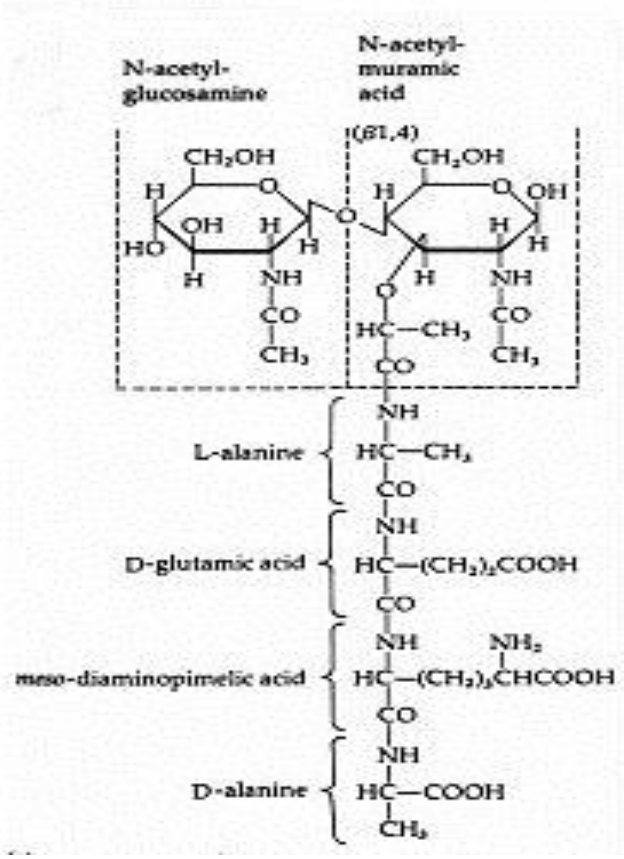

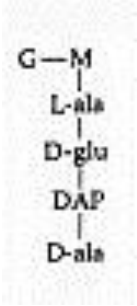

Figure 1.3.5

Two amino sugars

(N-acetyl- glucosamine =G
N- acetylmuramic acid=M)

1. 4 amino acids

(L-alanine=L-ala, D-glutamic acid=D-glu, diaminopemelic acid=DAP, D-alanine =D-ala

1.3.3.3 Core

All of the genetic materials and enzymes are in the core, in a very concentrated form. For dormancy or the resistance to environmental stresses, protection of the core is very important. A huge amount of DPA accumulates in the core which helps to reduce the water content and pH too. Water comprises 75% to 80% of the wet weight of the protoplast of a growing cell, whereas it makes up only 27% to 55% of the spore core wet weight depending of the species [19]. The spores of *Bacillus subtilis* mutants lacking DPA due to mutation in the *operon spoVF* that encodes *DPA synthetase* [12]; have a lower core wet density and sensitive to wet heat and theses spores are unstable and germinate spontaneously [12]. Stabilization and retention of dormancy by exogenous addition of DPA has also been reported. DPA is formed by a single oxidative reaction from as intermediate (dihydrodipiciolinic acid) in the biosynthetic pathway leading to the amino acid lysine. Biosynthesis of dipicolinic acid (pyridine-2, 6-dicarboxylic acid) is shown in Figure 1.3.6.

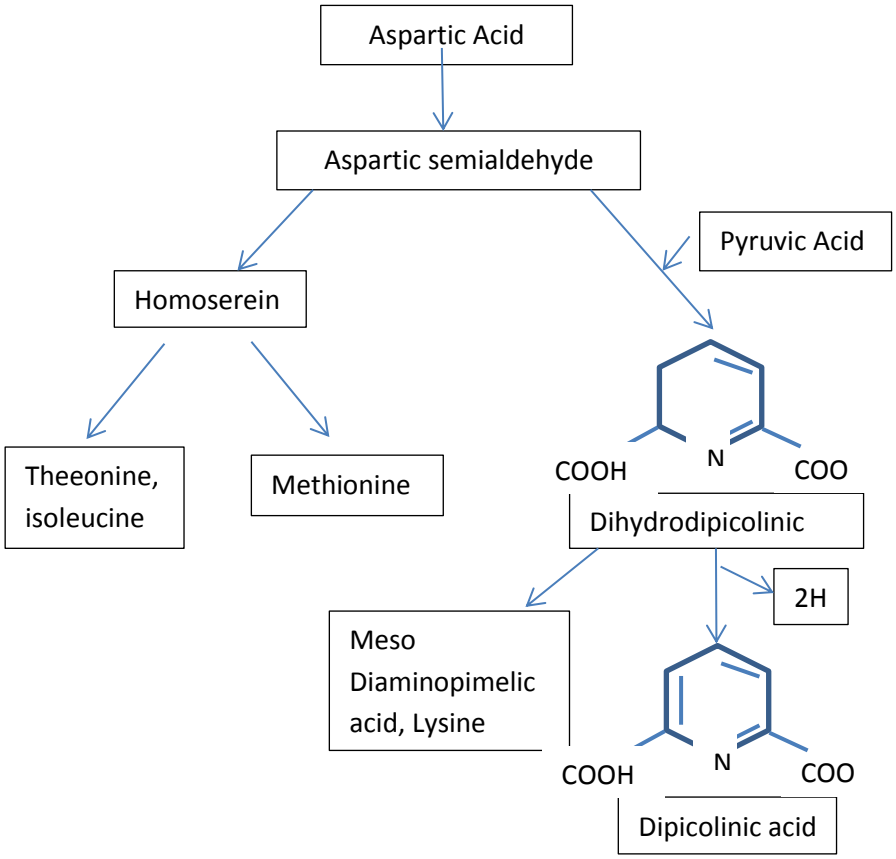

Figure 1.3.6 Pathway of Biosynthesis of Dipicolinic Acid Showing its Relationship to the Pathway of Biosynthesis of the Amino Acids: threonine, isoleucine, methionine and lysine (Taken from the reference 6)

DPA is associated with wet heat resistance but it does not seem to play any role with dry heat resistance [12]. On germination, along with lots of other changes spore losses its cortex along with a huge leakage of DPA. Mineralization (accumulation of Ca^{2+}) of the core is also helps with the reduction of water content. Ca^{2+} ions chelate with DPA and form a complex Ca-DPA (calcium dipicolanate).

In the core, there are small acid soluble proteins (SASPs) which are α, β, and γ bind with DNA and protect it from damaging agents like chemicals, heat, UV radiations, desiccation etc. α/β type SASPs change the shape of DNA from B conformation to A conformation by saturating it [13]. When an endospore gets favorable conditions, losses its dormancy within minutes and germinates [14].

1.3.3.4 Formation of Spore Layers

Formation of spore layers is a very complex process and controlled by lots of genes. Adam Driks proposed a model for the synthesis of spore layers. According to that model [9] coat proteins are synthesized in cytoplasm and then layered on spore surface.

In Figure 1.3.6, MC shows mother cell l and FC shows the forespore. First *SpolVA* protein accumulates on the outer surface of the membrane from the mother cell. It also helps with the synthesis of peptidoglycan between the membranes. Above *SpolVA* protein, *Cot*eE protein starts accumulating as shown in diagram (b) of Figure 1.3.6. There is a matrix between these two layers to glue them together (b). *CotE* directs the deposition of outer coat layers as show in diagram (c) of Figure 1.3.6. Inner coat forms as a layer underneath the CoatE shell as shown in (c) diagram of Figure 1.3.6 which is largely *CotE* independent. There are lots of other proteins of known and unknown functions play very important roles. For each and every step some genes are responsible which work in a very specific manner with a proper coordination with each other.

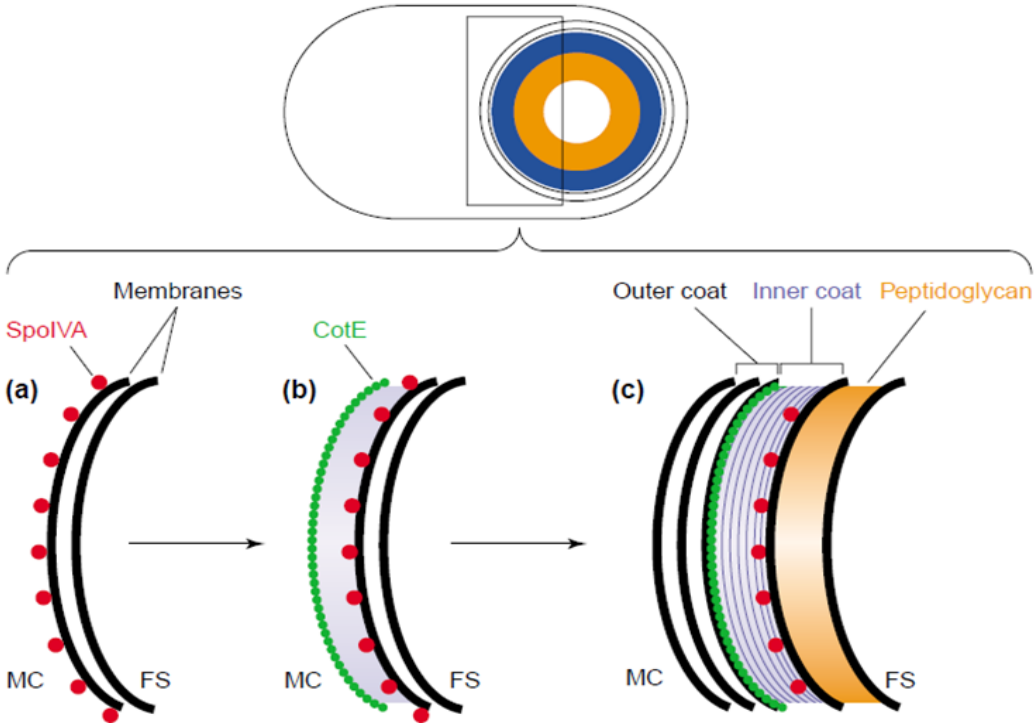

Figure 1.3.7 Model for Spore Coat Assembly; Upper diagram shows mother cell bearing spore before lysis. Lower diagram shows coat assembly of the boxed part in the above diagram. (Taken from the reference 9)

1.3.4 Conclusion

Bacterial spores are very different from the vegetative cells and lots of changes also take place during sporulation but still exact mechanisms of dormancy maintenance and the resistance to environmental stresses are not absolutely clear. Researchers have been trying to understand the mechanisms that take place in a bacterium or particularly in a spore so that techniques can be developed to inactivate them. Atmospheric pressure plasma can be used to sterilize different types of surfaces and equipment. It can also be used to remove dead cells or infectious proteins (prions). It is being used to perform lots of surgeries like cauterization and tissue de-vitalization [20], tissue desiccation [21], skin surgery [22], urology [14], gynecology, brain tumor surgery [23], gastroenterology [24], breast surgery [25], and bronchological endoscopy [26]. Atmospheric pressure cold plasma has immense physical and biological applications.

On the basis of above discussion a comparison between a bacillus vegetative and endospore is given below in table 1.

Property	Bacillus Vegetative cells	Bacillus Endospores
Cell wall	Peptidoglycan cell wall with teichoic acid	Thick protein spore coat, peptidoglycan cortex, inner spore wall
Under the microscope	Nonrefractile	Refractile
Metabolic Activities	present	absent
Macromolecular Synthesis	present	absent
Sensitivity to Lysosomes	Sensitive	resistant
Heat Resistance	Low resistance	High resistance
Chemical Resistance	Low resistance	High resistance
Radiation Resistance	Low resistance	High resistance
Water Content in Protoplast	Low	high
Presence of Dipicolinic acid	absent	present

Table 1- Comparison of a vegetative cell and endospore

1.3.5 References

[1] Stragier P and Losick R. Molecular genetics of sporulation in Bacillus subtilis. Annu. Rev. Genet. 30:297–341, 1996.

[2] Vreeland RH, Rosenzweig WD, and Powers DW. Isolation of a 250 million-year-old halo-tolerant bacterium from a primary salt crystal. Nature 407:897–900, 2000.

[3] Driks A. *Bacillus subtilis* Spore Coat. American Society for Microbiology. p. 1–20 Vol. 63, No. 1.

[4] Losick R and Stragier P. Crisscross regulation of cell-type-specific gene expression during development in *Bacillus subtilis*. Nature 355:601–604, 1992.

[5] Lansing M. Prescott. "Microbiology", 5th edition. The McGraw−Hill Companies, 2002.

[6] Stanier YR, Ingraham LJ, Wheelis LM, and Painter RP. The Microbial World. 5th edition. Prentice- Hall, Englewood Cliffs, New Jersey.

[7] Setlow P. Spores of Bacillus subtilis: their resistance to and killing by radiation, heat and chemicals. Journal of Applied Microbiology 101, 514–525, 2006.

[8] Nicholson WL, Munakata N, Horneck G, Melosh HJ, and Setlow P. Resistance of Bacillus endospores to extreme terrestrial and extra-terrestrial environments. Microbiology and Molecular Biology Review 64, 548–572, 2000.

[9] Driks A. Maximum shields: the assembly and function of the bacterial spore coat. TRENDS in Microbiology Vol.10 No.6, June 2002.

[10] Popham DL. Speciaized peptidoglycan of the bacterial endospore: the inner wall of lockbox. Cell Mol life Sci. 59:426-433, 2000.

[11] Murrel WG, and Warth AD. Composition and heat resistance of bacterial spores. In spores, vol 3 (Campbell LL and Halvorson HO, eds), pp. 1-24 American Society for Microbiology, Ann Arbor, Michigan, 1965.

[12] Paidhungat M, Setlow B, Driks A, and Setlow P. Characterization of spores of Bacillus subtilis which lack dipicolinic acid. J. Bacteriol. 182:5505-5512, 2000

[13] Setlow P. Mechanism for the prevention of Damage to DNA in Spores of Bacillus Species.Annu Rev Microbial 49:29 – 54, 1995.

[14] Paidhungat M, and Setlow P. Spore germination and outgrowth, p.537–548. *In* A. L. Sonenshein, J. Hoch, and R. Losick (ed.), *Bacillus subtilis* and its closest relatives. ASM Press, Washington, D.C., 2002.

[15] Bagyan I and Setlow P. Localization of the cortex lytic enzyme CwlJ in spores of *Bacillus subtilis*. *J. Bacteriol.* 184, 1219–1224, 2002.

[16] Hullo MF. CotA of *Bacillus subtilis* is a copper-dependent laccase. *J. Bacteriol.* 183, 5426–5430, 2001.

[17] Driks A. The Bacillus subtilis spore coat. Microbiol Mol Biol Rev 63, 1–20, 1999.

[18] Aronson AI, and Fitz-James P. Structure and morphogenesis of the bacterial spore coat. Bacteriol. Rev. 40:360–402, 1976.

[19] Gerhardt P. and Marquis RE. Spore thermoresistance mechanisms. In Regulation of Prokaryotic Development ed. Smith, I., Slepecky, R.A. and Setlow, P. pp. 43–63. Washington, DC: American Society for Microbiology, 1989.

[20] Raiser J and Zenker M. Argon plasma coagulation for open surgical and endoscopic applications: state of the art. J. Phys. D Appl. Phys. 39, 3520.70, 2006.

[21] Pollack S, Carruthers A, and Grekin RC. The History of Electrosurgery. Dermatol. Surg., 26, 904-908, 2000.

[22] Brand CU, Blum A, Schlegel A, Farin G, and Garbe C. Application of argon plasma coagulation in skin surgery. Dermatology 197152–7, 1998.

[23] Tirakotai W, Mennel HD, Celik I, Kolodziej M, Bertalanffy H, and Riegel T. Argon plasma coagulation (APC) in brain tumor surgery: experimental study and clinical experiences. Clini. Neuropathol. 23, 257–61, 2004.

[24] Ginsberg GG, Barkun AN, Bosco JJ, Burdick JS, Isenberg G A, Nakao NL, Petersen BT, Silverman WB, Slivka A, and Kelsey PB. The argon plasma coagulator. Gastrointestinal Endoscopy, Volume 55, No.7, 2002.

[25] Ridings P, Bucknall TE, and Bailey C. Argon Beam coagulation asan adjunct in breast-conserving surgery. Ann. R. Coll. Surg. Engl. 80, 61–2, 1998.

[26] Reichle G, Freitag L, Kullmann HJ, Prenzel R, Macha HN, and Farin G. Argon Plasma Coagulation (APC) in bronchology: A new method –alternative or complementary?. J. Bronchol. 7, 109–17, 2000.

Chapter 2

Electrical and Optical Characterization of Cold Atmospheric Pressure Plasma Torch (CAPPLAT – 9Ne) the Commercial unit and the Effects of N_2 gas on Argon Plasma Jet

2.1 Introduction

Normally, to produce non-equilibrium plasma, low pressure (about 10^{-4} to 10^{-2} kPa) is required. Maintenance of low pressure or vacuum, limits its use to batch processes besides that the size of the substrate and cost effectiveness are the main hurdles in the successful commercial use of non-equilibrium cold atmospheric plasmas. To overcome these problems, several novel atmospheric pressure plasma generating source**s** have been developed like arc discharges, plasma torches, barrier discharges, corona discharges, plasma jets and micro-plasma.

All over the world, people have been using plasma for a long time but the invention of non-equilibrium, atmospheric plasmas heralded a new era of their applications in different fields. Non-equilibrium plasmas like one atmosphere uniform glow discharge plasma (OAUGDP), atmospheric pressure plasma jet (APPJ), micro-beam plasma generator, plasma needle, plasma torches, plasma bullet etc. are often used for ozone generation, surface treatment [1-3], pollution control, radiation sources etc.. Bio-plasma is also a very fast emerging field of plasma applications. Efforts are being made to achieve specific parameters to kill different types of harmful microorganisms or diseased cells to treat some dreadful diseases. Actually, we also tried to characterize our handmade torch for its bio-application (sterilization).

At atmospheric pressure, a low temperature (22 to 35°C) , non-equilibrium plasma discharge generating device (CAPPLAT) fed by a high-voltage pulsed power source had already been

developed and used successfully for both chemical vapor deposition (CVD) and polymer surface treatment [5, 8-11]. That device had also been commercialized under the name of "CAPPLAT" by Cresur Corporation [6]. The CAPPLAT - 9 Ne, we used to conduct the experiments had a little bit different configuration from the basic CAPPLAT unit. The CAPPLAT - 9 Ne worked at higher sinusoidal feeding voltage (V_{pp} 20 kV) than the basic CAPPLAT unit manufactured by Cresur Corporation. To generate plasma discharge, Ar gas was used as a working gas or a primary gas, N_2 gas was mixed to achieve a homogeneous discharge. Electrical and optical properties of the homogeneous plasma discharge were characterized using a high voltage probe, current probe and optical emission spectroscopy. Finally, in order to investigate the effect of the stabilized plasma discharge on the viability of *Bacillus subtilis* endospores, the endospores (1.0×10^7 to 4.0×10^7 spores/ml) were exposed to the plasma for different durations. We could successfully inactivate a *Bacillus* endospore population of 1.0×10^7 to 4.0×10^7 endospores/ml. The experimental details about bacterial endospores are discussed in Chapter 4

2.2 Experimental Setup and Methods

2.2.1 Plasma Device

We used CAPPLAT-9 Ne (Figure 2.1) and a hand-made plasma torch (Figure 2.4) to generate non-equilibrium plasma at atmospheric pressure.

Figure 2.1 CAPPLAT- 9Ne (Cold Atmospheric Pressure Plasma Torch – 9 Ne). It is the commercial version of the basic CAPPLAT.

This device was based on the principle of dielectric barrier surface discharge. The schematic illustration of plasma torch is given in Figure 2.2. It comprised of two coaxial electrodes with a layer of dielectric barrier between them. The schematic illustration of electrode arrangements is given in Figure 2.3. The inner electrode was a copper tube with the outer diameter of 8 mm and the inner diameter of 7 mm. The inner electrode was connected to high sinusoidal voltage (V_{pp} 20 kV) at a frequency of 20 kHz. The outer electrode was a piece of copper foil of 20 mm width. The outer electrode was grounded. A silicone tube (Laboran® silicone tube) of thickness of 2 mm was sandwiched between two electrodes as a dielectric barrier. Arrangement of electrodes and dielectric barrier is illustrated in Figure 2.4. An inlet tube was also inserted into the copper tube to feed Ar gas (working gas) and N_2 gas (additive gas) into the hollow inner electrode. A glass capillary tube was inserted into the hollow inner electrode for the direct injection of other additive gases like O_2 or for the addition of H_2O_2 through bubbling with the argon gas as a carrier gas, to the plasma discharge. Our handmade plasma is shown in Figure 2.4.

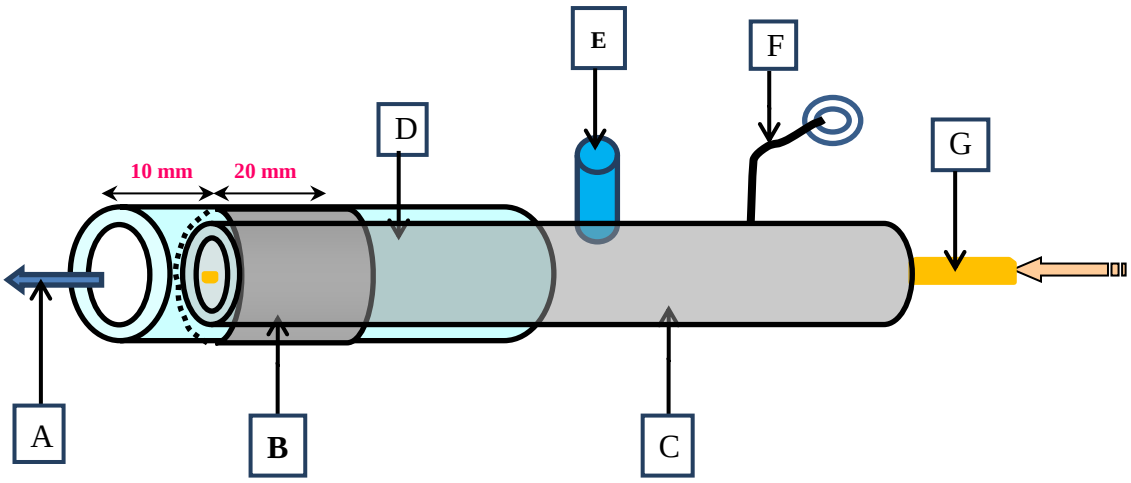

Figure 2.2 Schematic illustration of plasma torch; A: Plasma jet; B: grounded outer electrode; C: Inner copper electrode; D: Dielectric substance (silicon tube); E: Inlet for the mixture of Ar and N_2; F: Wire connecting inner copper electrode to a high voltage source; G: Glass capillary for other additive gases like O_2 or for the addition of other substances via bubbling.

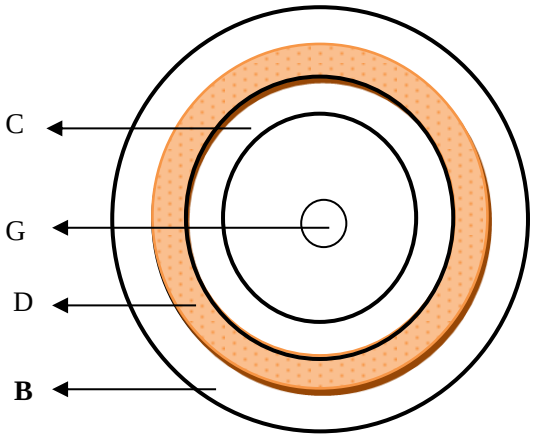

Figure 2.3 Schematic illustration of the Arrangement of electrodes and dielectric barrier C: inner high voltage electrode; G: glass capillary for direct gas injection into the plasma jet; D: dielectric substance (silicone tube); B: outer grounded electrode.

(The alphabets showing different parts, are the same as in Figure 2.2)

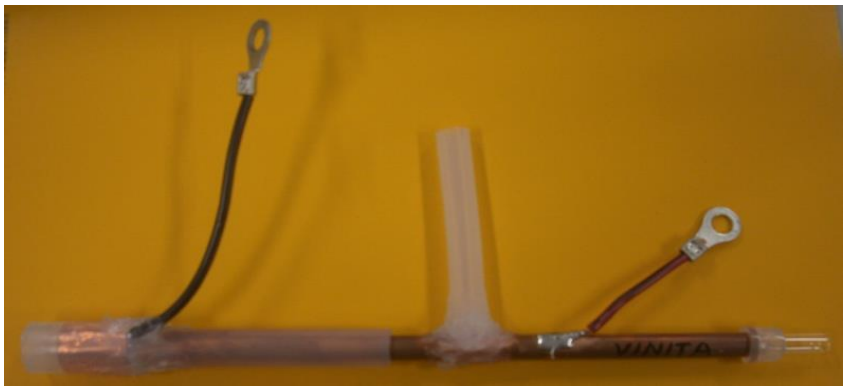

Figure 2.4 Handmade Plasma Torch

For plasma jet generation, 10 slm (standard liter per minute) of Ar gas as a working gas and the different volumes of N_2 gas (100 to 200 sccm (standard cubic centimeter per minute)) as an additive gas were used. All of the volumes were controlled by mass flow controllers installed in the CAPPLAT – 9Ne. Before feeding the mixture of gases into the hollow inner electrode, they were passed through a mixing device to have a uniform effect (quenching) of nitrogen gas on argon gas. N_2 could be added through the glass capillary inserted into the hollow inner electrode for the direct injection into the plasma discharge but it was not effective. There was no quenching effect of N_2 [5]

and the plasma discharge was as filamentary as it was before N_2 addition. To have quenching effect we need to add gases to direct plasma not to remote plasma (after-glow discharge).

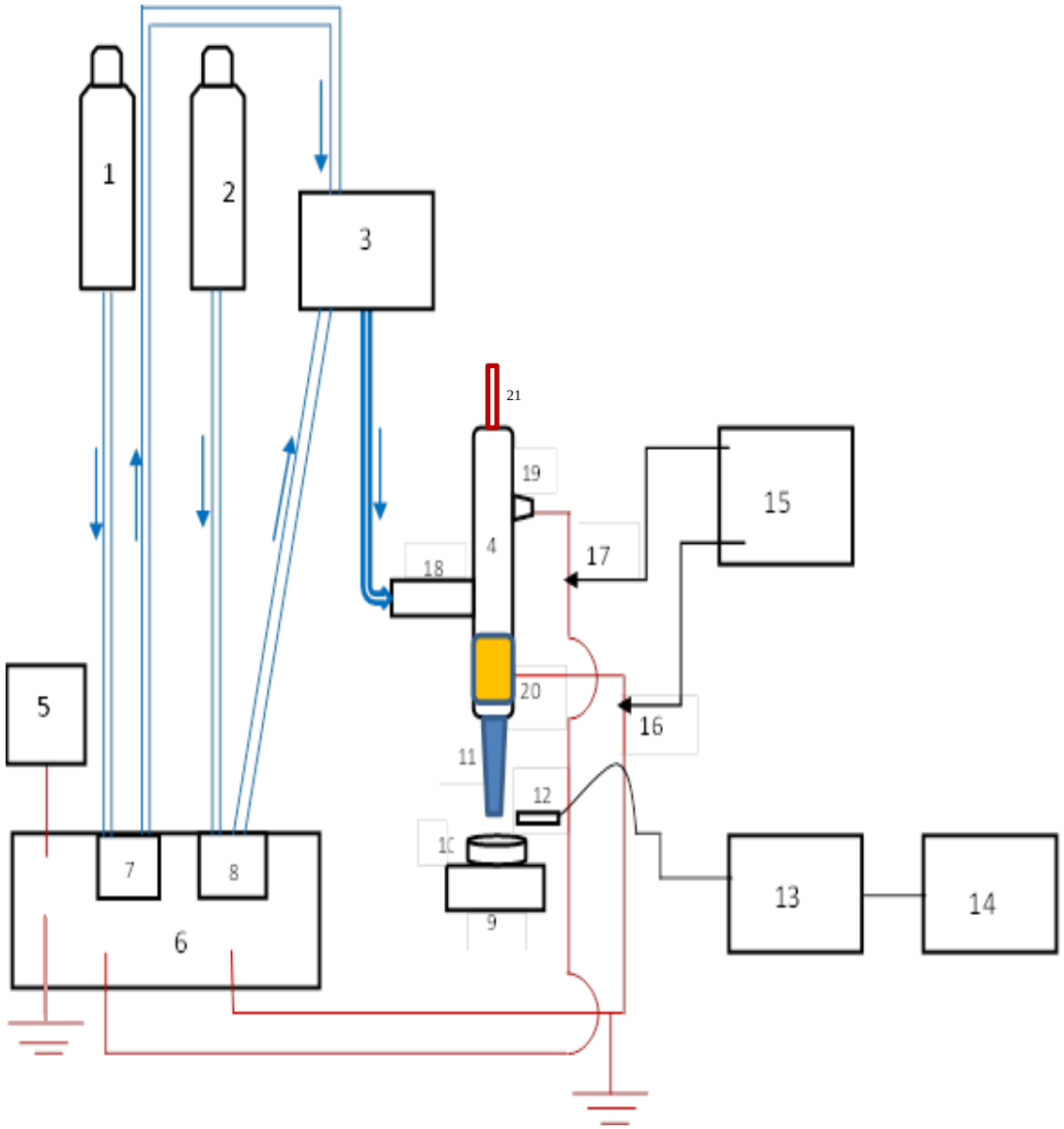

Figure 2.5 Schematic illustration for experimental setup and the setup for OES and electric measurements. 1: Ar gas (working gas); 2: N_2 gas (additive gas) ; 3: Gas mixing device; 4: Plasma torch; 5: A.C source; 6: CAPPLAT; 7 & 8: Mass flow controllers; 9: stage; 10: Substrate; 11: Plasma jet; 12: optical fiber ; 13: Optical emission spectroscopy; 14: Personal computer; 15: Oscilloscope; 16: Current probe; 17. Voltage probe; 18: Inlet for the mixture of Ar&N_2; 19: Inner electrode; 20: Outer electrode; 21: capillary to inject other gases into the plasma jet directly

When O_2 gas or H_2O_2 with Ar gas as a carrier gas were added through the capillary, there were

no effects on the appearance of the jet and consequently optical emission spectrum and the waveforms of current and voltage were also almost unaltered but the effects of the jet on the substrate were drastic. When O_2 was added to the mixture of Ar and N_2 it caused such a massive quenching that we couldn't get any plasma discharge so we added it to the plasma discharge directly (direct injection mode) through the capillary. Schematic illustration of the whole experimental set up is given in Figure 2.5 whereas to show the addition of Ar and N_2 is shown in Figure 2.8.

2.2.2 Electrical Measurements

The high sinusoidal voltage (V_{pp} 20 kV), applied to achieve the plasma discharge, was measured using a 1000:1 high-voltage probe (Tektronix P6015A). The voltage probe was attached to the inner electrode of the plasma torch. The capacitive current was monitored using a wide band current monitor (Pearson^{TM} current monitor) manufactured by Pearson Electronics Inc., Palo Alto, California, U.S.A.. The cable connected to the outer electrode was passed through the wide band current monitor. A digital phosphor oscilloscope (Tektronix TDS3012C) was inserted into the circuit to record the waveforms of voltage and current. The setup for electrical measurements is shown in Figure 2.5. Electrical measurements were recorded for filamentary plasma discharge (see Figure 2.6) when only Ar gas was being used and for stabilized plasma discharge (see Figure 2.7) when both Ar gas and N_2 gas were used to get a stabilized plasma discharge. Figure 2.8 has the schematic illustration of Ar-N_2 addition to the plasma discharge. The electrical wave forms are given in Figure 2.9 and Figure 2.10. To see the effect of the gas composition on total current, the current probe was attached to the outer electrode to check the total current in both cases; Ar discharge and Ar-N_2 discharge and the waveforms are shown in Figure 2.11.

2.2.3 Optical Emission Spectroscopic Measurements

The optical emission spectra of plasmas were collected using Multiband Plasma–process Monitor (MPM, Hamamatsu Photonics C7460). The spectral range was 200 nm to 950 nm with the wavelength resolution of < 2nm FWHM (full width at half-maximum). The optical fiber probe was kept 0.5 cm below and 1.5 cm away from the mouth of the plasma torch to capture the spectra of plasma emission. Monitoring and acquisition of data was carried out by a personal computer, connected to the multiband plasma-process monitor. The optical spectrum for Ar-plasma discharge is given in Figure 2.12. The spectrum for Ar-N_2 plasma discharge is shown in Figure 2.13. The comparison of spectra for different plasma discharges are given in Figure 2.14.

2.3 Results and Discussion

2.3.1 Electrical Characterization of Ar Plasma Jet and the Effects of the Additive gas (N_2)

Since Kanazawa et al. [7] generated homogeneous atmospheric plasma with He gas using dielectric barrier, lots of work about non-equilibrium homogeneous dielectric barrier discharge at atmospheric pressure has been done. Our hand-made torch is based on the principal of dielectric barrier surface discharge at atmospheric pressure. A high sinusoidal voltage (V_{pp} 20 kV, frequency 20 kHz) was used to generate the plasma discharge. Ar as a primary gas (working gas) generated highly filamentous plasma shown in Figure 2.6. Dielectric barrier substances are often used to achieve homogeneous discharges. The insulating nature of dielectric substance restricts the movement of the charge and subsequently there is a charge accumulation on the surface of dielectric barrier. In the other half cycle when the polarity of driving oscillation changes, the accumulated charge is expelled from the dielectric barrier surface to the other electrode. When the accumulation of charge exceeds its breakdown, micro-discharges (filaments) occur. In spite of the use of dielectric barrier, Ar gas plasma discharge was extremely filamentous as shown in Figure 2.6. To synergies the self-arresting power of dielectric barrier substance, N_2 gas was added to achieve a

stabilized plasma discharge shown in Figure 2.7. N_2 gas stabilized the plasma discharge by the process of quenching. With the addition of N_2, jet got stabilized but shorter in length and less intense.

Figure 2.6 A highly filamentous discharge obtained by applying a sinusoidal voltage (V_{pp} 20 kV) at the frequency of 20 kHz to Ar (10slm) only. The length of the jet was about 3.0cm.

Figure 2.7 A stabilized homogeneous plasma discharge obtained by applying a sinusoidal voltage (V_{pp} 20 kV) at the frequency of 20 kHz to the mixture of Ar (10 slm) and N_2 (100 sccm). The length of the jet was about 2.5cm.

Arrangement to feed gases into the plasma torch to get the plasma discharge is shown in Figure 2.8.

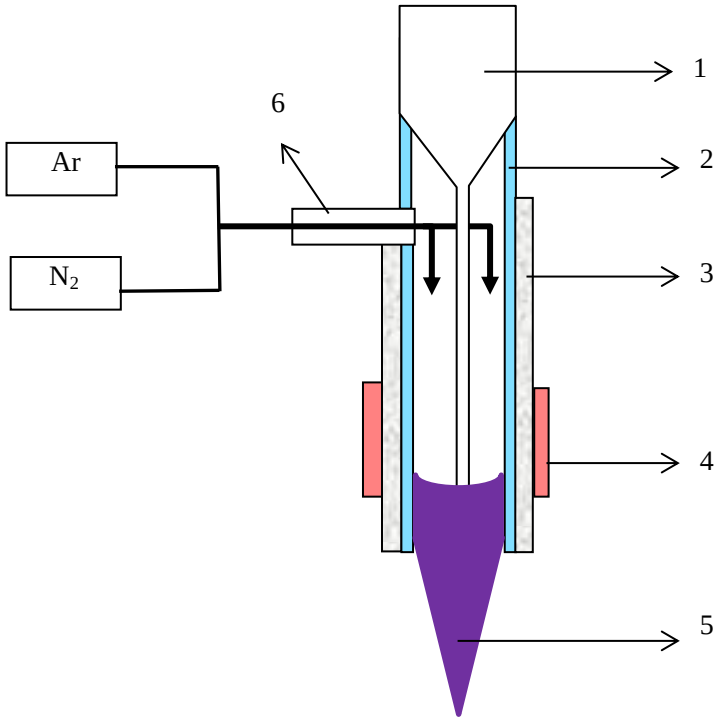

Figure 2.8 1: Capillary; 2: Inner electrode; 3: Dielectric barrier; 4: Outer electrode; 5: Plasma Jet; 6: Inlet for the mixture of gases (Ar and N_2)

The waveforms of time dependent current and applied voltage are shown in Figure 2.9 and Figure 2.10. To see the impact of micro-discharges on the current instead of average waveform,

single sequence waveforms were captured. The waveform of the capacitive current for Ar gas (10 slm) and N_2 gas (100 sccm) plasma discharge, as shown in Figure 2.10, was much smoother with only a few occasional microdischarges than the capacitive current waveform for only Ar gas (10 slm) plasma discharge, as shown in Figure 2.9.

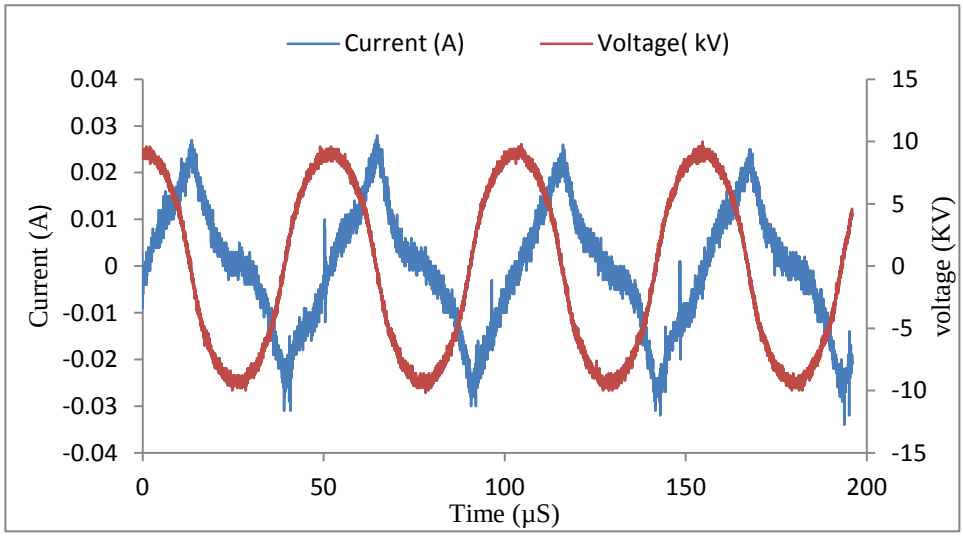

Figure 2.9 Typical waveforms of applied voltage and capacitive current for a single sequence for Ar (10 slm) plasma discharge, obtained by applying a sinusoidal voltage of 20 kV (peak to peak) at the frequency of 20 kHz. The blue line shows the current in ampere and the red line shows the voltage in kV.

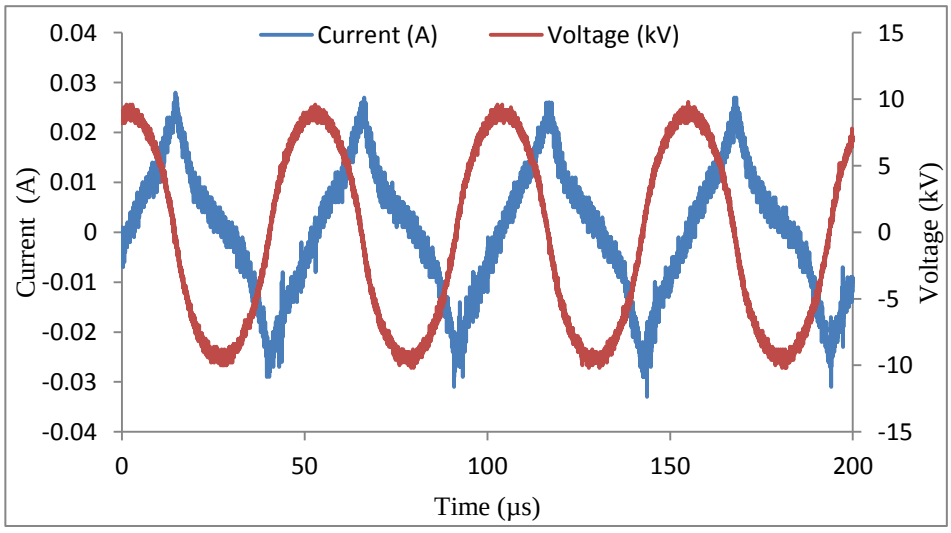

Figure 2.10 Typical waveforms of applied voltage and capacitive current for a single sequence for the mixture of Ar (10 slm) and N_2 (100 sccm) plasma discharge, obtained by applying a sinusoidal voltage of 20 kV (peak to peak) at the frequency of 20 kHz. The blue line shows the current in ampere and the red line shows the voltage in kV.

Both waveforms show that the amounts of voltage (V_{pp} 20 kV) and current (I_{pp} 60 mA) were almost the same which shows that the properties of micro-discharges in filamentary DBDs depend on feeding gas composition rather than the properties of external driving circuit (e.g. frequency, feeding voltage or the waveform) [5]. To see the effect of feeding gas composition on total current, the current probe was connected to the high voltage inner electrode and the average data was collected for the total currents for different feeding gas compositions (Figure 2.11).

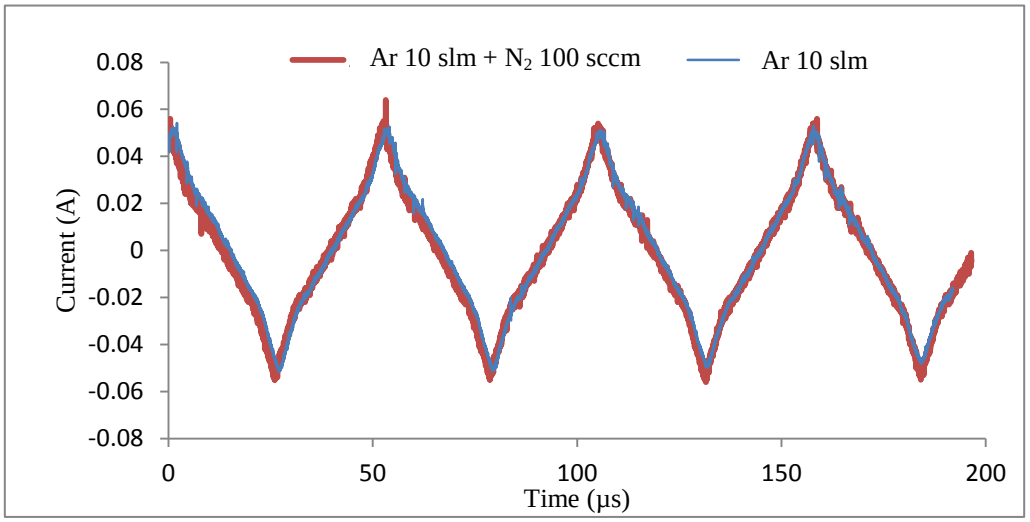

Figure 2.11 Comparison of waveforms of total current in Ar discharge before and after N_2 injection, obtained by applying a sinusoidal voltage (V_{pp} 20 kV) with the frequency of 20 kHz to the mixture of Ar (10 slm) The blue line shows the current of plasma discharge when only Ar (10 slm) was used. The red line shows the current discharge after mixing N_2 (100 sccm) into Ar gas to generate plasma discharge. The current probe was attached to the high voltage inner electrode.

As shown in Figure 2.11, the average total current increased a little bit when N_2 gas (additive gas) was added to the Ar gas (working gas) the feeding gas to achieve a stabilized plasma discharge. It could be assumed that the very slight increase in the amount of current is due to the ionization of some of the N_2 molecules by highly energetic electronic collisions. This ionization is different from penning ionization which requires much higher energy (18.7 eV).

$$e^{*} + N_2 \longrightarrow N_2^{+} + 2e$$

Most probably, the above transition is responsible for the slight increase in the current and this ionization process needs less energy (15.6 eV) than the energy required for penning ionization (18.7 eV).

For CAPPLAT 9-Ne, the characteristics of the power source can't be changed, only the added volume of N_2 gas (additive gas) to the working gas (Ar gas) can be manipulated in order to obtain a stabilized plasma discharge. So, we increased the amount of additive N_2 gas into the working gas Ar to achieve stabilized plasma. It was found that if we increase the volume of N_2 gradually, we need more than 200 sccm N_2 but if we add a surplus amount of N_2 in the beginning and then gradually decrease the amount of N_2 we can attain a stabilized plasma discharge with less amount of N_2. Initially, when there was 10 slm of Ar gas and 100 sccm of N_2 gas, the plasma jet was still quite filamentous. When, we started off adding N_2 gas with the volume of 200-250 sccm, the plasma discharge was highly stabilized from the beginning. Then we started decreasing the volume of N_2 gas and we could achieve a highly stabilized plasma jet with addition of just 100 sccm of N_2 gas. It could be explained by considering the fact that to prevent filamentary discharge; we need to have a minimum initial electron density and minimum ionization rate before breakdown [20]. Most probably, because of higher voltage of operation we had higher number of primary avalanches (α mode) and the released electrons caused the secondary emissions (γ mode). The series of avalanches led to microdischarges as dielectric barrier alone couldn't handle this much accumulation of charge. As we couldn't change the characteristics of the feeding power source so we increased the amount of N_2 gas excessively to quench the active charged species as much as possible in order to get stabilized plasma discharge by controlling electron density and ionization rate. Because of low electron density and ionization rate, dielectric barrier could handle the charge accumulation and subsequently microdischarges, when the amount of nitrogen was decreased

gradually. This way, we could maintain a stabilized plasma discharge at relatively lower volume of N_2 gas which was necessary for energetic plasma. When we decreased the volume of N_2 gas further we couldn't maintain the stabilized plasma discharge because of higher electron density and ionization rate which were too high to quench for the available N_2 molecules. Although we could stabilize plasma discharge (Figure 2.7) and we had a much smoother curve for current wave form (Figure 2.10) but visually and according to the current waveform, the plasma discharge was not a diffuse glow discharge it was filamentary glow discharge. For filamentary glow discharge we used the term stabilized plasma.

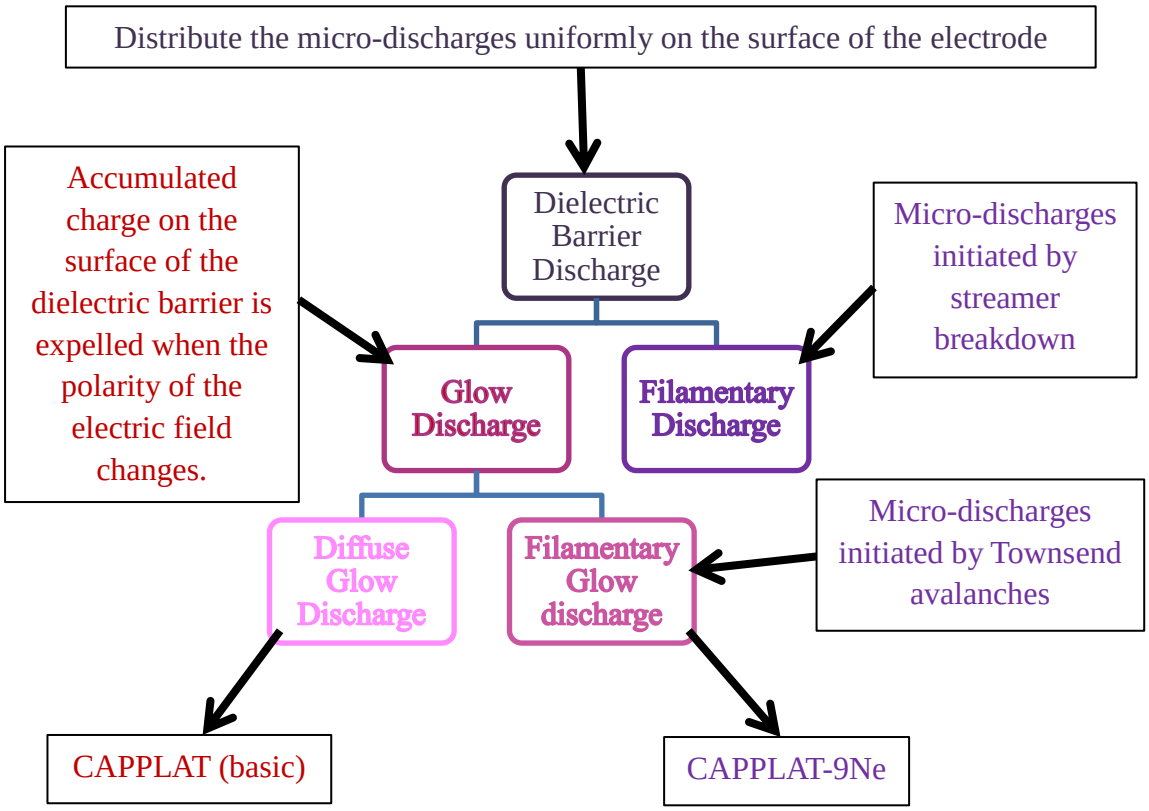

Figure 2.12 Difference between diffuse glow discharge and filamentary glow discharge

As shown in Figure 2.12, dielectric barrier is supposed to distribute the microdischarges uniformly on the surface of the electrode. But in most of the cases, a DBD discharge is not uniform. It consists of numerous non-steady-state local microdischarges distributed in the discharge volume

[17]. These microdischarges are also called filaments because of their appearance. The plasma discharge with these microdischarges or filaments is called filamentary discharge which is not suitable for lots of sophisticated industrial applications. Microdiscarges have already been explained in Chapter 1. The other mode of DBD plasma discharge is glow discharge (Figure 2.12). The glow mode of DBDs is not necessarily to be uniform but it can also be filamentary [17]. So, DBD glow discharge can be divided into two categories – diffuse glow discharge and filamentary glow discharge. The glow filaments are formed by Townsend avalanches unlike streamer breakdowns which cause filamentary discharges [Figure 2.12, 18, 19]. Diffuse glow discharge will be discussed later in chapter 3 with CAPPLAT. To have a volume-stabilized glow discharge, we should have enough pre-ionization electron density to have enough avalanches in order to get a glow discharge. Avalanches cause streamer formation but if we have enough avalanches to overlap and coalescence their primary heads in order to smooth out the space-charge field gradient, we can have glow discharge with avalanches. The discharge obtained this way can be called as a pulsed avalanche discharge. In case of CAPPLAT-9Ne, high voltage (Vpp 20kV) of operation provided enough electron density for a uniform pulsed avalanche discharge and because of these coalescent avalanches we had a glow discharge but because of avalanches the glow discharge was a filamentary glow discharge.

2.3.2 OES Characterization of Ar Plasma Discharge (Jet) and the Effects of N_2 Addition

The optical emission spectrum of the Ar plasma discharge in the wavelength range of 200 nm – 950 nm is shown in Figure 2.12. Some smaller emission peaks at the wavelengths of 337.13nm, 357.63nm, 380.27nm, 406.07nm belonging to the N_2 second positive system (N_2 ($C^3\prod_u$ — $B^3\prod_g$)) were observed, besides these emission peaks a prominent emission peak at 308 nm representing OH radicles ($A^2\Sigma^+$ — $X^2\prod$) was also observed. The information about these smaller peaks is

summarized in Table 1. These emission peaks were due to the ambient air or the impurities in the working gas shown in Figure 2.12.

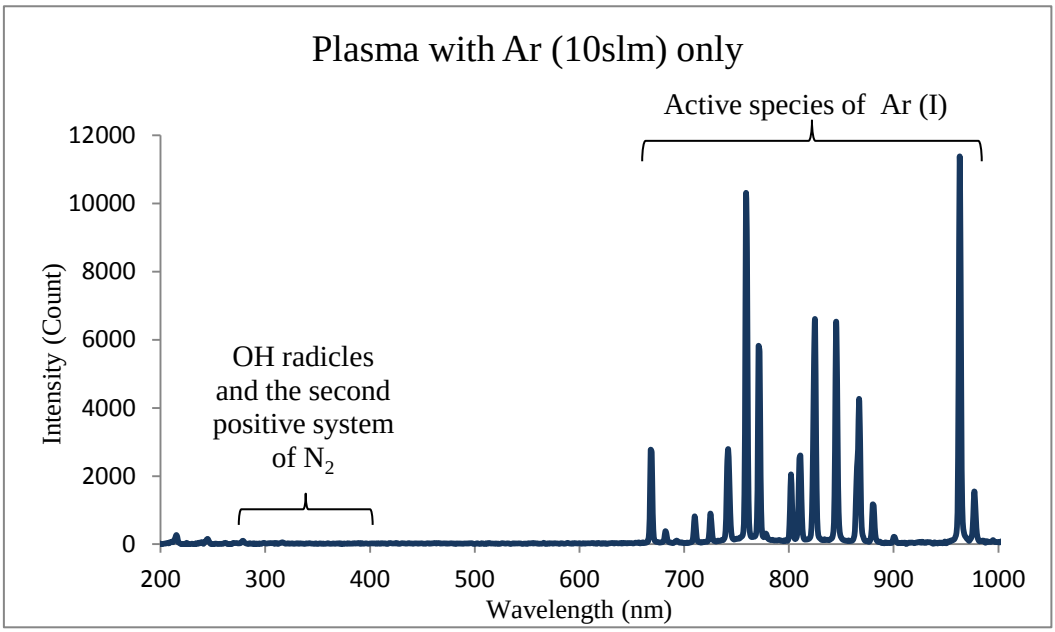

Figure 2.13 Optical emission spectrum of Ar (10 slm) plasma discharge, generated by high sinusoidal voltage (Vpp 20 kV) at the frequency of 20 kHz. The optical fiber probe was kept 0.5 cm below and 1.5 cm away from the mouth of the plasma torch to capture the spectra of plasma emission.

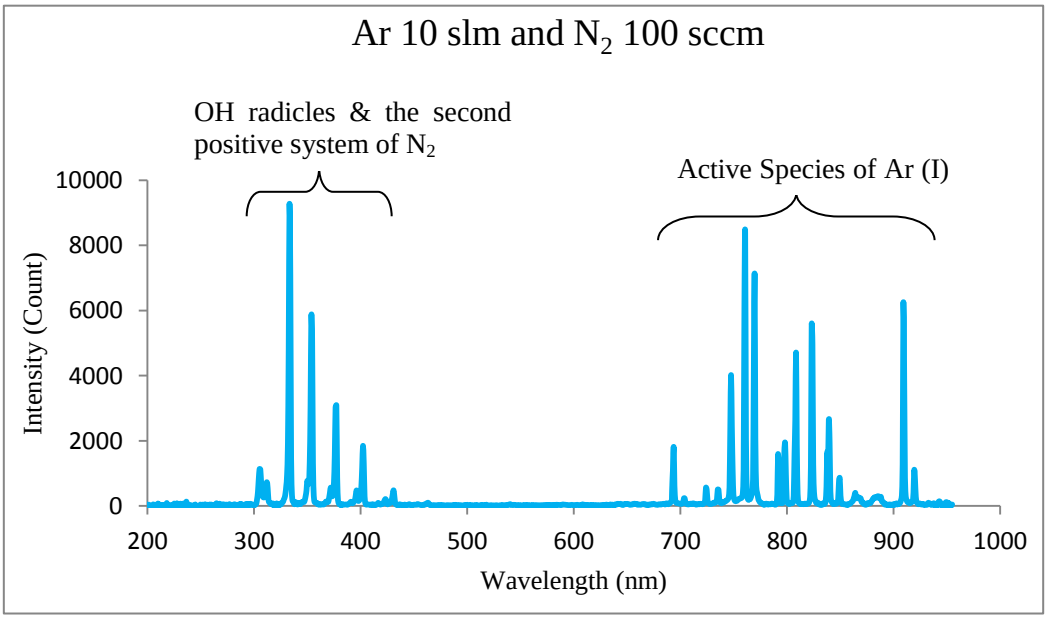

Figure 2.14 Optical emission spectra of Ar (10 slm) and N_2 (100 sccm) plasma jet generated by high sinusoidal voltage (V_{pp} 20 kV) at the frequency of 20 kHz. The optical fiber probe was kept 0.5 cm below and 1.5 cm away from the mouth of the plasma torch to capture the spectra of plasma emission.

All of the emission peaks for Ar atoms lie in the range from 696 nm to 922 nm [5, 12, and 15]. The intensities of emissions and transitions were coherent with NIST (National Institute of Standards and Technology). Almost all of the prominent peaks represented 4p-4s transition. Observed emission peaks with their wavelengths and transitions are summarized in Table 2.

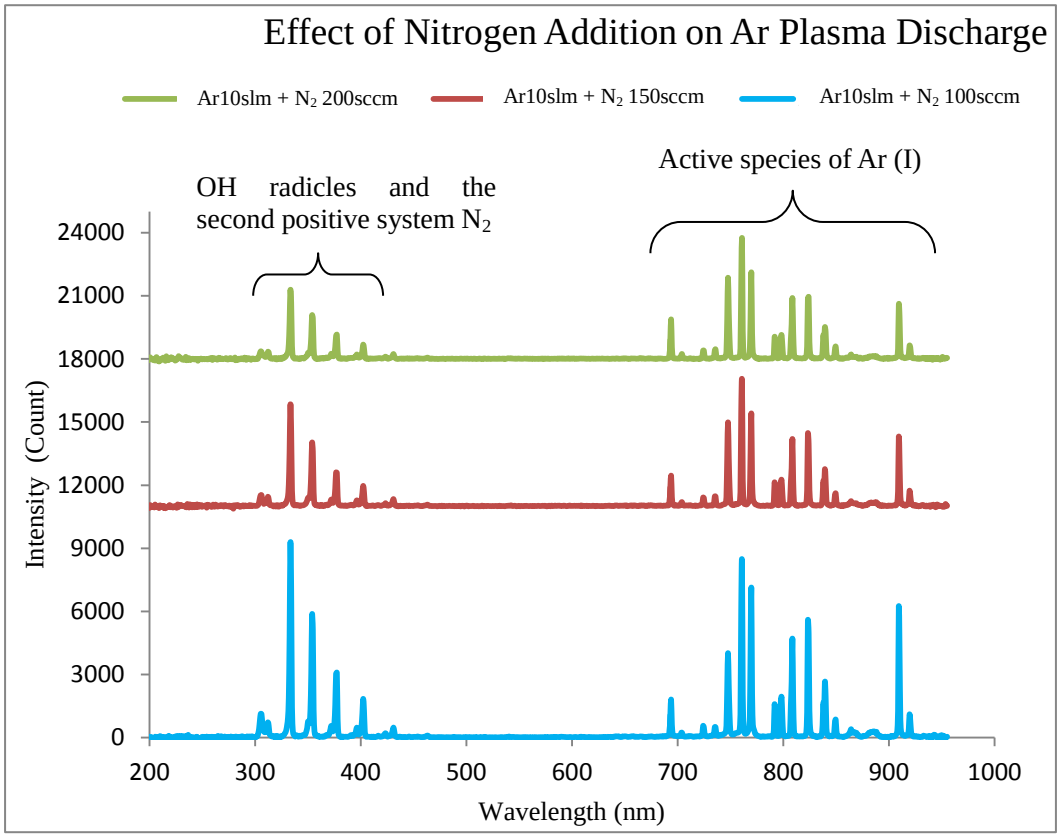

Figure 2.15 Comparison of different Optical emission spectra of Ar (10 slm) with different volumes of N_2 (100, 150 and 200 sccm) plasma jets generated by high sinusoidal voltage (V_{pp} 20 kV) at the frequency of 30 kHz. The optical fiber probe was kept 0.5 cm below and 1.5 cm away from the mouth of the plasma torch to capture the spectra of plasma emission.

With the addition of N_2 gas (additive gas) to the feeding gas (Ar gas), the emission intensities of Ar active species suppressed, but on the other hand the emission intensities for N_2 active species (N_2 ($C^3\prod_u$ — $B^3\prod_g$)) became quite abundant as shown in Figure 2.13. Initially, with the increase in the volume of N_2 gas, emission intensity of N_2 gas increases and the emission intensity of Ar active species decreases but later on with the increase in the volume of N_2 gas, the emission intensities of

both active species of Ar and N_2 gas decrease because initially even after quenching there were enough metastables to create active species of N_2 gas but later on there were not enough Ar-metastbles to create active species of N_2 gas as shown in Figure 2.14. In Figure 2.14, we captured the optical spectra for three different gas combinations. In each case, we had 10 slm of Ar gas (working gas) and 100 sccm, 150 sccm and 200 sccm of N_2 gas (additive gas). For stabilized plasma discharge, we got the highest emission peak intensities for Ar and N_2, when we had 10 slm of Ar gas (primary gas) and 100 sccm of N_2 gas (additive gas). So, we decided to use this combination of gases to generate plasma to use for bacterial inactivation.

Species	λ (nm)	Transition
N_2 second positive system	337.13	$C^3\prod_u \rightarrow B^3\prod_g$
	357.63	$C^3\prod_u \rightarrow B^3\prod_g$
	380.27	$C^3\prod_u \rightarrow B^3\prod_g$
	406.07	$C^3\prod_u \rightarrow B^3\prod_g$
OH	308.90	$A^2\Sigma^+ — X^2\prod$

Table 1: Summary of the some prominent active species of N_2 and OH species (wavelength range of 308– 426 nm) detected in Ar- N_2 plasma discharge.

Species	λ (nm)	Energy (eV) Upper level	Energy (eV) Lower level	Transition
Ar(I)	696.543	13.32	11.54	4p → 4s
	750.38	13.47	11.82	4p → 4s
	763.51	13.17	11.54	4p → 4s
	772.42	13.32	11.72	4p → 4s
	794.81	13.28	11.72	4p → 4s
	801.47	13.09	11.54	4p → 4s
	811.53	13.07	11.54	4p → 4s
	826.45	13.32	11.82	4p → 4s
	840.82	13.30	11.82	4p → 4s
	842.46	13.09	11.62	4p → 4s
	912.29	12.90	11.54	4p → 4s
	922.44	13.17	11.82	4p → 4s

Table 2: Summary of the prominent emission peaks for the active species of Ar atom detected in the plasma discharge in the range of 69 6nm to 923 nm of wavelength.

Penning ionization of N_2 molecules through the collisions with Ar metastables is not possible in CAPPLAT-9Ne for Ar plasma discharge because of its higher energy requirement (about 18.7 eV) and low electron density. That was why the first negative system of molecular nitrogen ion N_2^+ ($B^2\Sigma^+_u$ — $X^2\Sigma^+_g$) which is formed by penning ionization and accomplished with higher energy consumption (E ≈ 18.7 eV) was not observed [16]. The emission peaks for the second positive system of molecular nitrogen ion (N_2 ($C^3\prod_u$)) were observed. With the addition of N_2 gas, the emission peaks representing the second positive systems (N_2 ($C^3\prod_u$)) got prominent and the peaks

representing the argon meta-stables (Ar^m) got weaker which suggested that the energy of metastable Ar atoms transferred to the N_2 molecules to form second positive system of N_2 molecules. The energy of Ar metastable is about (E ≈ 11.5 to 11.8 eV) [13, table 1] which is close to the energy to the energy of N_2 molecules in the ground state (N_2 ($X^1\Sigma^+_g$)) (E ≈ 11.1) [14]. Therefore, a resonant reaction could easily occur between Ar metastables and ground-state molecular N_2 which explains the abundance of the N_2 second positive system (N_2 ($C^3\prod_u$ — $B^3\prod_g$)) emission peaks after the addition of N_2 gas. This whole process could be summarized by following transitions:

$$Ar^m + N_2(X^1\Sigma^+_g) \longrightarrow Ar^0 + N_2(C^3\prod_u)$$

$$N_2(C^3\prod_u) \longrightarrow N_2(B^3\prod_g) + h\nu$$

Before the addition of N_2 gas, argon metastables (A^m) were the main energy carriers in the Ar-plasma discharge but after the addition of N_2 gas to the feeding gas (Ar) this role was handed over to the second positive systems (N_2 ($C^3\prod_u$)) of nitrogen molecules.

2.4 Application of the Plasma Torch

This optically and electrically characterized CAPPLAT- 9Ne was used for plasma sterilization. *Bacillus* spores were collected form a 15 days old *Bacillus subtilis* culture. A spore suspension of about 1.0 X 10^7 to 4.0 X 10^7 endospores/ml was used to conduct all of the experiments. To ensure the presence of endospores, they were visually inspected under microscope (1000 times magnification) and were subjected to heat shock to kill the vegetative cells if there were any. For heat shock spores were kept in a water bath at 80˚C for 15 minutes. To check the total number of endospores, hemocytometer was used. The number of viable endospores was also checked by counting CFUs after serial dilutions. After plasma treatment the endospores were transferred to the nutritive agar medium. The colonies in the culture medium were counted after 18 hrs to check the inactivation of the endospores. The amount of released DPA (2, 6- pyridine dicarboxylic acid),

which is found only in the core of endospores, was also measured using Spectroflurophotometer to ensure the irreversible destruction of the endospores. DPA chelates with $TbCl_3$ to form a complex which gives a characteristic fluorescence. The emission peak intensity for the Terbium-DPA complex was measured as a function of plasma exposure time by measuring the emission peaks at 544 nm. The wave length of excitation radiation was 270 nm. Besides that SEM (Hitachi S-3000N, Scanning Electron Microscope) micrographs were also taken for visual inspection. We could completely inactivate a spore population of $1.0X10^7$ to $4.0X10^7$ endospores/ml in about 10 to 11 minutes. Unexposed to plasma bacteria are shown in Figure 2.16 and bacteria after the exposure of 5 minutes are shown in Figure 2.17. The effects of plasma on bacteria are discussed in detail in Chapter 4.

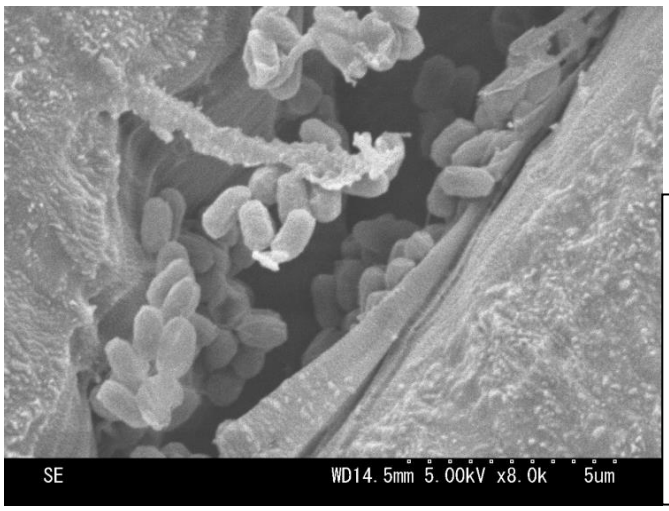

Figure 2.16 *Bacillus subtilis* Endospores without any exposure to the stabilized plasma jet

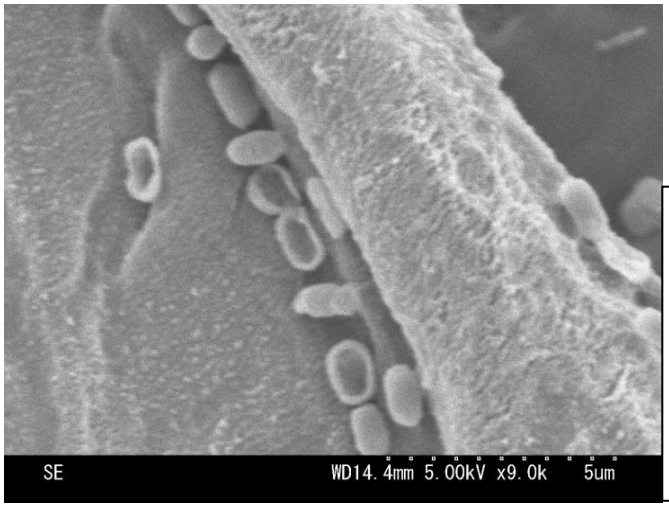

Figure 2.17 *Bacillus subtilis* Endospores after exposing to the stabilized plasma jet for 5 minutes.

2.5 Conclusions

In this study, we could stabilize and characterize a non-equilibrium plasma discharge at atmospheric pressure which was obtained in the form of a plasma jet. For this purpose we used our own designed plasma generating device named CAPPLAT-9Ne (Cold Atmospheric Pressure Plasma Torch-9Ne) and a hand-made torch. We studied the electrical and optical properties of plasma discharges in different experimental conditions by applying a high sinusoidal feeding voltage (V_{pp} 20 kV) at the frequency of 20 kHz. We also investigated the effects of the admixed gas N_2 on the properties of plasma discharge and analyzed our data for the characterization of the CAPPLAT-9Ne. We concluded that for CAPPLAT-9Ne, 100 sccm is the minimum amount of N_2 (additive gas) which is required for 10 slm of Ar gas (working gas) to achieve a stabilized plasma discharge. The additive gas (N_2) hardly affected the electrical properties of plasma discharge except a slight increase in the current after the addition of N_2 gas which could be due to the ionization of some of the N_2 molecules by highly energetic electronic collisions.

OES characterization exhibits that the main transition process for the excited Ar atoms is 4p-4s transition. Whereas the main transition process for active N_2 molecules is $C^3\prod_u \rightarrow B^3\prod_g$. After the addition of N_2 gas, the dominating emission intensity of the peaks representing the second positive system of the nitrogen molecules (N_2 $C^3\prod_u \rightarrow B^3\prod_g$) and the diminishing emission intensity of the peaks representing the active species of Ar gas suggest that the addition of N_2 gas (additive gas) into Ar gas (working gas) causes the quenching of Ar meta-stables by the formation of the second positive system of the nitrogen molecules (N_2 $C^3\prod_u \rightarrow B^3\prod_g$). In this quenching process the second positive system of the nitrogen molecules (N_2 $C^3\prod_u \rightarrow B^3\prod_g$) is the main energy transferring agent. When the amount of N_2 gas (additive gas) is further increased the emission intensities of Ar meta-stables and the second positive system of the nitrogen molecules (N_2 $C^3\prod_u \rightarrow$

$B^3\prod_g$) both decrease because of the absence of enough meta-stables which affect the formation of the second positive system of the nitrogen molecules (N_2 $C^3\prod_u \rightarrow B^3\prod_g$) too.

To identify the practical importance of our stabilized plasma as a sterilization tool, endospores of *Bacillus subtilis* were treated for different durations and we could successfully deactivate endospores (1.0X10^4 to 4.0X10^4) in about 11 to 12 minutes.

2.6 References

[1] Park J, Henins I, Herrmann HW, and Selwyn GS. J. App.l Phys., 89:20, 2001.

[2] Kim YH, Cho YH, and Park, JK. Surf. and Coat Techn., 174-175:535, 2006.

[3] Massines F, Ségur P, Gherardi N, Khamphan C, and Ricard A. Surf. and Coat Techn., 174-175:8, 2003.

[4] Boulos MI, Fauchais P, and Pfender E. Thermal plasmas: Fundamental and Applications. Volume 1, plenum Press, New York, ISBN: 0-306-44607-3, 452, 1994.

[5] Fei Xiaomeng, Kuroda Shin-ichi, Kondo Yuki, Mori Tamio, and Hosoi Katsuhiko. Comparison of High-density Polyethylene Surface Treatment Using Two Types of Cold Atmospheric Pressure Ar Plasma Jets, 2010.

[6] http://www.cresur.com/

[7] Kanazawa S, Kogoma M, Moriwaki T, and Okazaki S. J. phys D; Appl. Phys., 21, 838, 1998.

[8] Kuwabara A, Kuroda S, and Kubota H. Plasma Sources Sci. Techn., 15:328, 2006.

[9] Kasih TP, Kuroda S, and Kubota H. (2006). Chem Vap Depos., 13:1, 2006.

[10] Kuwabara A, Kuroda S, and Kubota H. Plasma Sci Techn., 9:181, 2007.

[11] Kuwabara A, Kuroda S, and Kubota H. Plasma Chem Plasma Process, 28:263,

2008.

[12] Yu QS, and Yasuda HK. Plasma Chem Plasma Process, 18:461, 1998.

[13] García MC, Varo M, and Martínez P.. Plasma Chem Plasma Process, 30:241, 2010.

[14] Yu QS, and Yasuda HK. Plasma Chem Plasma Process, 18:46, 1998.

[15] Tendro Claire, Tixier Christelle, Tristant Pascal, Desmaison Jean, and Leprince Philippe. Spectrochimica Acta Part B 61, 2005.

[16] Jackson GP and King FL. Spectrochim Acta B 58:185, 2003.

[17] Chirokov A, Gutsol A, and Fridman A. Atmospheric pressure plasma of dielectric barrier discharges. *Pure and Applied Chemistry*, 77(2), pp.487–495, 2005.

[18] Brauer I, Punset C, Purwins HG, and Boeuf JP. *J. Appl. Phys.* 85 (11), 7569–7572, 1999.

[19] Müller I, Punset C, Ammelt E, Purwins HG, and Boeuf JP. *IEEE Trans. Plasma Sci.* 27, 20, 1999.

[20] Kogelschatz U. Plasma Science, IEEE Transactions, 30 (4), pp. 1400 - 1408, 2002.

Chapter 3

Electrical and Optical Characterization of Cold Atmospheric Pressure Plasma Torch (CAPPLAT) the Basic Unit and the Effects of Addition of N_2 Gas, O_2 Gas and H_2O_2 on Argon Plasma Jet

3.1 Introduction

In Chapter 2, we discussed CAPPLAT–9Ne. In this chapter we will be discussing the basic unit of cold atmospheric pressure plasma torch (CAPPLAT). This CAPPLAT (Figure 3.1) was also manufactured by Cresur Corporation of Japan [1].

In the past cold atmospheric plasmas were produced at low pressure (10^{-4} to 10^{-2} kPa.), which has already been explained in Chapter 1 in detail. CAPPLAT (cold atmospheric pressure plasma torch) as its name shows, it is a non-LTE, cold plasma generating device but it is little bit different from the CAPPLAT–9Ne which has already been discussed in Chapter 2. CAPPLAT-9Ne, had high voltage AC power source whereas CAPPLAT the basic unit (or CAPPLAT) used a high voltage pulsed power source. CAPPLAT-9Ne had sinusoidal voltage of 20 kV whereas CAPPLAT the basic unit required an invariable voltage of 16 kV with square wave amplitude at a 50% duty cycle. The frequency for both CAPPLAT-9Ne and CAPPLAT the basic unit was 20 kHz. For both CAPPLATs, we used Ar as a primary or a working gas and N_2 as a secondary or the additive gas to attain a glow discharge or a stabilized plasma jet.. Both plasmas had almost the same range of the temperature (22°C to 35°C). The plasma jet from CAPPLAT the basic unit, has already been used for chemical vapor deposition and polymer surface treatment [2- 5] so this time, we tried to use it as a sterilization tool. For electric characterization we used a high voltage probe and a current probe. For optical characterization we used optical emission spectroscopy. Effects of addition of N_2 the

additive gas were also studied. N_2 was added directly into Ar the working gas whereas O_2 and H_2O_2 were added to the plasma through a capillary (direct injection mode). O_2 was added to the plasma jet alone whereas H_2O_2 was added to the plasma jet with the aid of a carrier gas (Ar gas). Then finally all different types of plasma were used for the inactivation of bacterial endospores which will be discussed in our next Chapter.

3.2 Experimental set up and methods

3.2.1 Plasma Device (Basic CAPPLAT)

We used CAPPLAT the basic unit (Figure 3.1) as a plasma generating device and a handmade torch (see Figure 2.2 for schematic representation and see Figure 2.4 for the torch) to generate non-equilibrium plasma discharge at atmospheric pressure.

Figure 3.1 CAPPLAT (Cold Atmospheric Pressure Plasma Torch). This is the basic unit.

This device is based on the principle of dielectric barrier surface discharge. The torch is comprised of two coaxial electrodes with a layer of dielectric barrier substance between them (see

Figure 2.3). The inner electrode was connected to high voltage pulsed power source of V_{pp}16 kV with square wave amplitude at a 50% duty cycle and a constant frequency of 20 kHz. The configuration of plasma torch and the experimental set up have already been explained in detail in Chapter 2 (2.2.1). Experimental set (Figure 3.2) up for CAPPLAT was very similar to that of the experimental set up for CAPPLAT - 9Ne with some minor changes. For plasma jet generation with CAPPLAT, 10 slm (standard liter per minute) of Ar gas and 300 sccm (standard cubic centimeter per minute) of N_2 were used to achieve a stabilized plasma discharge. We used 10 slm of Ar so that we could compare the effects with CAPPLAT - 9Ne. All of the flow rates were controlled by mass flow controllers. The mixture of Ar gas and N_2 gas was fed into the torch through the inlet tube. We fed O_2 (500sccm) through the capillary inserted into the hollow inner electrode to the plasma jet directly (see 2 in Figure 3.2).

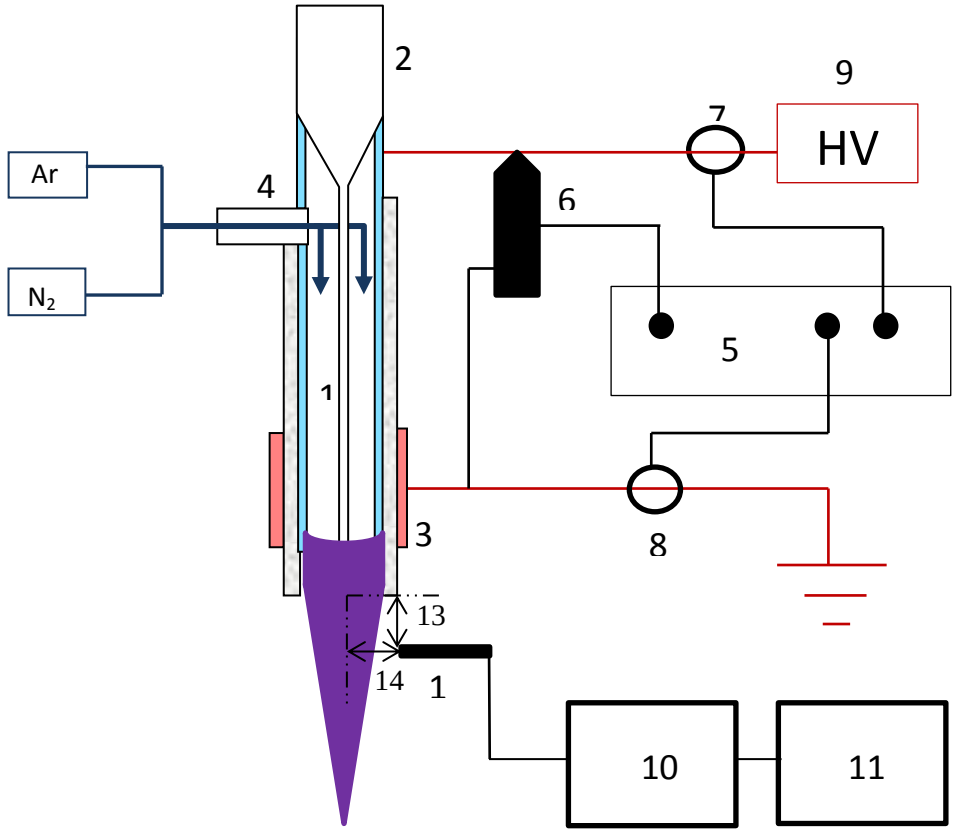

Figure 3.2 Experimental set up for electrical and optical measurements for Ar-N_2 plasma jet 1: Capillary; 2: Inner electrode; 3: Outer electrode; 4: Inlet for the mixture of Ar and N2; 5: Oscilloscope; 6: High- voltage probe; 7&8: Current probes; 9: High voltage pulsed power; 10: Optical emission spectroscopy; 11: Personal computer; 12: Optical fiber; 13 & 14: Vertical (0.5 cm) and horizontal (1 cm) distances of the optical fiber from the mouth of the torch

For the direct injection of H_2O_2 into plasma jet bubbling method was adopted. For bubbling 150 sccm of Ar gas was used as a carrier gas.

3.2.2 Electrical Measurements

The high-voltage pulsed power (V_{pp} 16 kV) with the frequency of 20 kHz, applied to achieve the plasma discharge which was measured using a 1000:1 high-voltage probe (Tektronix P6015A). The voltage probe was attached to the inner electrode of the plasma torch. The current was monitored using a wide band current monitor (PearsonTM current monitor) manufactured by Pearson Electronics Inc., Palo Alto, California, U.S.A.. The cable was passed through the wide band current monitor to monitor current. The waveforms for the total current and capacitive current were captured, so that the discharge current could be calculated. A digital phosphor oscilloscope (Tektronix TDS3012C) was inserted into the circuit to record the waveforms of voltage and current. The setup for electrical measurements is shown in (Figure 3.2).

3.2.3 Optical Emission Spectroscopic Measurements

The optical emission spectra of plasmas were collected using Multiband Plasma–process Monitor (MPM, Hamamatsu Photonics C7460). The spectral range was 200 nm to 950 nm with the wavelength resolution of < 2nm FWHM (full width at half-maximum). The optical fiber probe was kept 0.5 cm below and 1.0 cm away from the mouth of the plasma torch to capture the spectra of plasma emission. Monitoring and acquisition of data was carried out by a personal computer, connected to optical emission spectroscopy (Figure 3.2).

3.2.4 Addition of Gases to the Plasma Jet (Direct Injection Mode)

Different volumes of N_2 gas (additive gas) were added to the Ar gas (working gas) as shown in Figure 3.2. O_2 gas (500 sccm) was added to the plasma jet in a direct injection mode (Figure 3.3) through a capillary (Figure 3.3) passing through the hollow inner electrode (Figure 3.3). N_2 was mixed in to working gas (Ar) but there was no mixing of O_2 into the mixture of Ar and N_2.

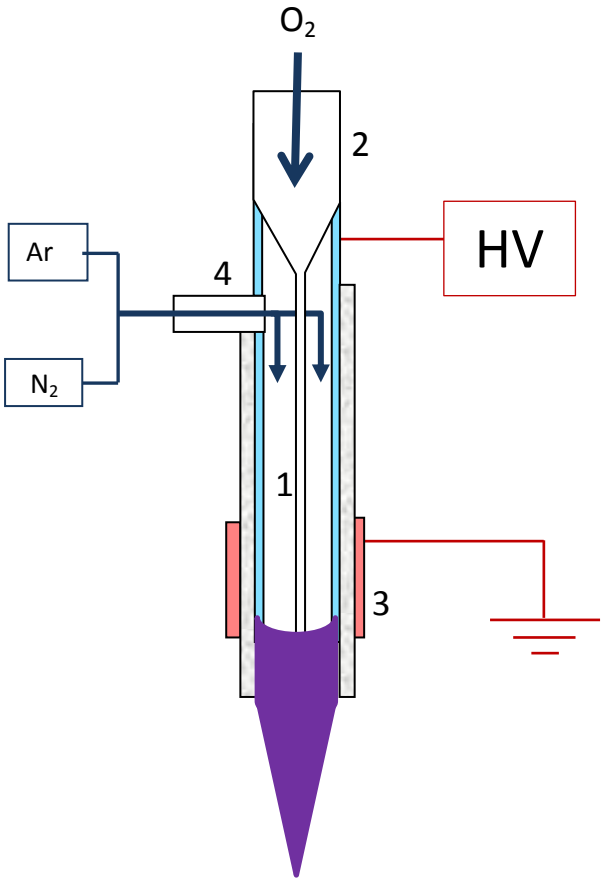

Figure 3.3 Experimental set up for direct O_2 addition to the Ar-N_2 plasma jet 1; 2; 3; & 4 refer to Figure 3.2

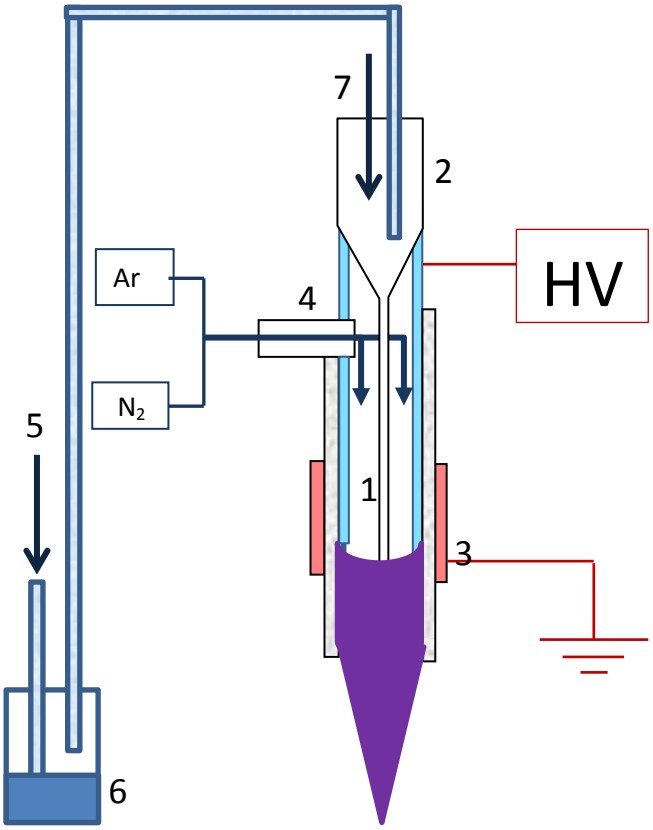

Figure 3.4 Experimental set up for direct H_2O_2 addition to the Ar-N_2 plasma jet 1; 2; 3; & 4 refer to Figure 3.2; 5: Ar gas; 6: H_2O_2; 7: H_2O_2 vapor carried by Ar gas to the plasma jet

H_2O_2 was also added in the same way as we added O_2 i.e. direct injection mode the but H_2O_2 was added to the plasma jet through bubbling method and Ar gas was used as a carrier gas (Figure 3.4). H_2O_2 easily disintegrates into H_2O and O_2 that is why after every 20 minutes, we used fresh H_2O_2 to add to the plasma jet through bubbling. For H_2O_2 addition, first Ar gas (5 of Figure 3.4) was being passed through the H_2O_2 (6 of Figure 3.4). Lots of bubbles were formed then the Ar loaded with H_2O_2 vapor was taken to the plasma jet (7 of Figure 3.4)

3.2.5 Effect of the Plasma Jet from CAPPLAT on the Viability of Endospores

Revival of culture, collection of endospores then the preparation of agar disc, medium and other buffers, solutions, plasma exposure, collection of plasma treated spores, estimation of DPA and colony counting etc. will be explained in detail in Chapter 4. Just like CAPPLAT - 9Ne, spores were treated with plasma for different durations and after treatment colonies were counted. The number of viable CFUs was plotted as the function of the time of plasma exposure. The decimal reduction time because of plasma exposure (D_P value), the time of exposure to reduce D_P value by one log cycle (Z_P) and the time required to kill the whole population of spores (F_P) at SATP (Standard Ambient Temperature and Pressure which refers to 25°C (298.15 K) and pressure of 101. 325 kPa) were calculated.

3.3 Results and Discussion

3.3.1.1 Electrical Characterization of Ar Plasma Jet Obtained from CAPPLAT and the Effect of N_2 Addition

Normally, in dielectric barrier discharges, electrodes are separated by a distance of few millimeters to ensure the stable plasma ignition [6] but our plasma torch is based on dielectric barrier discharge principal. There is no space between electrode and dielectric barrier so we need not to consider the sheath effect also. Depending on working gas composition, voltage and frequency of excitation, the discharge can be filamentary or glow [7, 8]. Dielectric barrier limits the discharge current and distributes the steamers randomly on the electrode surface in order to achieve

homogeneous discharge. Figure 3.5 shows the wave forms for nominal applied voltage (black line) and total current (pink line). The nominal applied voltage was 16 kV (peak to peak) but the voltage according to the waveform, shown in Figure 3.5, is about 14.5 kV (peak to peak). The drop in potential is because of the ionization of the gases and subsequent charge accumulation. The waveform also shows the square wave form of the voltage with 50% duty cycle. The current from peak to peak in the circuit is about 0.8 A.

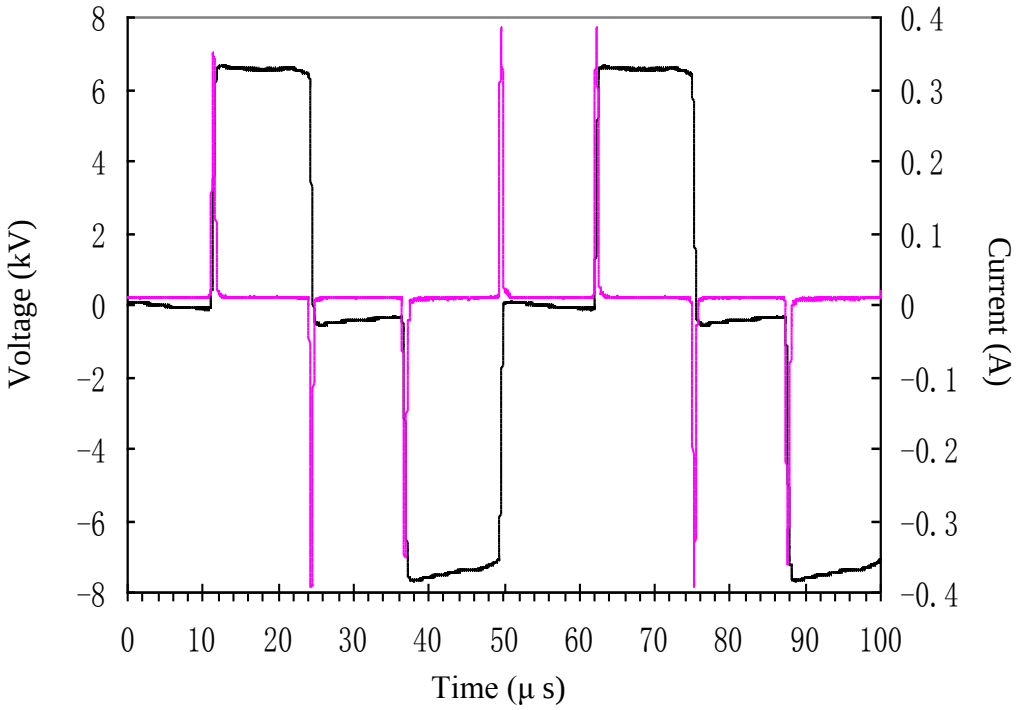

Figure 3.5 Typical waveform of applied nominal voltage V_{pp} 16 kV (black line) voltage and the total current (pink line); Ar (10 slm) and N2 (300 sccm)

.

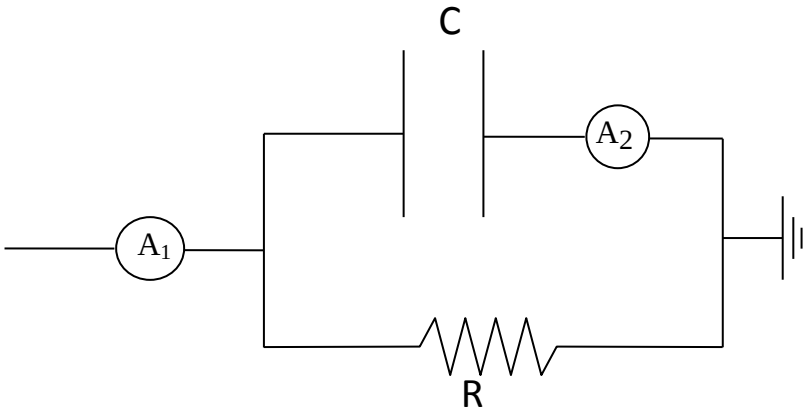

Figure 3.6 an equivalent circuit model for surface dielectric barrier discharge A_1 measures the total current; A2 measures the capacitive current; C: capacitor; R: resistance

Generally, electrical measurements allow the determination of the impedance of the entire load rather than the impedance of the plasma only. To evaluate the characteristics of the plasma jet, we can consider our circuit equivalent to an *R*-*C* parallel circuit [9-11] as shown in Figure 3.6. According to the circuit, *C* is the capacitance of the dielectric barrier between two electrodes and *R* is the resistance of the discharge. So, we can say the total current (A_1) will be the sum of the capacitive current (A_2) and the discharge current. So, the discharge current can be calculated as (A_1- A_2).

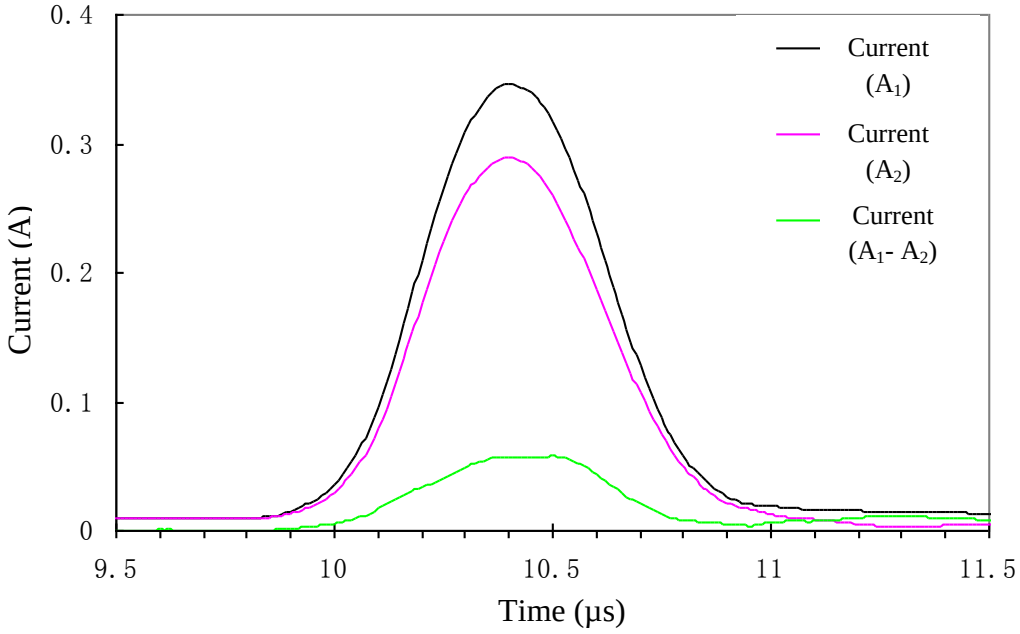

Figure 3.7 Waveform of total current (current A_1), capacitive current (Current A $_2$) and discharge current (A_1-A_2)

Total current was measured by connecting the current probe to the inner electrode and the capacitive current was measured by connecting the current probe to the grounded electrode. Figure 3.7 shows all the three currents according to the Figure 3.7, the discharge current is about 60 mA and the pulse width is about 1 μs. Current pulses due to microdischarges were also not observed [12] which is the indication of glow like (homogeneous) discharge. The filamentary plasma discharge has spiky current waveform. The spikes show the presence of microdischarges. Microdischarges are tiny individual breakdown channel which are formed by charge accumulation at certain points (memory effect). Formation of microdischarges has already explained in chapter 1.

The microdischarges are like weakly ionized transient plasma discharges. These short lived plasma discharge currents are the small spikes of spiky current waveforms of filamentary discharges.

We could successfully, produce glow plasma discharge with this CAPPLAT. To Produce glow discharge with both CAPPALT – 9Ne and CAPPLAT we added N_2 gas (additive gas) into Ar (working gas). For glow discharge pre-ionization electron density should be high enough to cause overlap and coalescence of primary avalanche heads to make the charge distribution smoother. Above discussion explains the importance of low frequency (1 kHz to 100 kHz), high voltage [13] and short pulse duration for glow discharge [6]. Our plasma producing device also satisfied these conditions.

To quench extra metastables, in order to get glow discharge, we added N_2 gas into Ar gas in both CAPPLATs. In case of CAPPLAT-9Ne, we added just 100 sccm of N_2 gas (additive gas) into 10 slm of Ar gas (working gas) whereas we had to add 300 sccm of N_2 gas (additive gas) into 10 slm of Ar gas (working gas). In both cases, we compared the total current before the addition of N_2 gas with the total current after the addition of N_2 gas. Figure 3.8 shows the comparison for CAPPLAT the basic unit and Figure 2.11 (Chapter 2) shows the comparison for CAPPLAT – 9Ne. Although the current didn't change a lot but in case of CAPPLAT– 9Ne, there was a slight increase in total current after the addition of N_2 whereas (Figure 2.11), in case of CAPPLAT the basic unit, there was a slight decrease in total current (Figure 3.8). Besides current, different amounts of N_2 gas (additive gas) were used with the same amount of Ar gas (10 slm) which also indicated two different Mechanisms for CAPPLAT–9Ne and CAPPLAT the basic unit to achieve glow discharge.

The glow mode of DBD could be uniform or filamentary. In case of DBD glow discharge the filaments are formed because of avalanches rather than streamers. In glow discharge filaments are initiated by Townsend ionization whereas filamentary dielectric barrier discharge is because of streamer breakdown [16, 17]. Actually, the glow discharge with the CAPPLAT–9Ne, was filamentary glow discharge, which has already explained in chapter 2, whereas the glow discharge

with the CAPPLAT the basic unit, was diffuse glow discharge (see Figure 2.12). In case of CAPPLAT – 9Ne, because of higher voltage, we had higher ionization electron density which caused the pulsed avalanche discharge. In pulsed avalanche discharge, we needed higher number of avalanches so that the primary heads of all of the avalanches could overlap and coalescence to have a volume-stabilized glow discharge. Because of the requirement of higher number of avalanches (higher preionization electron density), we needed less amount of N_2 to stabilize the plasma.

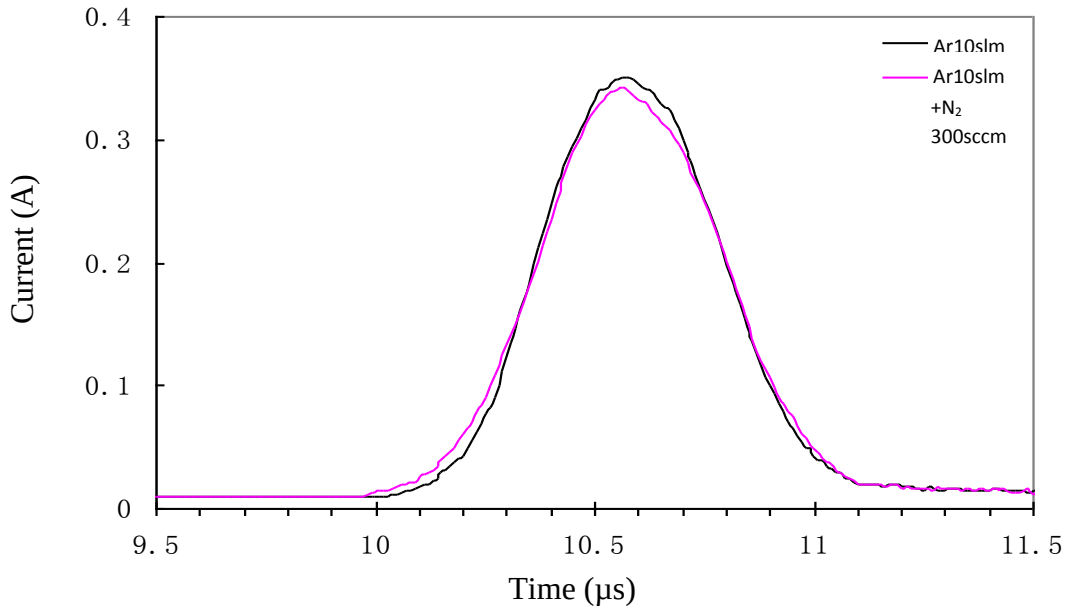

Figure 3.8 Comparison of waveforms of total current in Ar (10 slm) discharge before addition of N_2 (black line) and the total current after addition of N_2 (300sccm) shown by pink line, during polarity change

Most probably the higher electron density was responsible for the slight increase in the current after the addition of N_2 gas into Ar gas. For the diffuse glow discharge from the CAPPLAT, as Tepper et al. [18] demonstrated, dielectrics are capable of accumulating appreciable amounts of charges on the surface. Supported by the applied voltage the charges are trapped uniformly on the surface. When the electric field changes its polarity and exceeds a certain threshold value, the charge carriers are expelled spontaneously from the surface and initiate a homogeneous discharge. Obviously, we required less electron density and less pre ionization and subsequently less avalanches for diffuse glow discharge. That is why we needed higher quenching or higher volume

of N_2 gas the additive gas for the same volume of Ar gas (10 slm) and lower electron density or higher quenching caused slight decrease in the total current after the addition of N_2 gas.

3.3.1.2 Effect of O_2 and H_2O_2 Additions on the Electrical Characterization of Ar-N_2 Plasma Jet Obtained from CAPPLAT

Addition of O_2 or H_2O_2 to Ar-N_2 plasma didn't bring any changes in the electrical properties of the plasma discharge (Figure 3.9 and Figure 3.10).

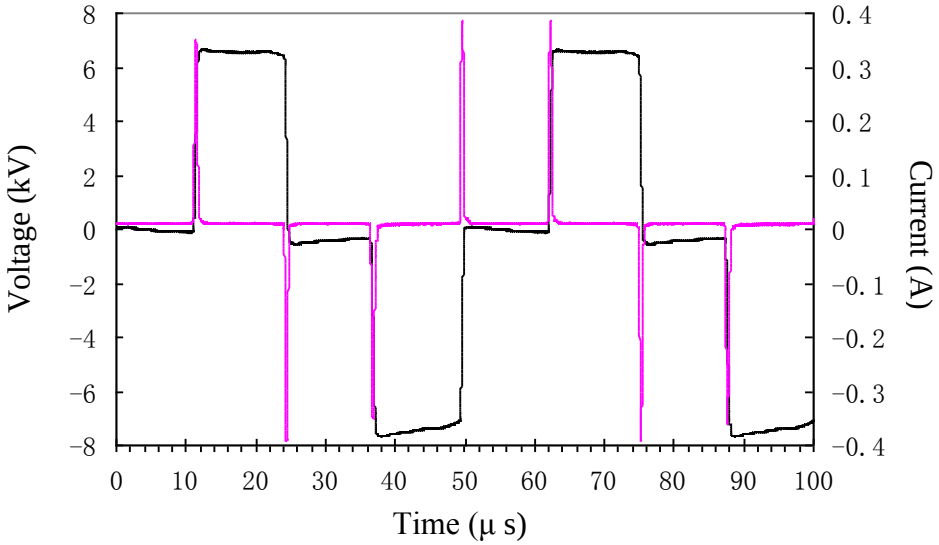

Figure 3.9 Typical waveform of applied nominal voltage V_{pp} 16 kV (black line) voltage and the total current (pink line; Ar (10 slm) + N_2 (300 sccm) + O_2 (500 sccm)

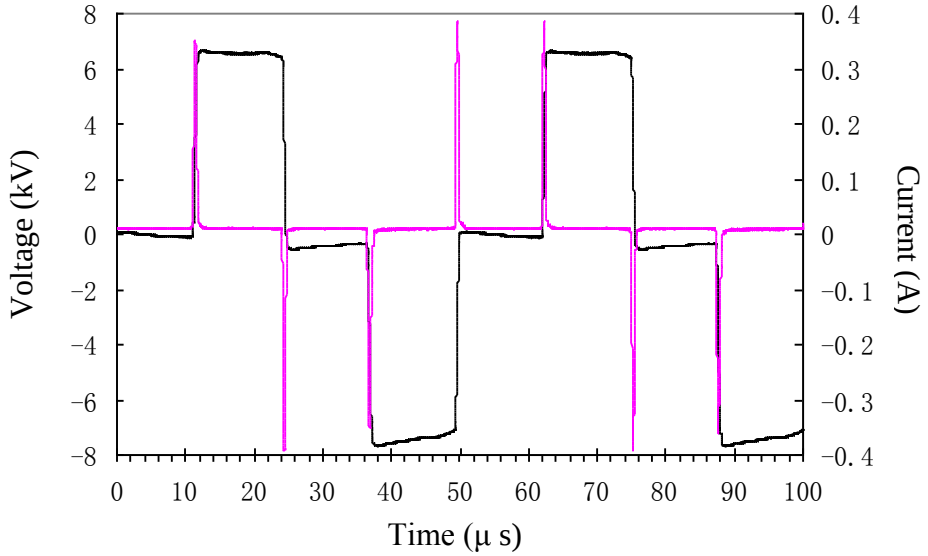

Figure 3.10Typical waveform of applied nominal voltage V_{pp} 16 kV (black line) voltage and the total current (pink line; Ar (10 slm) + N_2 (300 sccm) + Ar (150 sccm) carried the vapor of H_2O_2 to the plasma jet through the capillary

Actually, in both cases, we added O_2 or H_2O_2 through the capillary into the plasma jet directly.

Because of the addition of the additives in the remote plasma not into the active plasma, didn't change the waveforms for the current and voltage.

3.3.2.1 OES Characterization of Ar Plasma Jet and the Effects of N_2 Addition

The optical emission spectrum of the Ar plasma discharge in the wavelength range of 200 nm – 950 nm is shown in Figure 3.11. All of the emission peaks for Ar atoms lie in the range from 696 nm to 922 nm [14, 15]. Almost all of the prominent peaks represented 4p-4s transition. The smaller emission peaks at the wavelengths of 337.13nm, 357.63nm, 380.27nm, 406.07nm belonging to the N_2 second positive system (N_2 ($C^3\prod_u$ — $B^3\prod_g$)) were also observed besides these emission peaks a prominent emission peak at 308 nm representing OH radicles ($A^2\Sigma^+$ — $X^2\prod$) was also observed.

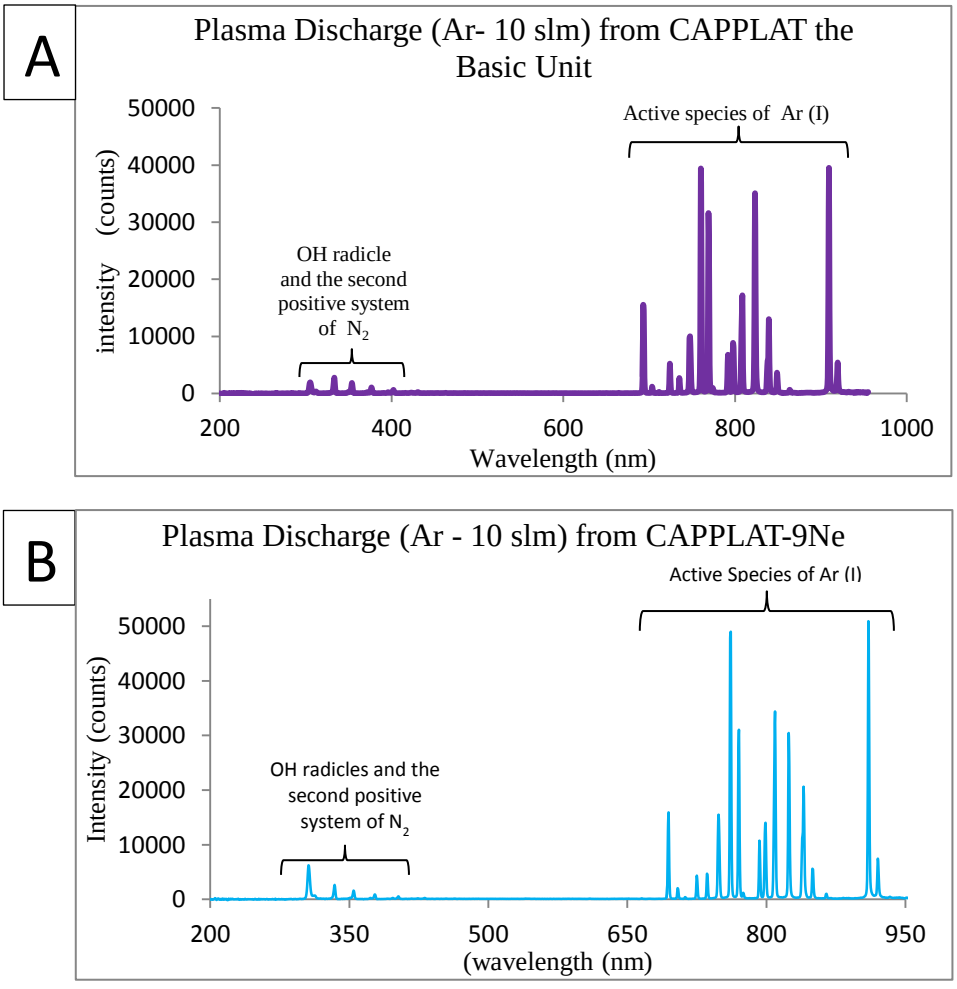

Figure 3.11 Glow discharges for both CAPPLATs: (A) CAPPLAT the basic unit Optical emission spectrum of Ar (10 slm) plasma jet generated by a pulsed voltage (Vpp 16 kV) at the frequency of 20 kHz with 50% duty cycle. (B) CAPPLAT – 9Ne Optical emission spectrum of Ar (10 slm) plasma jet generated by a sinusoidal voltage (Vpp 20 kV) at the frequency of 20 kHz.

All of the optical emission spectra show the same peak which shows that both of the CAPPLATs follow the same mechanism to make active species and make the same kind of the species which has already explained in detail in Chapter 2. The information about the peaks is summarized in Table 1 & 2, are also given in Chapter 2. Plasma discharges for Ar only with both CAPPLATs are given in Figure 3.11: A, shows the optical emission spectra for CAPPLAT the basic unit and B shows the optical emission spectra for CAPPLAT – 9 Ne.

Comparison of spectra A and B (Figure 3.11) shows that higher the voltage, higher is the intensity of active species. To achieve glow discharge with CAPPLAT - 9 Ne, we needed 100 sccm of N_2 gas for 10 slm of Ar with the CAPPLAT we required 300 sccm of N_2 gas for 10 slm of Ar gas.

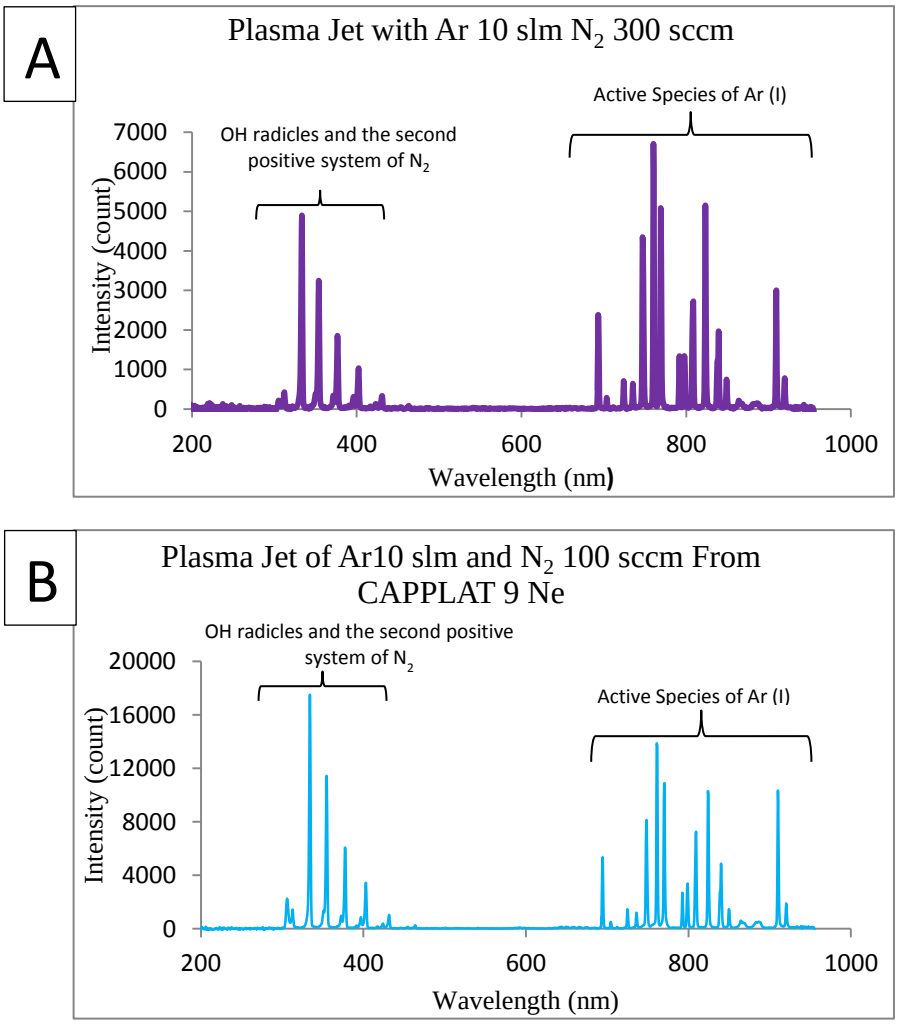

Figure 3.12 Glow discharges for both CAPPLATs: (A) CAPPLAT the basic unit Optical emission spectrum of Ar (10 slm) and N2 300 sccm plasma jet generated by pulsed voltage (V_{pp} 16 kV) at the frequency of 20 kHz with 50% duty cycle. (B) CAPPLAT- 9Ne Optical emission spectrum of Ar (10 slm) and 100 sccm plasma jet generated by a sinusoidal voltage (V_{pp} 20 kV) at the frequency of 20 kHz.

We needed different volumes of N_2 gas to the feeding gas, we got homogeneous discharge, and it has also been explained with electrical characterization. The emission intensities of Ar active species suppressed but on the other hand the emission intensities for N_2 active species (N_2 ($C^3\prod_u$ — $B^3\prod_g$) enhanced as shown in Figure 3.12: A, shows the spectra for CAPPLAT and B, shows the spectra for CAPPLAT- 9Ne, it has also been explained in Chapter 2. Formation of different active species has also been explained in Chapter 2.

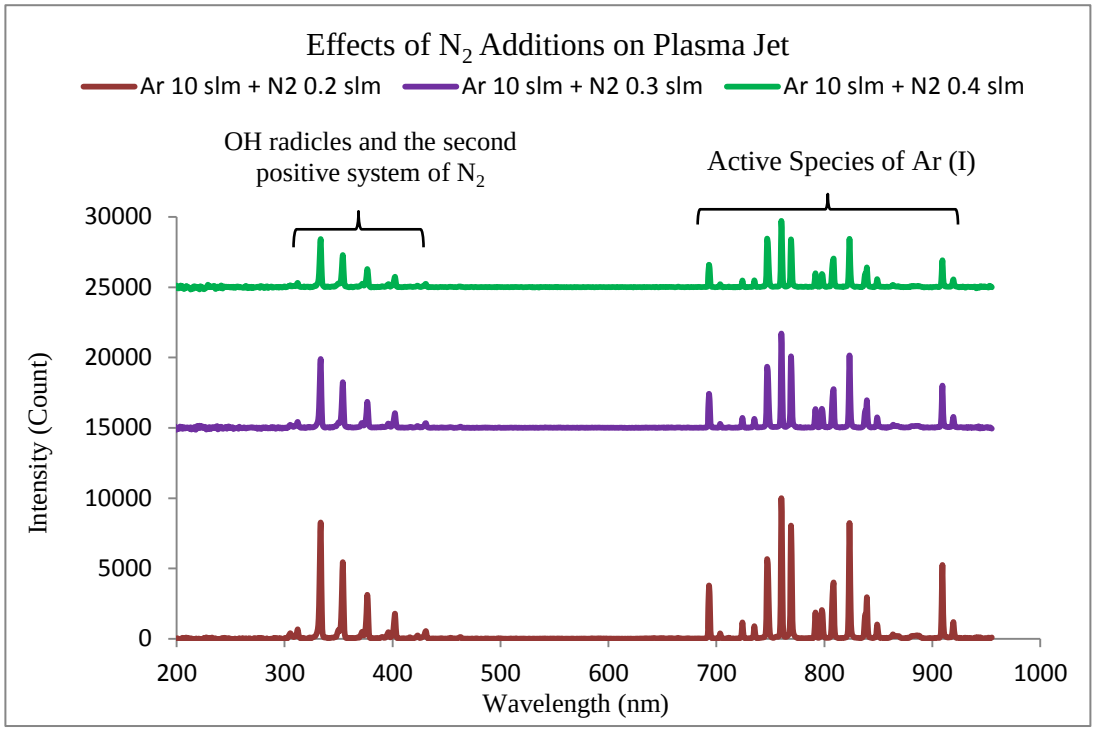

Figure 3.13 Comparison of different optical emission spectra of Ar (10 slm) with different volumes of N_2 (0.2, 0.3, and 0.4 slm) plasma jets generated by a nominal applied voltage (V_{pp} 16 kV) at the frequency of 20 kHz with 50% duty cycle. The optical fiber probe was kept 0.5 mm below and 1.0 mm away from the mouth of the plasma torch to capture the spectra of plasma emission.

3.3.2.2 Effect of the Addition of O_2 & H_2O_2 on the OES Characterization of Ar-N_2 Plasma Jet

If we compare Figure 3.14 and 3.15 with Figure 3.12, there are no changes in the number of emission peaks, after adding O_2 and H_2O_2. It is because of the addition of the additives into afterglow plasma zone through a capillary. There was slight decrease in the intensity of the emission peaks representing the second positive system of N_2 (Figure 3.14) only when O_2 was added and there was slight decrease in the intensity of all of the emission peaks of Ar (I), and the second

positive system of N_2 (Figure 3.15) H_2O_2 was added.

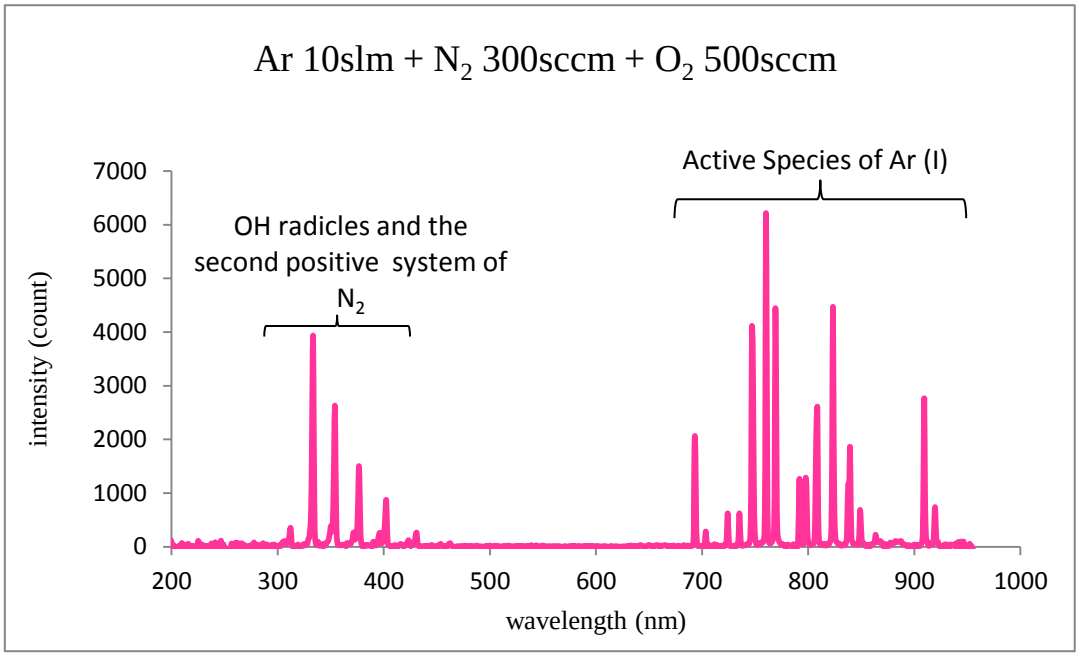

Figure 3.14 Optical emission spectrum of Ar (10 slm); N_2 300 sccm: O_2 500 sccm; plasma jet generated by pulsed voltage (Vpp 16 kV) at the frequency of 20 kHz.

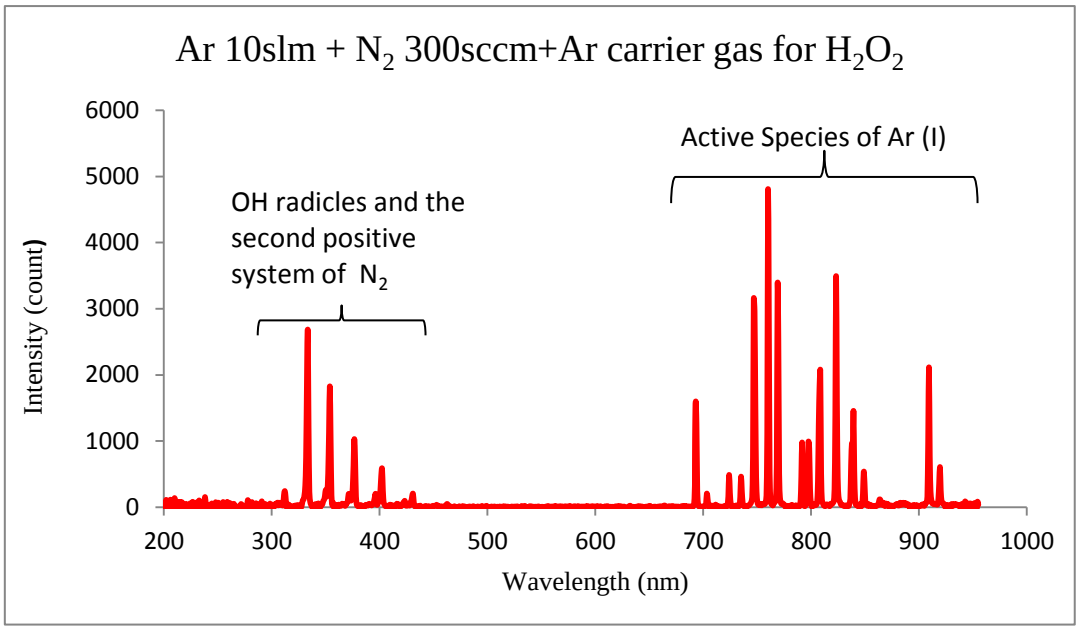

Figure 3.15 Optical emission spectrum of Ar (10 slm); N_2 300 sccm: H_2O_2 vapor carried by 150 sccm of Ar gas as a carrier gas; plasma jet generated by pulsed voltage (Vpp 16 kV) at the frequency of 20 kHz.

In the afterglow zone, there are no charged species so the Ar metastables and the second positive systems of N_2 (N_2 ($C^3\prod_u$ — $B^3\prod_g$) are responsible for the new active species. It was

reported that the most probable channel for the formation of O atoms was through collisions between the oxygen molecular ions (O_2^+) and electrons [19]. Oxygen molecular ions (O_2^+) formation is not possible because it needs higher energy (E ≈ 18.2 eV) for penning ionization which is higher than the energy of Ar metastables' energy (E ≈ 11.5 eV [20]. However oxygen atoms can probably be generated through the following channels in Ar discharge [20, 21-23]:

$$Ar^* + O_2 (X^3\Sigma^-_g) \rightarrow O (^1D) + O (^3P) + Ar^0 \quad (1)$$

$$e^* + O_2 (X^3\Sigma^-_g) \rightarrow e + [O (^1D) \text{ or } O (^1S)] + O (^3P) \quad (2)$$

$$e^* + O_2 (X^3\Sigma^-_g) \rightarrow 2e + O_2^+ (b^4\Sigma^-_g) \quad (3)$$

$$e^* + O_2^+ (b^4\Sigma^-_g) \rightarrow 2O (^3P) \quad (4)$$

Considering the electron density and the electron energy, reaction (1) is the only channel for the generation of O atoms in Ar plasma jet generated by CAPPLAT which can combine with other molecules or can easily make O_3 easily.

$$O + O_2 + M \longrightarrow O_3 + M \quad (5)$$

Where *M* could be O, O_2, or O_3, M is the third collision partner.

Both O and O_3 are very strong oxidizing agents. That is why addition of O_2 is very lethal but still we are not able to see any peaks.

The second positive system of nitrogen N_2^* can also lead to the formation of oxygen atoms by the following reactions [24]. Reaction 6, 7, and 8 explains the decrease in the intensity of the emission peaks of second positive system of nitrogen N_2^* as it happened in both cases when we added O_2 and H_2O_2

$$N_2^* + O_2 \longrightarrow N_2 + 2O \quad (6)$$

$$N_2^* + O_2 \longrightarrow N_2O + O \quad (7)$$

$$O + O_2 + M \longrightarrow O_3 + M \quad (8)$$

Addition of H_2O_2, further enhanced the sporocidal effects of the plasma jet. But we couldn't find any new peaks related to the O_2 or O atoms (Fig.14). OES spectra show that the Ar

metastables and the second positive systems of N_2 (N_2 ($C^3\prod_u$ — $B^3\prod_g$)) are responsible for the inactivation of the endospores but this jet was stronger than Ar- N_2 jet and Ar-N_2- O_2 jet. H_2O_2 is a very strong oxidizing agent itself and it further disintegrates very quickly which enhances its effect.

$$2H_2O_2 \longrightarrow 2\,H_2O + O_2 \quad \text{(ionization energy of -O-O- is 1.95 eV)}$$

$$2H_2O_2 + \text{e Impact} \longrightarrow OH^* + OH^* \quad \text{(Ionization energy is 2.2 eV)}$$

$$OH^* \longrightarrow O^* + H^* \quad \text{(Ionization energy is 4.4 eV)}$$

As above mentioned reactions show, the low ionization energy is needed for ionization, this energy can be supplied by Ar metastables (E ≈ 11.5 eV) [2], second positive systems of N_2 (E ≈ 11.8 eV) or some highly energetic electrons. The byproducts of H_2O_2 i.e. H_2O and O_2 further ionized to produce more free radicles which assist sterilization. The ionization energies of H_2O are in the range of 16.95 to 26.80 eV which is not possible for Ar metastables (E=11.5eV) to provide.

$$2\,H_2O_2 \longrightarrow 2\,H_2O + O_2 \quad \text{(ionization energy of -O-O- is 1.95 eV)}$$

The ionization energies of H_2O are in the range of 16.95 to 26.80 eV which is not possible for Ar metastables (E=11.5eV) or second positive systems of N_2 (E ≈ 11.8 eV) to provide.

$$H_2O + e \longrightarrow H^+ + OH + 2e \quad \text{(Not Possible)}$$

Water molecules' excitation energy is 7.5 eV. With the energy of by Ar metastables or second positive system of nitrogen molecules, lots of dissociative reactions are possible.

$$H_2O^* + H_2O^* \longrightarrow H_2O_2 + H_2 \quad \text{(E= 3.2 eV)}$$

$$H_2O^* + H \longrightarrow H_2 + OH \quad \text{(E=0.9 eV)}$$

$$H_2O^* + OH \longrightarrow H_2O_2 + H_2 \quad \text{(E=3.6 eV)}$$

$$H_2O + e \longrightarrow H^* + OH^* \text{ (dissociation energy is 5.1 eV)}$$

We had O_3 molecules in Ar-N_2-O_2 Plasma. Breathing ozone is known to cause chest pain, impair respiratory function, and damage lung tissue [25]. O_3 molecules can be dissociated by the byproducts of H_2O_2 and H_2O dissociation by the following reactions [26].

$$OH^* + O_3 \longrightarrow HO_2^* + O_2$$

$$H^* + O_3 \longrightarrow OH^* + O_2$$

$$HO_2^* + O_3 \longrightarrow OH^* + 2\,O_2$$

The increasing number of oxygen species with the addition of H_2O_2 to the plasma jet, explained, the further decrease in the intensity of the emission peaks representing the second positive system of nitrogen N_2^*. Increasing number of second positive system of nitrogen N_2^* affected the intensity of emission peaks of Ar metastable as explained in Chapter 2. Although the intensity of the peaks decreased with addition of the oxidants (O_2 and H_2O_2) but the sterilization effects of plasma jet was increased. So, it could be assumed that when the oxidants were added to the plasma jet then not only Ar metastables and the second positive system of nitrogen N_2^* but the other species formed because of Ar metastables and the second positive system of nitrogen N_2^* were also responsible for more efficient sterilization.

3.3.2.3 Effect of the Ar-N_2-O_2 Plasma Jet and Ar-N_2-H_2O_2 Plasma Jet on the Viability of *Bacillus subtilis* Endospores

Both plasma discharges had sporocidal property. We could inactivate spores successfully the endospores in both cases. The number of viable CFUs was plotted as the function of the time of plasma discharge exposure for both plasmas to see the effect of plasma exposure on the viability of the endospores. When we compared the effects of H_2O_2 and O_2, it was found that the Ar-N_2 plasma jet had enhanced sporocidal power when H_2O_2 or O_2 was added to the plasma jet but the effect was more pronounced in case of H_2O_2 than O_2.It will be explained in detail in Chapter 4.

3.4 Conclusion

CAPPLAT the basic unit and CAPPLT-9Ne, both can produce flow discharge. The glow discharge of CAPPLAT the basic unit was diffuse glow discharge and the glow discharge of CAPPLAT–9Ne was filamentary glow discharge because they were using different types of

voltages. CAPPLAT-9Ne had sinusoidal voltage of 20 kV whereas this CAPPLAT the basic unit worked on invariable voltage of 16 kV with square wave amplitude at a 50% duty cycle whereas CAPPLAT-9Ne had sinusoidal voltage of 20 kV although the frequency for both CAPPLAT-9Ne and CAPPLAT the basic unit was 20 kHz. To stabilize the plasma discharge, we added 300 sccm of N_2 into 10 slm of Ar in case of CAPPLAT the basic unit but CAPPLAT- 9Ne got stabilized plasma discharge with 100 sccm of N_2 and 10 slm of Ar. Both CAPPLATs have similar OES spectra but CAPPLAT the basic unit had less intense emission peaks than the CAPPLAT- 9 Ne. Both CAPPATs could be used for very effective sterilization but CAPPLAT- 9Ne was more effective then CAPPLAT the basic unit which shows that to inactivate endospores high voltage is preferable. Although we couldn't identify the new active species in plasma jet because of the addition of O_2 and H_2O_2 but there was a visible impact on the number of CFUs. We could inactivate bacteria with Ar and N_2, but the addition of O_2 and H_2O_2 enhanced the inactivation of endospores. Particularly, addition of H_2O_2 enhanced the bactericidal property the most.

3.5 References

[1] http://www.cresur.com/

[2] Kuwabara A, Kuroda S, and Kubota H. Plasma Sources Sci. Technol.15, 328, 2006.

[3] Kasih TP, Kuroda S, and Kubota H. Chem. Vap. Depos. 13, 1, 2007.

[4] Kuwabara A, Kuroda S, and Kubota H. Plasma Sci. Technol. 9, 181, 2007.

[5] Kuwabara A, Kuroda S, and Kubota H. Plasma Chem. Plasma Process. 28, 263, 2008.

[6] Tendro C, Tixier C, Tristant P, Desmaison, and Leprince P. Spectrochimica Acta Part B 61, 2005.

[7] Massines F, and Gouda G. A comparison of polypropylene-surface treatment by filamentary, homogeneous and glow discharges in helium at atmospheric pressure, J. Phys. D: Appl. Phys. 31 – 3411 – 3420, 1998.

[8] Yokoyama T, Kogoma M, Moriwaki T, and Okazaki S. The mechanism of the stabilisation of glow plasma at atmospheric pressure, J. Phys. D: Appl. Phys. 23- 1125–1128, 1990.

[9] Laimer J, and Stŏri H. Plasma Process. Polym. 3, 573, 2006.

[10] Laimer J, and Stŏri H. Plasma Process. Polym. 4, 266, 2007.

[11] Li HP, Sun WT, Wang HB, Li G, and Bao CY. Plasma Chem. Plasma Process. 27, 529, 2007.

[12] Wagner HE, Brandenburg R, Kozlov KV, Sonnenfeld A, Michel P, and Behnke JF. Vacuum 71, 417, 2003.

[13] Kogelschatz U. Fundamentals and applications of dielectric- barrier discharges. ABB Corporate Research Ltd., 2000.

[14] Yu QS, and Yasuda HK. Plasma Chem Plasma Process, 18:461, 1998.

[15] García MC, Varo M, and Martínez P. Plasma Chem Plasma Process, 30:241, 2010.

[16] Brauer I, Punset C, Purwins HG, and Boeuf JP. Appl. Phys. 85 (11), 7569–7572, 1999.

[17] Müller I, Punset C, Ammelt E, Purwins HG, Boeuf JP. IEEE Trans. Plasma Sci. 27, 20, 1999.

[18] Tepper J, Lindmayer M, and Salge J. Hakone VI, Cork, Ireland. 123-127, 1998.

[19] Léveillé V, and Coulombe *S.* (2006). Plasma Process. Polym. 3, 587, 2006.

[20] Yu QS, and Yasuda HK. Plasma Chem. Plasma Process. 18, 461, 1998.

[21] Lee C, Graves DB, Lieberman MN, and Hess DW. J. Electrochem. Soc. 141, 1546, 1994.

[22] Eliasson BU, and Kogelschatz U. “Basic Data for Modeling of Electrical Discharge in Gases: Oxygen’’, Research, Asea Brown Boveri Corporate, KLR-11C CH5405, 1986.

[23] Lee D, Park J, Hong SH, and Kim Y. IEEE Trans. Plasma Sci. 33, 949, 2005.

[24] Ahn HS, Hayashi N, Ihara S, and Yamabe C. Ozone generation characteristics by superimposed discharge in oxygen-fed ozonizer, Jpn.J. Appl. Phys.42-6578-6583, 2003.

[25] Sung Kil Kang, Myeong Yeol Choi, Il Gyo Koo, Paul Y Kim, Yoonsun Kim, Gon Jun Kim, Abdel-Aleam H. Mohamed, George J Collins, and Jae Koo Lee1. Applied Physics Letters 98, 143702, 2011.

[26] Soloshenko I A, Tsiolko V V, Khomich, V A, Bazhenov Yu. V, Ryabtsev A. V, Schedrin A I, and Mikhno I L. IEEE Trans. Plasma Sci. 30,1440, 2011 .

Chapter 4

Effects of Cold Atmospheric Pressure Plasma Torch (CAPPLAT- 9Ne) on the viability of *Bacillus subtilis* Endospores

4.1 Introduction

Bacteria are indispensable in our food-product industries and pharmaceuticals but on the other hand they cause a huge loss of money and lives. So, we often need sterilization to remove bacteria, infect all of the living things from a particular environment. But many gram positive bacteria like *Bacillus* and *Clostridium* in response to starvation form the most resilient type of cell, called endospore that can withstand extremes of heat, radiation, chemical assault and time [1, 2]. Their durability is even more remarkable, considering that dormant spores convert back to actively growing cells, through a process called germination, almost immediately after nutrients return to the environment [3]. Removal of endospores is always the biggest challenge for any sterilization methods. For all of their lethality and industrial values, the best studied spore forming bacteria with no special power other than the ability to be readily manipulated in the laboratory is *Bacillus subtilis* [4]. The information about different aspects of *Bacillus Subtilis* is used to understand other highly virulent bacteria like *Bacillus anthraces.* The process of spore formation follows essentially the same morphological sequences in all endospore forming organisms including the round shaped *Sporosarcina* species [5]. Sporulation involves asymmetric cell division i.e. closer to one cell pole rather than at mid cell, and during which a copy of the genome is partitioned into each of the sister cells [6, 7] and the smaller cell, or forespore develops into a mature spore and the larger cell or the mother cell, contributes to the differentiation process but undergoes autolysis following its

completion to release the endospore into the surrounding medium [8]. The process of sporulation has already been explained in detail in Chapter 1.

On germination along with lots of other changes spore losses its cortex and there is a huge leakage of DPA. DPA (Dipicolinic acid or Pyridine-2, 6- dicarboxylic acid) is exclusively found in the protoplast of an endospore and it constitutes about 5 to 15 % of the endospore's dry weight [9]. It is synthesized in the mother cell and subsequently transferred to the spore cell.

The development of wet heat resistance is closely related to the massive uptake of divalent cations Ca^{2+} ions and the synthesis of DPA in large amount. The role of DPA in dry heat sterilization is not very clear yet. Ca^{2+} ions and DPA are present in the molar ratio of 1:1 which indicates that Ca^{2+} ions chelate with DPA and form a complex Ca-DPA (calcium dipicolanate). For the fluorimetric quantification of DPA, Rosen et al introduced the terbium dipicolinate fluorescence method [10] which was further improved by Hindle and Hall for determination of nanomolar concentrations up to 2nM which correspond to 10^4 spores/ ml [11]. Estimation of DPA was performed to confirm the breakdown of the cortex which will assure the either germination or the release of genetic materials form protoplast. DPA has high binding affinity toTb^{3+} ions which gives a green luminescence under UV excitation at 270 nm. Inhibition of the bonding between Tb^{3+} ions and DPA by phosphate ions has also been reported whereas the addition of $AlCl_3$ can ameliorate the inhibition to a great extent.

Wet heat inactivation or use of harmful chemicals has detrimental effects on food products, heat sensitive medical equipment and some of the polymers. Post sterilization sanitation, particularly after using lethal chemicals, sterilization processing time and the inactivation of spores without disturbing the bulk properties of the substrate have been challenges. Plasma modifies only the surface of the substrate, as it penetrates only about 100 Å [12] from the surface without disturbing the bulk. The energy of active species is high enough to inactivate the spores and there is

no need to have post sterilization sanitation as the active species are very short lived and they exist as long as there is an external source of energy to ionize the gas or the mixture of gases.

4.2 Experimental Set up and Methods

4.2.1 Plasma Device and Electrical and Optical Emission Spectroscopic Measurements

We used, our indigenously designed and characterized, plasma generating device CAPPLT-9Ne (Cold Atmospheric Pressure Plasma Torch- Ne) and a hand-made plasma torch to generate non-equilibrium plasma at atmospheric pressure and a low temperature (22 to 35°C). The CAPPLAT-9Ne worked at a sinusoidal feeding voltage of V_{pp} 20 kV and a frequency of 20 kHz, manufactured by Cresur Corporation [13]. To generate the stabilized plasma discharge, we used 10 slm of Ar gas as a working gas and 100 sccm of N_2 gas as an additive gas for quenching in order to achieve a homogeneous plasma discharge. The details of the system's structure and characteristics have already been discussed in Chapter 2.

The high sinusoidal voltage (V_{pp} 20 kV), applied to achieve the plasma discharge, was measured using a 1000:1 high-voltage probe (Tektronix P6015A). The voltage probe was attached to the inner electrode of the plasma torch. The capacitive current was monitored using a wide band current monitor (Pearson TM current monitor). The cable connected to the outer electrode was passed through the wide band current monitor. A digital phosphor oscilloscope (Tektronix TDS3012C) was inserted into the circuit to record the waveforms of the voltage and current.

The optical emission spectra of plasmas were collected using Multiband Plasma–process Monitor (MPM, Hamamatsu Photonics C7460). The spectral range was 200 nm to 950 nm with the wavelength resolution of < 2nm FWHM (full width at half-maximum). The optical fiber probe was kept 0.5 mm below and 1.0 mm away from the mouth of the plasma torch to capture the plasma emission spectra for active species. All of the waveforms, OES spectra, mechanisms and effects of additive gas N_2 have already explained in Chapter 2.

4.2.2 Culture Conditions and Isolation of Endospores

To investigate the effects of homogeneous Ar-N_2 plasma discharge from CAPPLAT- 9Ne on bacterial endospores, *Bacillus subtilis subsp. Subtilis* culture (NBRC No. – NBRC 13719) was used. *Bacillus subtilis subsp. subtilis* culture obtained from NBRC (NITE Biological Research Center), where NITE stands for National Institute of Technology and Evaluation, was revived in a liquid broth. The composition of the liquid broth, for 1 liter water was; 10 g polypepton, 2 g yeast extract, 1 g $MgSO_4 \cdot 7H_2O$ at pH 7. The autoclaved medium was used. The Culture was allowed to grow for 24 hours. 100 µl of the freshly revived culture was inoculated by spreading over NAM (Nutritive Agar Medium) and let it incubated at 32°C for 15 days to assure complete depletion of nutrients from the culture medium. The chemical composition of NAM was - 10 g polypepton, 2 g yeast extract, 1 g $MgSO_4 \cdot 7\,H_2O$ and 15 g agar, dissolved in 1 liter water at pH 7. The autoclaved medium was used. The spores were collected from the 15 days old culture and centrifuged (Kubota 6800) at 10000 rpm at 4°C for 10 minutes, the supernatant was discarded and spores (pallet) were again washed with double distilled autoclaved water. Heat shock was given to the spore suspension for 10 minutes at 80°C to have the spore suspension free from any vegetative cells.

A

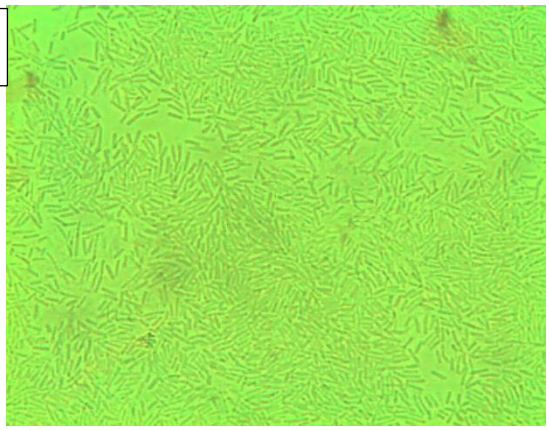

Figure 4.1 (A) *Bacillus subtilis subsp. Subtilis* (NBRC No. – NBRC 13719) as seen under the microscope (OLYMPUS CX41) after 24 hours of culture revival with the magnification of 1000 times

B

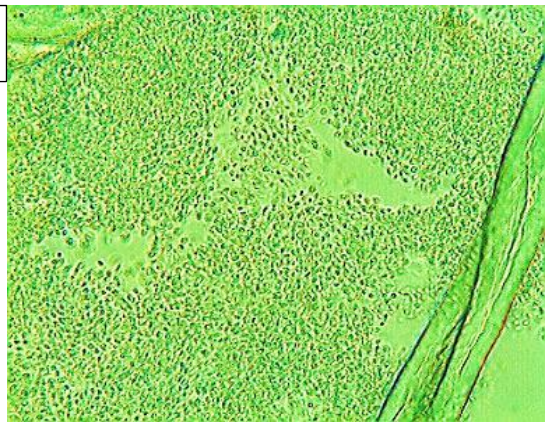

Figure 4.1 (B) *Bacillus subtilis subsp. Subtilis* (NBRC No. – NBRC 13719) endospores, as sheen under the microscope (OLYMPUS CX41) with the magnification of 1000 times (They were harvest from a 15 days old culture)

The spore sample was observed under microscope to ascertain the purity of the sample. Figure 4.1 (A) show 24 hours old freshly revived culture & Figure 4.2 (B) shows 15 days old culture. In 15 days, all of the nutrients were depleted as a result all of the living bacteria changed into endospores. Number of spores was adjusted to the 1.0 to $1.4X10^7$ spores/ml and counted by serial dilution method, using autoclaved physiological saline solution. The number of spores was also counted by hemocytometer too.

4.2.3 Air Dried Agar Disc for spores for Plasma Treatment

The spores were dried on an agar disc for plasma treatment. To prepare agar disc, autoclaved mixture of 0.64 g agar dissolved in 20 ml of deionized water, then it was poured into a sterilized petridish and let it dry at 60°C in a drier oven for 2 days. Small discs of about 2 to 2.5 cm in diameter were cut out from the dried film of agar obtained after two days of desiccation. 15 µl of spore suspension was dried on the agar disc for 2 hours at 35°C. These *Bacillus* spore inoculated agar discs were exposed to the stabilized plasma discharge for different durations from 1 minute to 15 minutes. The distance of the substrate from the mouth of the plasma torch was about 1 cm. After exposing to the stabilized plasma discharge (plasma jet) for different durations, discs were washed with 1.5 ml deionized water for 30 minutes in a vortex shaker to remove all of the spores or spore debris from the disc. This plasma treated spore suspension was used to check the viability of the spores by CFU (Colony Forming Unit) counting method and the amount of released DPA, after plasma treatment. For viability test, the spore suspensions were further diluted into several dilutions by serial dilution method and 100 µl of each dilution was inoculated and incubated for 24 hours before CFU counting. Autoclaved physiological saline was used for dilutions and the nutritive agar medium was used for all of the cultures. All experiments were conducted in triplicates and then the average of the data was used. The remaining spore suspensions were centrifuged to separate water soluble DPA (supernatant) from cellular debris (pallet) and then filtered to separate cellular debris and DPA. In some previous studies, spores were dried on filter paper or on glass plates. The high absorptive power of the tissue paper and the hydrophilic nature of the glass resulted into stalked

layers of endospores, as shown in Figure 4.2 (A). So we decided to use bacterial resistant dried agar discs because it was easy to spread spores much more evenly on the surface, as shown in Figure 4.2 (B).

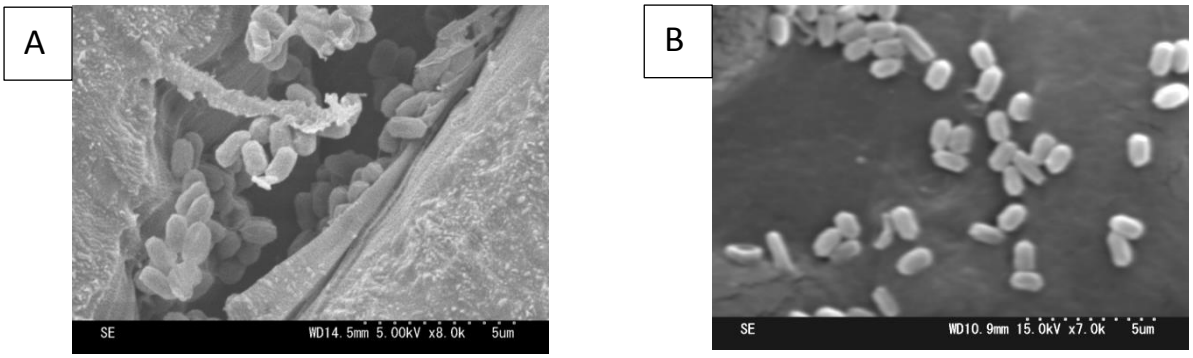

Figure 4.2 (A) SEM (Hitachi S-3000N, Scanning Electron Microscope) Micrograph showing stalked *Bacillus subtilis* endospores on filter paper

(B) SEM (Hitachi S-3000N, Scanning Electron Microscope) Micrograph showing uniformly distributed *Bacillus subtilis* endospores on agar disc.

The penetrating power of the plasma is hardly about 100 Å. So, to see the effect of plasma, stalked layers or lumps of spores are highly undesirable. To check the effectiveness of agar disc, spores were spread over both agar disc and filter paper disc. After plasma treatment the amount of released DPA was higher in case of Agar disc and it took less time to inactivate the spores by plasma exposure (Data is not included.) After spreading spores on agar discs, spores were dried at 35°C for 2 hours, to avoid any sublethal temperature activation of the spores.

4.2.4 Measurement of Released DPA (Dipicolinic acid or Pyridine-2, 6- dicarboxylic acid)

The fluorimetric quantification of DPA is based on the enhanced photoluminescence emission of DPA as a $[Tb\ (DPA)\ (H_2O)_6]^+$ complex which is obtained by binding of DPA with terbium ions (Tb^{3+}) from $TbCl_3.6H_2O$. We used DPA (Sigma-Aldrich) to prepare DPA solutions of known concentrations for the calibration curve and $TbCl_3.6H_2O$ (Aldrich) for 100 µM freshly prepared $TbCl_3.6H_2O$ solution in 0.1M sodium acetate buffer. In a cuvette, containing 1.7 ml of 0.1 M sodium acetate buffer, 850 µl samples and 850 µl freshly prepared $TbCl_3$ solution in 0.1 M sodium acetate buffer were added and then the relative fluorescence intensity was measured by RF-1500

Spectrofluorophotometer (Shimadzu). The excitation wavelength was 270 nm. The emission spectra were recorded from 475 nm to 600 nm wavelength range. For everything, to decide on the intensity of emission peak to work on throughout the experiment, to achieve the calibration curve, to measure the amount of released DPA after plasma exposure and to measure the amount of released DPA after wet heat sterilization, exactly the same method was used. To measure the amount of released DPA as a result of wet heat sterilization, the aliquots of different number of spores/ml were autoclaved for 15 minutes at 121°C, under 15 psi (pounds per square inch) pressure. To measure the amount of released DPA as a result of plasma exposure, the same spore suspension, dried agar discs, was used to expose to the stabilized plasma discharge for different durations. Then, all of the treated spore suspension samples were centrifuged (Kubota 6800) at the speed of 10,000 rpm at 4°C to remove cellular debris without any further disintegration. Centrifuged spore suspensions were filtered by using filter paper with the pore size of 0.22 µm. DPA salt is soluble in water so only supernatant was used for DPA estimation. The pallets of cellular debris were very clearly visible in autoclaved aliquots of spore suspension but not in plasma treated spore suspensions.

4.3 Results and Discussion

4.3.1 Electrical and Optical Characterization

Ar plasma discharge was quite filamentary (Figure 2.6, Chapter 2) so to achieve homogenous plasma discharge (Figure 2.7, Chapter 2) N_2 was added for quenching. The waveforms of voltage and current showed that the discharge sinusoidal voltage peak to peak voltage (V_{pp}) was of about 20 kV and the capacitive current was about 60 mA current (Figure 2.9, Chapter 2). The current got smoother (Figure 2.10, Chapter 2) after the addition of N_2 gas because of quenching which indicated homogenous plasma discharge. The optical emission spectra (Figure 2.13, Chapter 2) was dominated by active species of Ar representing 4p – 4s transition, nitrogen active species representing N_2 second positive system (N_2 ($C^3\prod_u$)) and a small peak representing OH radicals because of ambient air were also visible. Although OH radicals are known for their destructive effects on living cells but this time we can ignore their effects because of a very small quantity.

The wave forms of voltage, current (Figure 2.9 and 2.10, Chapter 2) and the optical emission spectra for CAPPLAT- 9 Ne (Figure 2.13 and 2.14, Chapter 2) have already been explained in Chapter 2 in detail. The homogeneous plasma discharge from CAPPLAT- 9 Ne had a very strong sporicidal effect because of the active species. The mechanism of the formation of active species had already been explained in Chapter 2. The energetic electrons collide with Ar molecules and make Ar metastables (Ar^m) and these energetic metastable sometimes de-excite along with the emission of radiation or change nitrogen molecules in the ground state into second positive systems (($N_2 (C^3\prod_u)$)which is the main energy carrier. These processes could be summarized as:

$$e^* + Ar \longrightarrow Ar^m + e$$

$$e^* + Ar^m \longrightarrow Ar^* (4p) + e$$

$$e^* + Ar^m \longrightarrow Ar^* (4s) + e$$

$$Ar^* (4p) \longrightarrow Ar^* (4s) + h\nu$$

$$Ar^m + N_2 (X^1\Sigma^+_g) \longrightarrow Ar^0 + N_2(C^3\prod_u)$$

$$N_2 (C^3\prod_u) \longrightarrow N_2(B^3\prod_g) + h\nu$$

4.3.2 Effects of Plasma Exposure on Endospores

4.3.2.1 The Viability Check of Endospores by CFU (Colony Forming Unit) Counting

To check the effect of the plasma exposure on the viability of endospores, the number of viable CFUs (Colony Forming Units) or survivors was plotted as the function of the time of plasma discharge exposure (Figure 4.3). The decimal reduction time because of plasma exposure (D_P value), the time of exposure to reduce D_P value by one log cycle (Z_P) and the time required to kill the whole population of spores (F_P) at SATP (Standard Ambient Temperature and Pressure which refers to 25°C (298.15 K) and pressure of 101kPa.) were calculated. D_P value shows the time in which the number of microorganisms is reduced by one log cycle (90% inactivation).

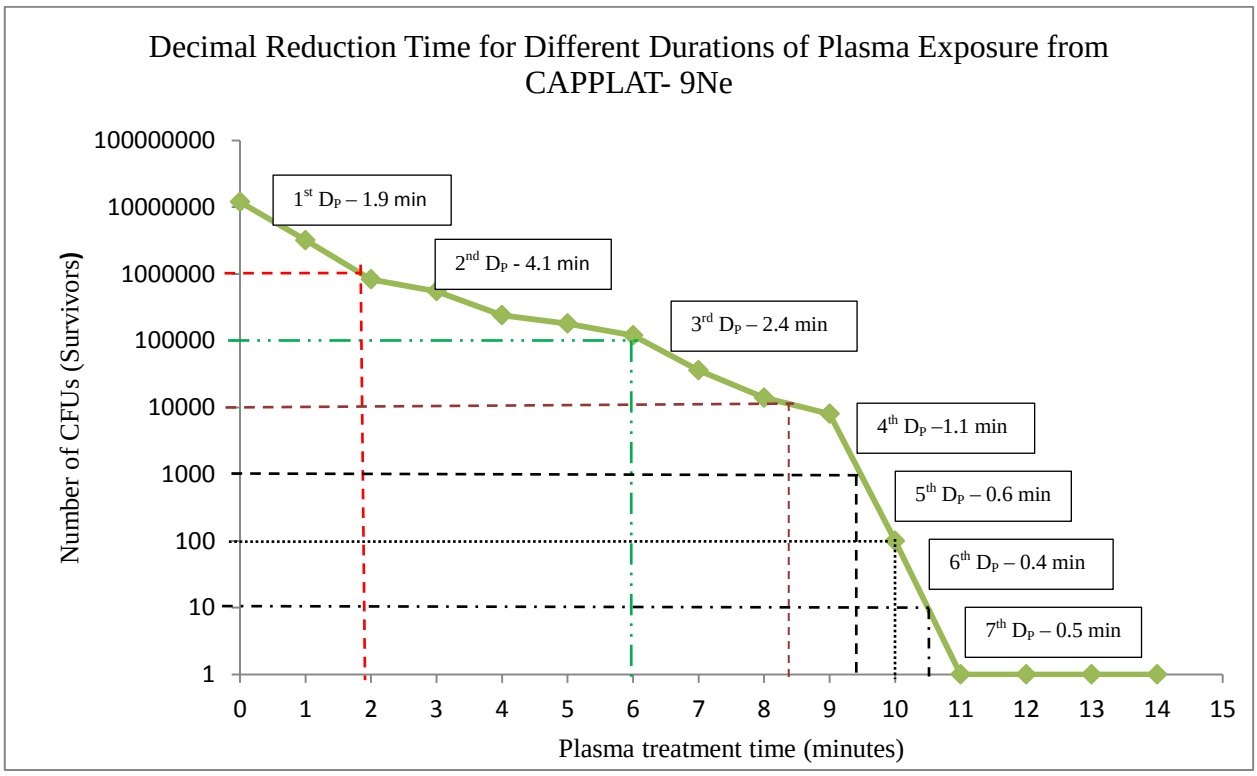

Figure 4.3 The number of viable CFUs as the function of the time of plasma discharge exposure from CAPPLAT- 9Ne. The biphasic survival curve of *Bacillus* endospores showing the time in minutes taken by each decimal reduction due to plasma exposure (D_p). The samples were exposed to the plasma (Ar 10 slm, and N_2 100 sccm) for different durations.

According to the Figure 4.3, for the total inactivation of the endospores we needed 7 D_Ps (1st D_P - 1.9 min, 2nd D_P - 4.1 min, 3rd D_P - 2.4 min, 4th D_P -1.1 min, 5th D_P - 0.6 min, 6th D_P - 0.4 min and 7th D_P - 0.5 min). From 2nd D_P to 6th D_P the decimal reduction value because of plasma exposure (D_P) had reduced by one log cycle. One log cycle reduction in decimal reduction value because of plasma exposure is Z_P. It means the Z_P value for this sterilization would be about 8.7 minutes. The time required for the complete sterilization was about 11 minutes. After 11 minutes, occasionally 1 or 2 colonies were observed. These colonies could be experimental errors or because of some super resistant endospores. But we never observed any colonies after the plasma exposure for 14 minutes.

The inactivation was a biphasic inactivation. Although the first phase of inactivation had several linear segment but there was a striking difference between the first and the second phase of inactivation. The second phase of inactivation was due to super dormant endospores or due to the spores underneath the cellular debris. The population represents these stubborn super dormant

endospores was less than 0.1% of the whole population. The second phase of inactivation was much shorter than the first phase. It could be because of the continuous cumulative effects of plasma exposure during the first phase on endospores. The inactivation in the second phase was comparatively very fast as all of the endospores were inactivated in less than one minute. Most probably, in the first phase they sustained serious injuries to their outer coats and cortex but still their protoplast was intact and they survived but in the second phase without their outer protective coverings (spore coat layers) they were more vulnerable for plasma exposure and easily in less than one minute they succumbed to complete decontamination. So, we could say that in the second phase, they were more like bacteria rather than spores, as far as their resistance was concerned, or we could call them de-coated spores. This deactivation was not because of direct DNA damage, actually there was not enough protection for DNA. So, DNA damage was the secondary effect. It is somewhat similar to the wet heat sterilization as the wet heat kills the spores by disrupting the inner membrane permeability barrier of the core and denaturing the core enzymes and other essential proteins not by damaging the DNA [26]

Exposing microorganisms of a given type to conventional sterilization systems such as autoclaves, ovens and EtO generally yield survival curves with an unique straight line: the whole inactivation process up to sterilization is an exponential function of time [2, 7]. In contrast, exposure to plasma (be it direct or in its afterglow) provides survival plots with 2 or 3 different linear segments, as shown in [Figure 4.4 taken from reference 37 and 4.5 taken from reference 38]. This implies that the number of surviving microorganisms decreases to a first approximation, as an exponential function of time also, but with different time constants, i.e., different kinetics [14, 35]. Figure 4.4 shows the biphasic inactivation curve for *Bacillus aureus* (spore forming bacteria) and *E.coli* (vegetative cell). Figure 4.5, shows a tri-phasic curve for *Bacillus subtilis*. The inactivation curves are multiphasic, unlike classical straight line survival curve or convex, sigmoid, or concave curves from thermal inactivation [39] as shown in Figure 4.6. It proves that the inactivation of gaseous plasma follows a higher order of inactivation kinetics.

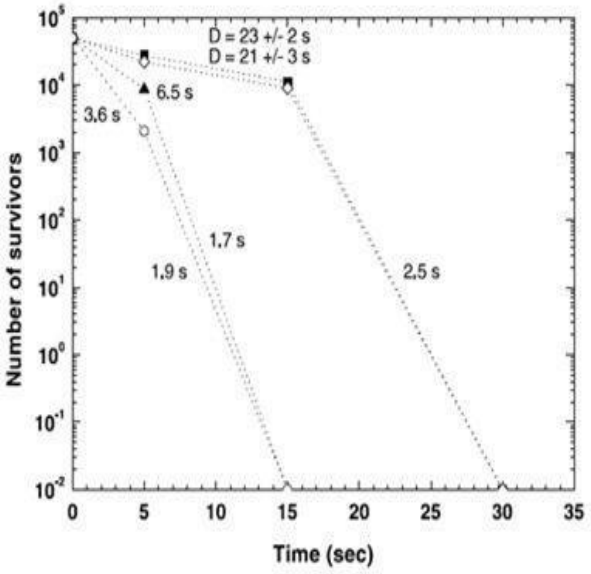

Figure 4.4 Survival curve of *S. aureus* and *E. Coli* cells (5.0×10^4) seeded on polypropylene samples and exposed to a DBD-type discharge in air at atmospheric pressure: *S. aureus* cells exposed unwrapped (◊) and in semi-permeable bags (■), *E. coli* cells (○) exposed unwrapped and in semi-permeable bags (▲) after Kelly-Wintenberg et al., 1998).

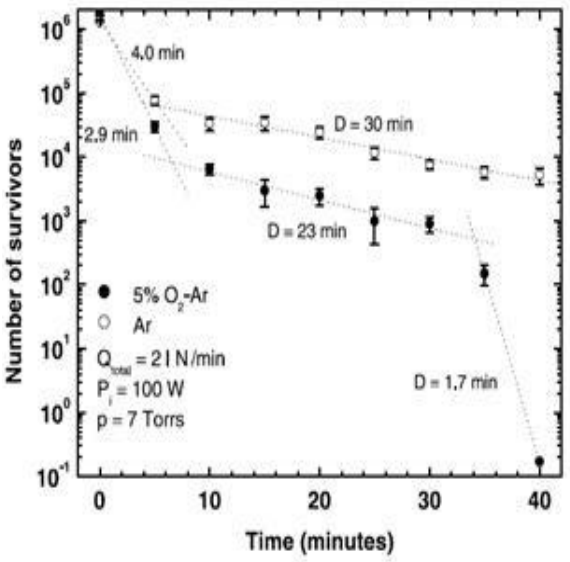

Figure 4.5 Survival curves of *B. subtilis* spores subjected to a flowing afterglow. Adding molecular oxygen to argon gas in the discharge leads to complete inactivation of the spores in 40 min (Moreau et al., 2000).

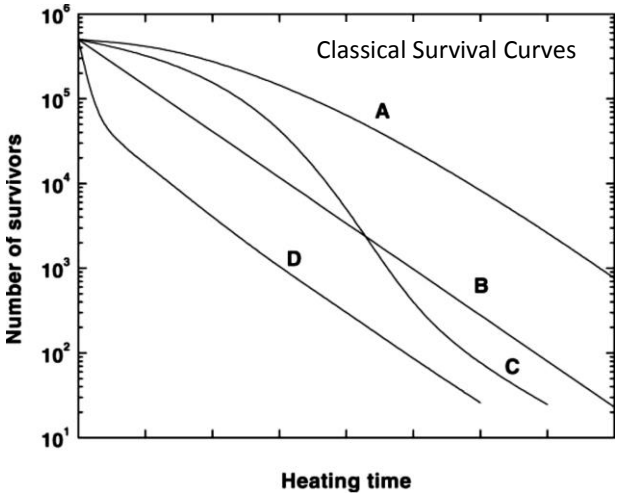

Figure 4.6 Classical survival curve (B) and three other commonly observed non-exponential survival curves (A, C, and D) designated as convex, sigmoid and concave curves, respectively, resulting from thermal inactivation (after Moats, 1971). Taken from reference 39

Higher order of inactivation kinetics shown in above graphs explains the different decimal reduction values. The very initial decimal reduction value (1^{st} D_P - 1.8 min) was comparatively small and after that it kept increasing for few more log reductions. After third decimal reduction time ($3D_P$ - 2.4 min) the inactivation of the spores was very rapid. For the fourth decimal reduction

(4 D_P), it required just 1.3 minutes. The last 3 log decimal reduction happened in less than 3 minutes.

4.3.2.2 Estimation of DPA to Confirm the Irreversible Cortex Lysis

Sometimes, apparently inactivated (dead) spores are not really inactivated (dead). These apparently inactivated spores can activate in certain conditions. This type of inactivation could be misleading. Setlow et al were trying to inactivate *Bacillus subtilis*, using acid, alkali and ethanol. They observed that in case of alkaline inactivation they got comparatively less amount of DPA. They also found, that apparently alkali killed *Bacillus subtilis* were completely recovered by *lysozyme* (required for spore cortex lysis) treatment [34]. Without cortex lysis, bacteria can't germinate and we won't be able to have any colonies for viability test, even though we still have viable endospores (temporarily inactivated endospores). The confirmation of cortex lysis and subsequent core lysis, is the release of DPA. So, we checked the amount of DPA, as an indicator of cortex lysis and then the core lysis or in other words the confirmed inactivation of the endospores.

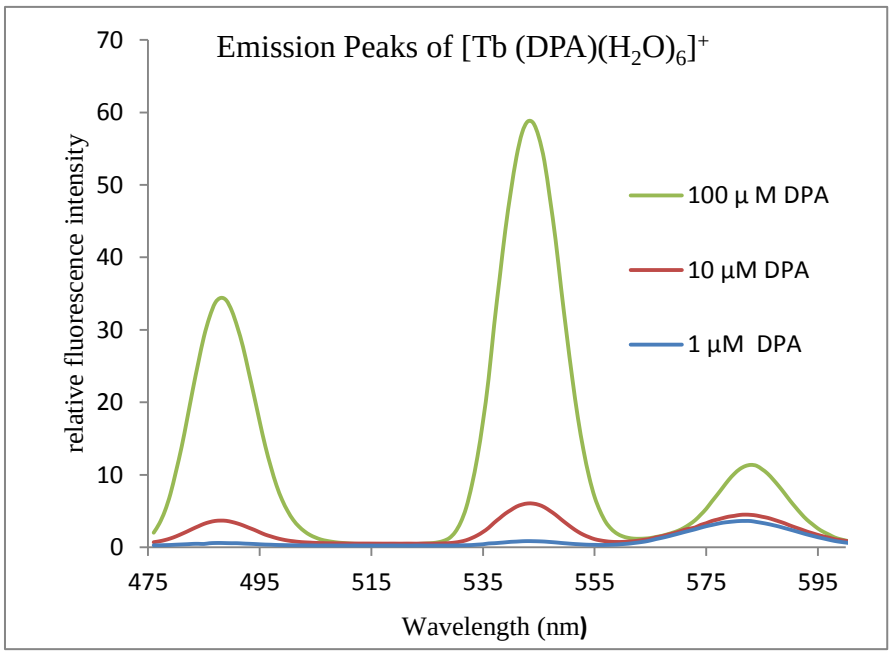

Figure 4.7 Fluorescence emission spectra of $[Tb(DPA)(H_2O)_6]^+$ recorded at the excitation wavelength 270 nm and emission wavelength range from 475 nm to 600nm for different concentrations of DPA (1µM, 10µM, 100µM) solution with 100 µM TbCl3·6H2O solution in 0.1 M sodium acetate buffer .

Excitation of the [Tb (DPA)$(H_2O)_6]^+$complex for known concentrations of 1µM, 10µ M and 100µM concentrations, gave three typical emission peaks at 487nm, 544nm and 582 nm at the excitation of 270 nm (Figure 4.7).

Throughout the study the highest peak (544 nm) was considered for all of the calculations (Figure 4.7). To make the calibration curve (Figure 4.8), the known concentrations of DPA from 1µM, 10µ M were used in the same way as explained in methods.

All of the intensities were also recoded at the wavelength 544 nm. The R^2 (linear regression) value was almost 1 (Fig. 7). To calculate the amount of the DPA following equation was used

$$Y = 0.4814. X$$

Where Y= the intensity of the peak

X= concentration of DPA (µM)

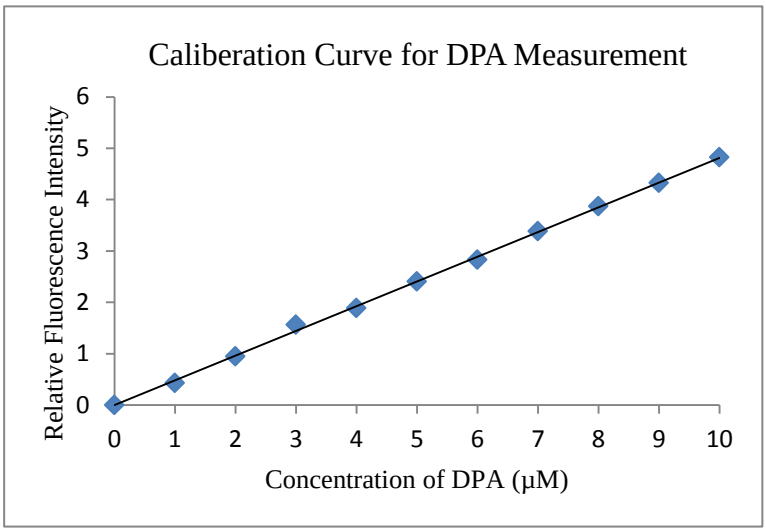

Figure 4.8 Calibration Curve for DPA Measurements. Relative Fluorescence emission intensities of [Tb (DPA) $(H_2O)_6]^+$ were recorded at the excitation wavelength 270 nm and emission wavelength 544 nm for different concentrations of DPA solution (1µM to 10µM,) with 100 µM $TbCl_3.6H_2O$ solution in 0.1 M sodium acetate buffer. The linear regression is 0.9991. The equation y=0.481x was used to calculate the amount of DPA(x).

The amounts of DPA, after wet heat sterilization (autoclaving) (Figure 4.9) and plasma treatment (Figure 4.9) were very different from each other which indicated that plasma treatment has a different mechanism for spore inactivation then the wet heat inactivation.

In case of wet heat sterilization, the amount of DPA was increased in exponential way with the exponential increase in the number of bacteria. Although the spore loses its dormancy earlier than the release of DPA but it should keep increasing on until all of the DPA is released. It didn't happen with plasma sterilization. In the beginning, the amount of released DPA increased with the time but then it decreased (Figure 4.10).

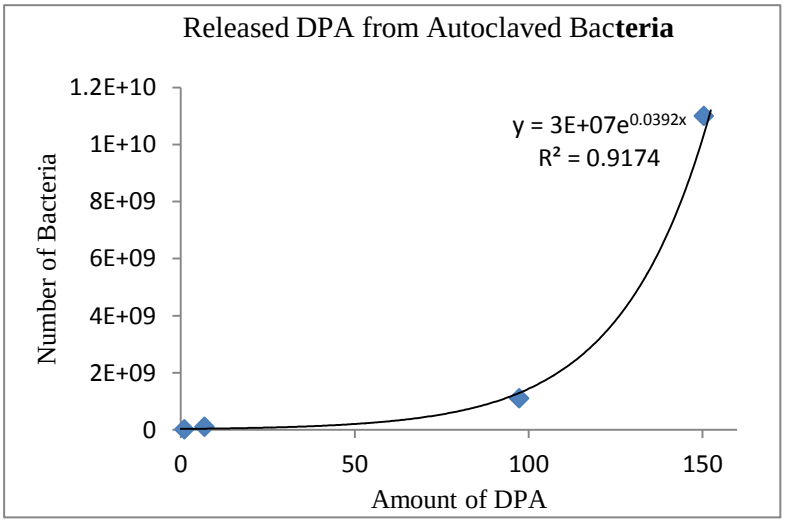

Figure 4.9 Amount of DPA in µM, released from the spores after wet heat sterilization at 121°C and 15 psi. The graph of released DPA as a function of the number of spores (10^6, 10^7, 10^8, 10^9) by checking the intensity of fluorescence emission at the excitation wavelength 270 nm and emission wavelength 544 nm and using the equation derived for the calibration curve (y=0.481x).

According to the Figure 4.10, for DPA release, in first 6 minutes, we had the maximum released DPA, and then it started decreasing. Although maximum number of spore inactivation was in the first 7 minutes it could be due to legged release of DPA. Although the amount of DPA should have kept increasing or remained constant but it didn't happen. It could be assumed that the amount of DPA was increasing but at the same time the active species of plasma discharge were disintegrating it. In gaseous phase DPA has 5 isomers. The ionization potential for all of these isomers is about 9eV [27] which is less than the energy of argon metastables (E ≈ 11.1 *eV*) and second positive system of nitrogen (E ≈ 11.5 *eV*). So, the energetic active species of plasma disintegrated DPA.

Estimation of DPA was used as an indicator of the bacterial germination or spore inactivation. The amount of DPA was not very consistent. There could be several other reasons too. To get DPA all of the outer walls of the protoplast must be disintegrated. So, even if a spore was dead, it might possible that they got stuck into debris or the spores got clumped and didn't get enough plasma exposure to lose outer cell wall. Different bacteria might have different amounts of DPA or the varying ratio of some already dead spore in a certain aliquot. After a certain point, DPA stopped releasing but plasma kept disintegrating it, so the overall amount of DPA started decreasing.

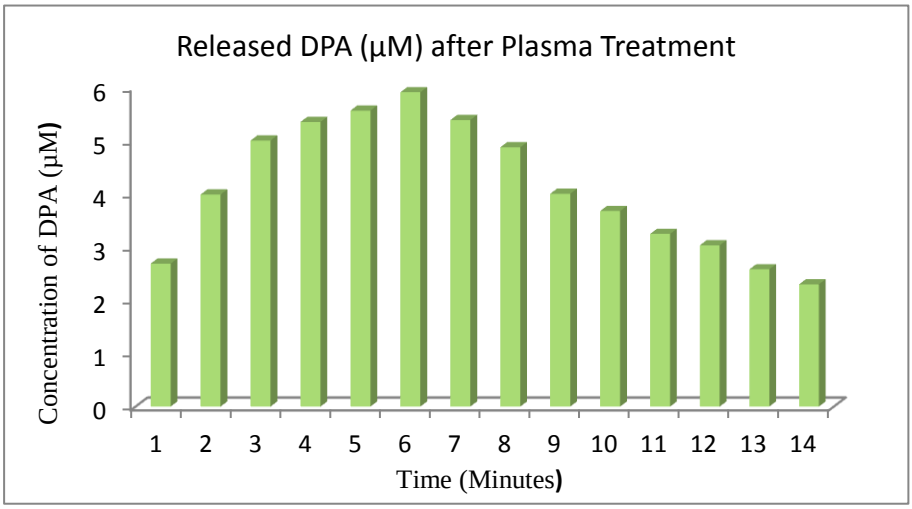

Figure 4.10 Amount of DPA (µM) released from the spores after plasma exposure from 1 minute to 14 minutes. The graph of released DPA as a function of time of plasma exposure by checking the intensity of fluorescence emission at the excitation wavelength 270 nm and emission wavelength 544 nm and using the equation derived for the calibration curve (y=0.481x).

4.3.2.3 Visual Inspection by SEM Micrographs

For the visual inspection SEM (Hitachi S-3000N, Scanning Electron Microscope) micrographs were taken. The changes in SEM micrograph of *Bacillus subtilis* spores exposed to the plasma discharge for 0 minutes (Fig. 11), 5 minutes (Fig.12), 7 minutes (Fig.13) showed that endospores suffered the collapse of the cell wall. There were sort of ghost cells which have lost the protoplast with all of the genetic materials. These cells look like empty containers. These drastic effects can't be reversed by any self defense mechanisms of the spore. The number of spores was

also hugely decreased without any traces which further supported the formation of volatile compounds. The fatal effect of plasma increased with time.

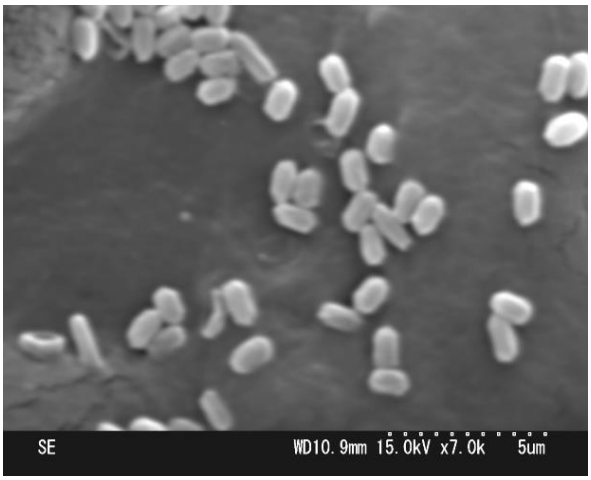

Figure 4.11 *Bacillus subtilis* spores without exposing to the homogeneous plasma discharge (0 minutes).

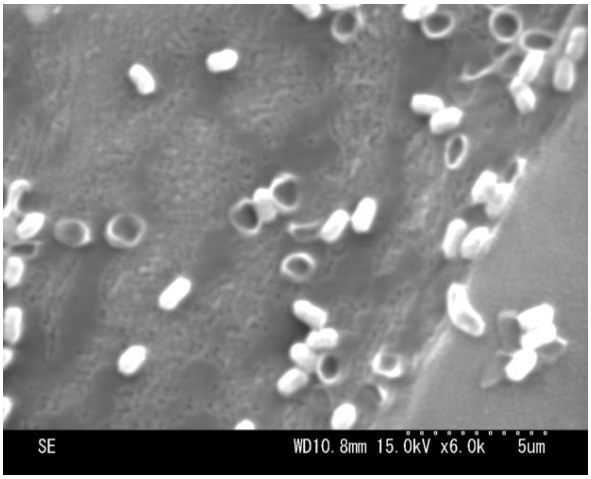

Figure 4.12 *Bacillus subtilis* spores after exposing to the homogeneous plasma discharge for 5 minutes.

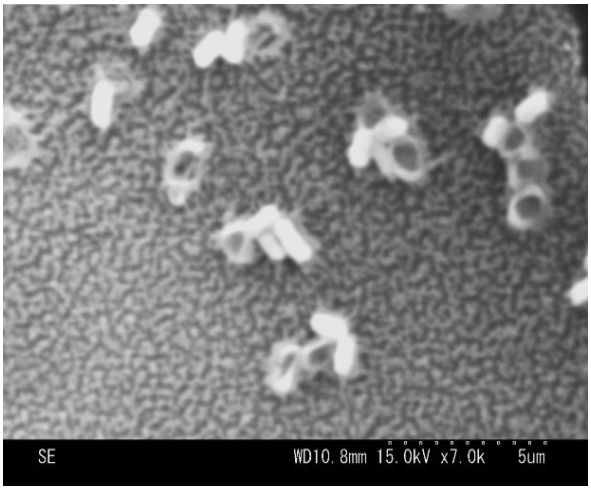

Figure 4.13 *Bacillus subtilis* spores after exposing to the homogeneous plasma discharge for 7 minutes.

4.4 Mechanism of Endospore Inactivation

The exact physiochemical process of inactivation is not fully understood yet. So far, the most

accepted processes happen during the plasma sterilization are inactivation of genetic materials by UV irradiation, erosion of microorganisms by etching and erosion of microorganisms through intrinsic photodesoption, [14]. In the plasma discharge, we had charged species, excited Ar metastables, OH radicles, second positive system of N_2 molecules, electrons and the de-excitation of active species occurred with the emission of radiation. We also had some transitions in UV region (220 – 390) too but the effect of the UV radiation is not clear in case of atmospheric pressure plasmas yet, whereas it plays a very important role in reduced pressure plasmas. Although UV radiation is well known for its effect on DNA and other nucleic materials but according to M. Moissan et al the sporicidal effect of atmospheric plasma is not affected by the presence or absence of UV radiation [14]. UV photons at atmospheric pressure are strongly reabsorbed by the plasma, preventing them from reaching to the sample [36] so, there are not enough UV photons to reach the substrate. On the other hand highly energetic metastables play an important role in inactivation of microorganisms. Plasma sterilization is possible with glow discharge and afterglow discharge but of course, sterilization in afterglow takes longer than the glow discharge because afterglow discharge has less charged particles. It is mainly consists of neutral atoms, radicles and molecules. It might have some excited species. Although metastables have short life but they have a comparatively longer life than the charged species [14]. So, the metastables de-excite by the collision with other molecules by energy transfer rather than just emitting radiations. Due to these collisions or energy transfers, sometimes bonds are broken or other processes like photodesorption, etching and alteration in chemical environment initiate. During the process of erosion of microorganisms by intrinsic photodesorption or etching, volatile compounds are formed. After plasma exposure when the spore suspensions were centrifuged, no cellular debris was observed but wet heat sterilized spore suspensions got cellular debris (pellet) which supported the formation of volatile byproducts

The mechanism of sterilization by reduced pressure is quite well understood but the mechanism of atmospheric plasma is not very clear yet [38]. If we compare the inactivation at

reduced pressure (Figure 4.14) with inactivation at atmospheric pressure (Figure 4.15), we can clearly see that the both survival curves are multiphasic unlike classical straight line survival curve or convex, sigmoid, or concave curves from thermal inactivation [39].

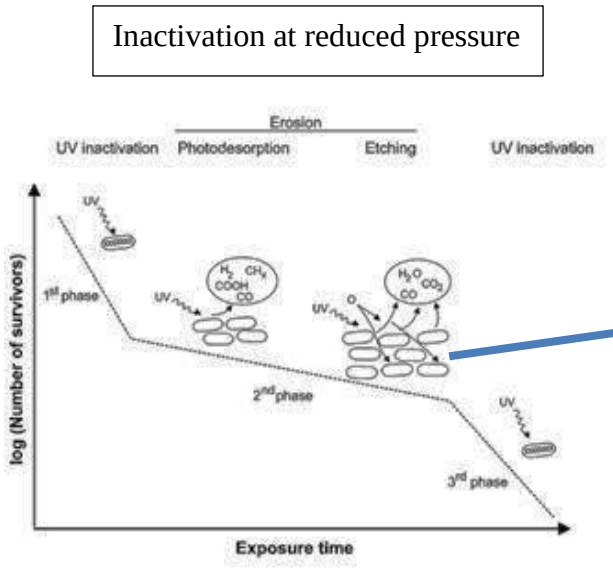

Figure 4.14 Schematic illustration of the triphasic survival curve characterizing plasma sterilization, showing the mechanisms predominantly acting during 1each phase. (Taken from reference 38)

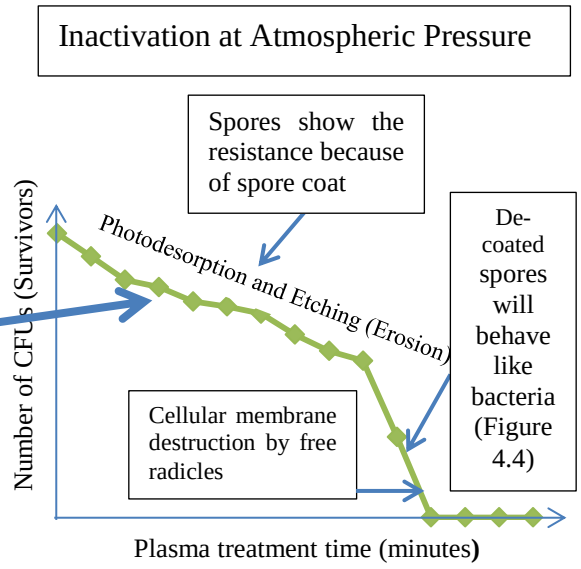

Figure 4.15 Reproduction of graph 4.3; showing biphasic survival curve after receiving plasma treatment for different durations

In case of reduced pressure, it is very clearly tri-phasic (Figure 4.14) whereas in case of atmospheric pressure, it is biphasic (Figure 4.14). In case of reduced pressure, the first phase shows the inactivation because of UV radiation and as we previously discussed that in case of atmospheric pressure plasma, UV radiation doesn't play any role in the process of inactivation. Most probably, that is why we don't have the first very distinct phase. The first phase of our survival curve (Figure 4.15), at atmospheric pressure is very similar to the second phase of the survival curve under reduced pressure which indicates that the main dominating process for inactivation at atmospheric pressure is erosion (photodesorption and etching). If we observe Figure 4.4, we can see bacterial spores are taking much longer than the bacterial cells. The biggest difference between a spore and a bacterium is the cell wall. In the beginning of the first phase of the inactivation at atmospheric pressure, the inactivation was comparatively faster (Figure 4.15) because in this phase, plasma

inactivated the spores which were not stacked or present on the surface of stacked spores. In time, the cellular debris accumulated over spores which slowed down the process of inactivation of the spores underneath the debris. Once plasma could remove the debris second phase was executed very quickly. Most probably, longer exposure also helped with the inactivation of super dormant spores in the second phase. It also explains different D_p values for the survival curve. In the second phase, the spores were like de-coated spores which were like bacteria (or germinating spore). The free radicles which were formed because of active plasma species would change the fluidity and permeability of the inner cell wall which was exposed after spore coat destruction. Change in fluidity and the permeability would inactivate the enzymes because of disturbed pH, and would start disrupting the cell wall which eventually it would inactivate the spore by releasing out the genetic materials from the core.

On the basis of our comprehension and the available information we tried to postulate a mechanism for endospore inactivation (Figure 4.17). The removal of outer spore membrane and the coat proteins do not the affect the wet heat resistance of the spores. It means spore coat does not play any direct role in dormancy, but infect, it acts as a first line of defense against any foreign intrusions. It protects the cortex which is susceptible to the peptidoglycan enzymes like *lysozyme*; it also provides resistance against some other oxidizing agents like chlorine dioxide, hypochlorite, ozone and peroxyinitrite [15] but has a minor role in hydrogen peroxide resistance [16]. Disintegration of cortex means either germination of the spore or the death of the spore. Even if spores germinate, they will be inactivated much more easily than the spores.

Bacillus subtilis spores have ridges about 85 nm thick and 12 nm in height along the long axis of the *B subtilis* spores. Chada et al [33] found circular bumps of 7 to 20 nm in diameter in ridges present on the surface of spores and small pores of estimated size of 24 nm or smaller were present between the bumps [17, 1 8, 1 9]. As shown in Figure 4.16, these pores act like a sieve and let selected molecules go into the spore. These pores allow small amino acids like as L-alanine or inosine to interact with germination receptors and keep harmful things out. Spore has a thick

proteinceous outer coat about 70 to 200 nm thick and then inner coat is about 70 nm thick which cover the cortex, germ cell wall and protoplast shown in Figure 4.16. The penetration power of glow discharge is just about 100 Å. It means plasma discharge can't go all the way up to the core where it has all of the genetic material which must be released in order to inactivate the spore or to germinate the spore (bacterium). There must be some other processes which assist the inactivation which is initiated by plasma discharge.

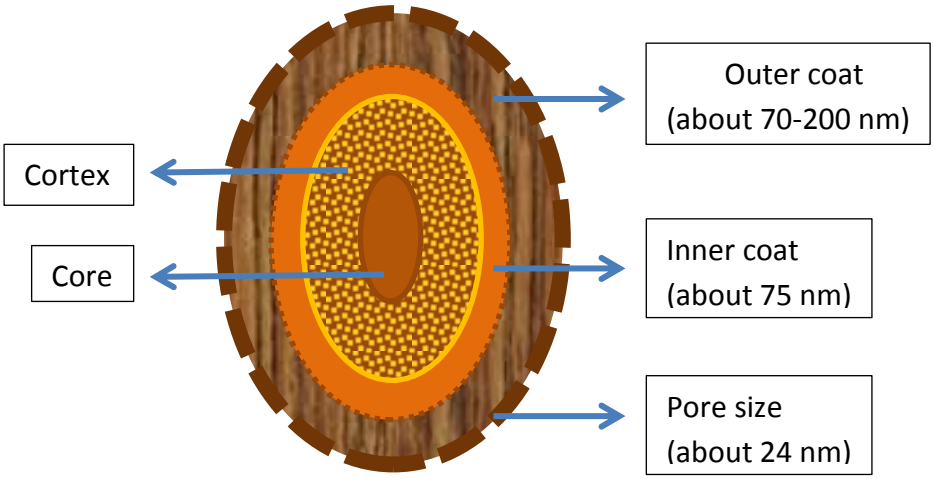

Figure 4.16 showing the thickness of outer and inner coat and the pore size of an endospore

Most probably (see Figure 4.17), the surface of the outer coat gets etched by active species which are in direct contact with the surface. The collision with the surface can lead to physical sputtering or chemical reactions like oxidation which will result into formation of volatile compounds between the active species and surface (spore layer) atoms. The energy of Ar^m (Argon metastables) is about ($\Delta E \approx 11.1$ eV) and the energy of N_2 second positive system (N_2 ($C^3\prod_u$ — $B^3\prod_g$)) is about ($\Delta E \approx 11.5$ eV) [20, 21]. These active species can break the weak hydrogen bonding, which holds the proteins in the functional form, of highly cross linked spore coat proteins and then other peptide bonds of the protein, composing the endospore coat, which can lead to the formation of some micro-capillaries to help the propagation of the active species, particularly free radicles, that are formed by the collision of active species or formed by previously formed free radicles, into the spore.

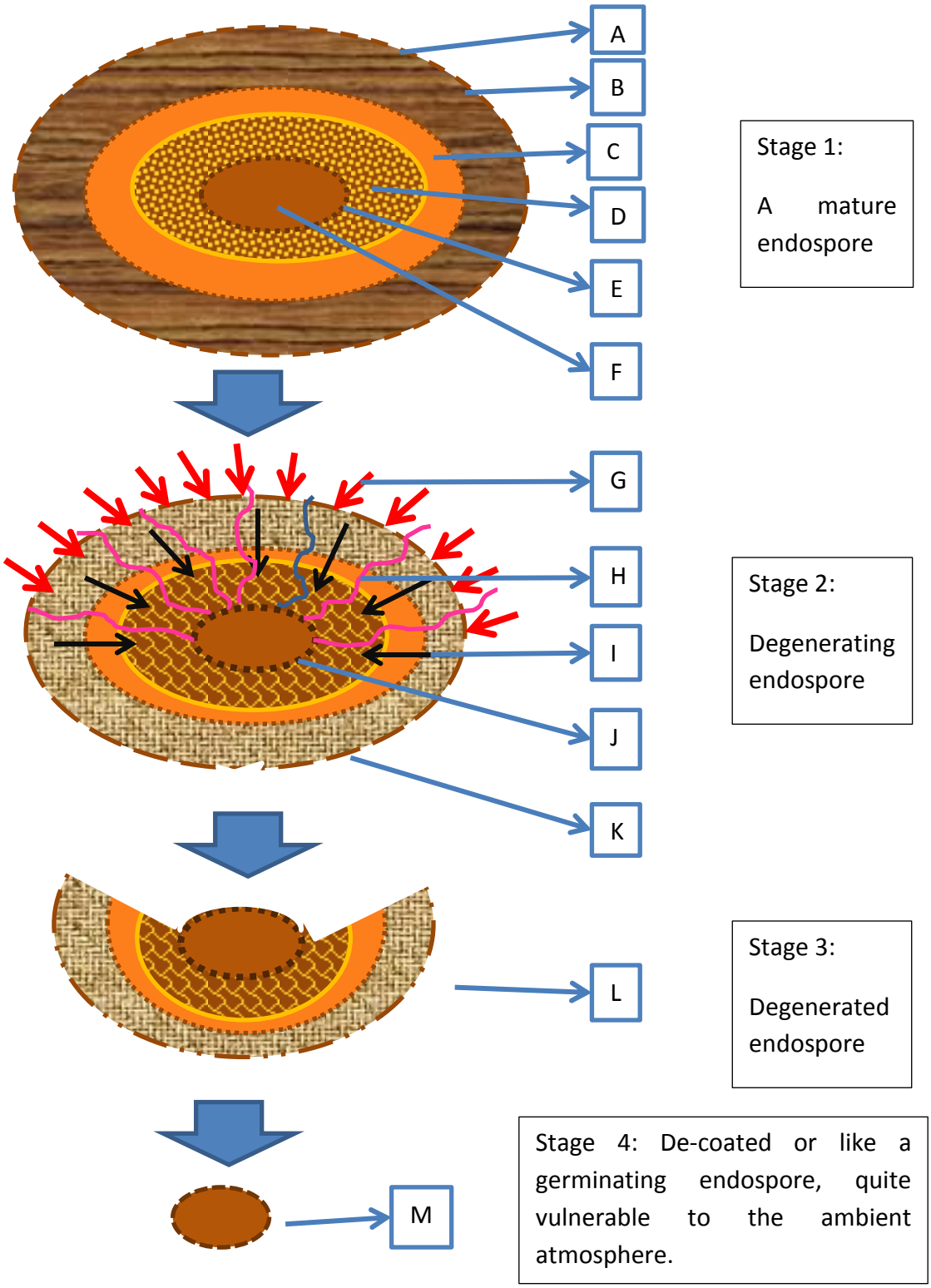

Figure 4.17 Possible mechanism of Spore destruction in *Bacillus subtilis*; Stage 1: A: small pores in the outer surface B: outer spore coat; C: inner spore coat; D: cortex; E: germ cell wall; F: core; G: attack of active species on the outer coat of then spore; H: diffusion of free radicles and active species into the spore; I: release of cortex lytic enzymes form the disintegrating spore coat; J: changes in the permeability of the germ cell wall; K: dilating pores in the surface of the spore; L: degenerated spore in the germination like conditions (germinating spore); M: Bacterium or de-coated spore, vulnerable to the ambient conditions

The outer coat has some small pores with etching they might dilate. These alterations could lead to the diffusion of free radicles, atoms and excited molecules to the core of the spore [22] and expose more surface for active species and free radicles. These metastable or sputtered species and the electrons from electron dense outer coat can initiate intrinsic photodesoption too. The outer coat has some lytic enzymes which help to hydrolyze the cortex which is a necessary condition for either germination or the death of the spore [4, 23]. Cortex is made up of peptidoglycan, similar to vegetative cells with some spore specific modifications [24]. Endospore cortex is made up of three repeating subunits muramic lactum subunit without any attached amino acid, alanine subunit with only an L- alanyl residue and a tetra peptide subunit bearing the sequence L-al-D-glu-meso-DAP-D-ala. These subunits represent 55%, 15%, and 30% of the total. There is comparatively less cross-linking between peptide chains [25] than the vegetative cells, which further makes the breakdown of the cortex easier.

Breakdown of cortex, releases DPA (*dipicolinic acid*) which further activates coat associated enzyme CwIJ which is a cortex lytic enzyme. Lysis of sporecoat and subsequent lysis of cortex is just like the conditions, we have when a spore germinates. Germinating spores are highly vulnerable to their environmental stresses. Under the cortex there is germ cell wall which is like a bacterial cell wall and its permeability is also altered by free radicles, these alterations will facilitate the diffusion of free radicles, atoms and excited molecules to the core of the spore. It might possible that the cell wall would have a kind electroporation by free radicals or other active species formed by plasma active species and other byproducts of catastrophic reactions with free radicles. Without outer walls, the genetic material from the core leaks out and the spore gets inactivated. So, the plasma has a dual effect i.e. the active species disintegrate a spore from outside i.e. extrinsic effect and sets off a chain of catastrophic, multifaceted mode of operation to inactivate the spores from inside i.e. intrinsic effects. There is a similarity with the inactivation under reduced pressure. In both cases, first spore is germinated and then the plasma treatment kills the bacterium which is highly susceptible to the plasma treatment via particularly free radicles.

4.5 Conclusion

We could successfully inactivate a population of $1.0X10^7$ to $4.0X10^7$ *Bacillus subtilis* endospores/ml in about 11 minutes (F_p). To inactivate the spores, we used our originally designed and characterized plasma generating device called CAPPALT- 9Ne (Cold Atmospheric Pressure Plasma Torch- 9Ne). The inactivation was biphasic. The first phase of inactivation was much longer than the second phase. The decimal reduction value (D_p) changed with time. It varied from 1.9 minutes to 0.4 minutes. The Z_p value i.e. one log reduction in D_p value was 8.7 minutes. We measured the amount of released DPA to understand the deactivation and to confirm the destruction of cortex. We tried to figure out the mechanism. It could be concluded that the highly energetic active species, particularly argon metastales and excited second positive system of N_2 molecules, of plasma discharge were responsible for the inactivation of the spore through the process of etching or physical sputtering via volatile compound formation. Some other intrinsic destructive reactions also participated in the process of inactivation. The active species worked on the surface of the spore (extrinsic effect) and made free radicles and other active species which entered in to the spore (intrinsic effect).This dual effect of highly active species and free radicles and other active species were responsible for the inactivation of the spores.

Although the basic unit of CAPPLAT had already been successfully used for both chemical vapor deposition (CVD) and polymer surface treatment [28 to32] but the CAPPLAT- 9Ne the commercial unit has never been used for any research purposes after this research we concluded that the CAPPLAT- 9Ne can successfully be used as a sterilization tool. The conventional methods of sterilization have some drawbacks like they are time consuming, not user and environment friendly and sometimes affect the bulk properties of the substrate, whereas plasma sterilization treats only the surface. The active species are short lived so they are user and environment friendly, no after use sanitation problems and very time efficient process.

The biggest drawback is its poor penetration power but I think it can be used as its biggest strength. Though, still more extensive researches are required, but it can easily replace the

hazardous chemo-therapy for cancerous cell without killing healthy cell because of its short working distance and only surface penetration. It could be really very effective tool to eradicate undesired diseased or dead microorganisms/cells. Bio-plasma is a very fast emerging field of plasma applications. Efforts are being made to achieve specific parameters to kill different types of harmful microorganisms or diseased cells to treat some dreadful diseases.

4.5 References

[1] Aronson AI, and Fitz-James P. Structure and morphogenesis of the bacterial spore coat: *Bacteriol. Rev.* 40, 360–402, 1976.

[2] Driks A. *Bacillus subtilis* spore coat: *Microbiol. Mol. Biol. Rev.*, 63, 1–20, 1999.

[3] Driks A. Maximum shields: the assembly and function of the bacterial spore coat. TRENDS in Microbiology, Vol.10 No.6, 2002.

[4] Hullo MF. CotA of *Bacillus subtilis* is a copper-dependent laccase. *J. Bacteriol*, 183, 5426–5430, 2001.

[5] Mazanec K, Kocusr M, and Martinec T. Electron microscopy of ultrathin sections of Sporosarcina urea: J. Bacteriol, 90:808–16, 1965.

[6] Errington J. Regulation of endospore formation in Bacillus subtilis: Nat. Rev. Microbiol, 1:117–26, 2003.

[7] Piggot PJ and Hilbert D W. Sporulation of Bacillus subtilis: Curr. Opin. Microbiol, 7:579–86, 2004.

[8] Adriano OH, and Charles P M Jr. Structure, Assembly and Function of the Spore Surface Layers: Annu. Rev. Microbiol, 61:555–88, 2007.

[9] Murrel WG, and Warth, AD. Composition and heat resistance of bacterial spores. In spores, Vol. 3 (Campbell LL and Halvorson HO, eds), pp. 1-24 American Society for Microbiology, Ann Arbor, Michigan, 1965.

[10] Rosen DL, Sharpless C, and McGown. LB. Bacterial spore detection and determination by use of terbium dipicolinate photoluminescence. Anal. Chem., 69:1082–1085, 1997.

[11] Hindle AA and Hall EA. Dipicolinic acid (DPA) assay revisited and appraised for spore detection, Analyst 124:1599–1604, 1999.

[12] Bhat M V and Benjamin YN. Text. Res. J., 69, 39, 1999.

[13]http://www.cresur.com/

[14] Moissan M, Barbeau J, Moreau S, Pelletier J, Tabrizian M, and Yahia LH. Low-temperature sterilization using gas plasmas: a review of the experiments and an analysis of the inactivation mechanisms. International Journal of Pharmaceutics 226: 1–21, 2001.

[15] Genest PC, Setlow B, Melly E. and Setlow P. Killing of spores of Bacillus subtilis by peroxynitrite appears to be caused by membrane damage. Microbiology 148, 307–314, 2002.

[16] Riesenman PJ and Nicholson WL. Role of the sporecoat layers in Bacillus subtilis resistance to hydrogen peroxide, artificial UV-C, UV-B, and solar radiation. Appl Environ Microbiol 66, 620–666, 2000.

[17] Aronson AI, and Fitz-James P. Structure and morphogenesis of the bacterial spore coat. *Bacteriol. Rev.* 40:360–402, 1976.

[18] Chada VGR, Sanstad EA, Wang R, and Driks A. Morphogenesis of Bacillus spore surfaces. J. Bacteriol. 185:6255–61, 2003.

[19] Holt SC, and Leadbetter ER. Comparative ultrastructure of selected aerobic sporeforming bacteria: a freeze-etching study. Bacteriol. Rev. 33:346–78, 1969.

[20] García MC, Varo M, and Martínez P. Plasma Chem Plasma Process, 30:241, 2010.

[21] Yu QS, and Yasuda HK. Plasma Chem Plasma Process, 18:46, 1998.

[22] Boucher (Gut) RM. Seeded gas plasma sterilization method. US Patent 4 207 286, 1980.

[23] Bagyan I, and Setlow P. Localization of the cortex lytic enzyme CwlJ in spores of Bacillus subtilis. J. Bacteriol. 184, 1219–1224, 2002.

[24] Popham DL. Specialized peptidogycan of the bacterial endospore: the inner wall of the lockbox. Cell Mol Life Sci 59, 426–433, 2002.

[25] Stanier RY, Ingraham. JL, Wheelis ML, and Painter PR. The Microbial World. 5th edition. Prentice- Hall, Englewood Cliffs, New Jersey.

[26] Setlow P. Resistance of bacterial spores. In: Storz, G., Hengge-Aronis, R. (Eds.), Bacterial Stress Responses. American Society of Microbiology, Washington DC, pp. 217–230, 2000.

[27] Richard D, Massaro, and Estela Blaisten-Barojas. Density functional theory study of dipicolinic acid isomers and crystalline polytypes. Computational and Theoretical Chemistry 977: 148–156, 2011.

[28] Fei X, Kondo Y, Mori T, Hosoi K, and Kuroda S. J. Materials Life Soc., 23, 120-127, 2011.

[29] Kuwabara A, Kuroda S, and Kubota H. Plasma Sources Sci. Technol., 15, 328, 2006.

[30] Kasih TP, Kuroda S, and Kubota H. Chem. Vap. Depos., 13, 1, 2007.

[31] Kuwabara A, Kuroda S, and Kubota H. Plasma Sci. Technol., 9, 181, 2007.

[32] Kuwabara A, Kuroda S, and Kubota H. Plasma Chem. Plasma Process, 28, 263, 2008.

[33] Chada VGR, Sanstad E A, Wang R, and Driks, A. Morphogenesis of *Bacillus* spore surfaces. *J. Bacteriol.* 185:6255–61, 2003.

[34] Setlow B, Loshon CA, Genest,PC, Cowan AE, Setlow C, and Setlow P. Journal of Applied Microbiology, 92, 362–375, 2002.

[35] Cariou-Travers S, and Darbord JC. Le vide: Sci. Tech. Appl. 299, 34–46, 2001.

[36] Kelly-Wintenberg K., Montie TC, Brickman C, Roth JR, Carr AK, Sorge K, Room temperature sterilization of surfaces and fabrics with a one atmosphere uniform glow discharge plasma. J. Indust. Microbiol. Biotechnol. 20, 69–74, 1998.

[37] Moreau S, Moisan M, Tabrizian M, Barbeau J, Pelletier J, Ricard A. Using the flowing afterglow of plasma to inactivate Bacillus subtilis spores: influence of the operating conditions. J. Appl. Phys. 88, 1166–1174, 2000.

[38] Moisan M, Barbeau J, Marie-Charlotte C, Jacques P, Nicolas P, and Bachir S. Plasma sterilization. Methods and mechanisms. IUPAC, Pure and Applied Chemistry 74, 349–358, 2002.

[39] Moats WA. Kinetics of thermal death of bacteria. J. Bacteriol. 105, 165–171, 1971.

Chapter 5

Effects of Cold Atmospheric Pressure Plasma Torch (CAPPLAT) the Basic Unit on the Viability of *Bacillus subtilis* Endospore and the Enhancement of the Sterilization Efficiency of the Plasma Jet

5.1 Introduction

In Chapter 2 and 3, the cold atmospheric plasma torches which we explained, were CAPPLAT–9 Ne the commercial Unit and CAPPLAT the basic unit. We discussed the optical and electrical characterization and their mechanisms in detail. In chapter 4, we discussed the bio application of Cold Atmospheric Pressure Plasma Torch – 9Ne (CAPPLAT- 9 Ne) as a sterilization tool. We successfully inactivated a population of $1.0X10^7$ to $4.0X10^7$ *Bacillus subtilis* endospores/ml. We also discussed the method and different aspects of the inactivation process and finally, we proposed a tentative inactivation mechanism. In this Chapter (5), we will be discussing the effect of plasma jet from CAPPLAT the basic unit on *Bacillus subtilis* endospores. We used the spore suspension of the same strength i.e. $1.0X10^7$ to $4.0X10^7$ *Bacillus subtilis* endospores/ml, we used the same methodology, as we used for our previous investigations with CAPPLAT-9Ne the commercial unit. Just like Chapter 4, we exposed the endospores, dried on an agar disc, to the plasma for different durations. Then we had the same inoculation process, incubation time and CFU counting process to make survival curves in order to check the check the viability of the endospores. From the survival curves, we calculated Dp, Zp and Fp values. We also checked the amount of released DPA to confirm the cortex lysis and then the disintegration of protoplast which is the indication of irreversible bacterial inactivation.

This time, we also studied the effects of addition of O_2 and H_2O_2 on endospore inactivation. Then we compared all of our results to see which CAPPLAT was more effective and what conditions were the most appropriate to inactivate endospores.

5.2 Experimental Set Up and Methods

5.2.1 Plasma Device.

We used CAPPLAT the plasma generating device (3.1, Chapter 3) and a handmade torch to generate non-equilibrium plasma discharge at atmospheric pressure. The configuration of plasma torch (see 2.2, Chapter 2) and the experimental set up (see 3.2, Chapter 3) have already been explained. For plasma jet generation with CAPPLAT, 10 slm (standard liter per minute) of Ar gas (working gas) and 300 sccm (standard cubic centimeter per minute) of N_2 gas (additive gas) were used to achieve homogeneous plasma discharge. It worked on an invariable voltage of 16 kV with square wave amplitude at 50% duty cycle. The mixture of Ar and N_2 was fed into the torch through an inlet tube (see 3.2, Chapter 3). We fed O_2 through the capillary, inserted into the hollow inner electrode, to the plasma jet directly (see 3.3, Chapter 3). For the direct injection of H_2O_2 into plasma jet, bubbling method was adopted (see 3.4, Chapter 3). For bubbling 150 sccm of Ar gas was used as a carrier gas.

5.2.2 Electrical Measurements

To see the experimental set up, please see the Figure 3.2. The method for electrical measurements is given in 3.2.2 (see Chapter 3).

5.2.3 Optical Emission Spectroscopic Measurements

To see the experimental set up see the Figure 3.2. The method for electrical measurements is given in 3.2.3 (see Chapter 3).

5.2.4 Addition of Gases to the Plasma Jet (Direct Injection Mode)

Experimental set ups for the addition of O_2 is shown in Figure 3.3 and for H_2O_2 is shown in Figure 3.4. The method is explained in 3.2.4 (Chapter 3).

5.2.5 Effect of the Plasma Jet from CAPPLAT on the Viability of Endospores

Revival of culture, collection of endospores then the preparation of agar disc, medium and other buffers, solutions, plasma exposure, collection of plasma treated spores, estimation of DPA and colony counting etc. have already been explained in detail in Chapter 4. Just like CAPPLAT-9Ne, spores were treated with plasma for different durations and after plasma treatment colonies were counted. The number of viable CFUs was plotted as the function of the time of plasma discharge exposure to get the survival curves for different conditions. The decimal reduction time because of plasma exposure (D_P value), and the time required to kill the whole population of spores (F_P) at SATP (Standard Ambient Temperature and Pressure which refers to 25°C (298.15 K) and pressure of 101kPa.) were calculated.

5.3 Results and Discussion

5.3.1 Electrical Characterization of Ar Plasma Jet Obtained from CAPPLAT and the Effects of the Additions of N_2, O_2 and H_2O_2

It has already been discussed in 3.3.1.1 (Chapter 3) for the addition of N_2 and the addition of O_2 and H_2O_2 have also been explained in 3.3.1.2. The waveforms for N_2 addition is given in figure 3.5 and the waveforms for O_2 addition and H_2O_2 additions are given in Figure 3.10.

5.3.2 OES Characterization of Ar Plasma Discharge (Jet) and the Effects of the Additions of N_2, O_2 and H_2O_2

The optical emission spectra of the Ar plasma discharges in different conditions have already been discussed in 3.3.2.1 and 3.3.2.1.

5.3.3. Effects of Ar –N_2 Plasma Jet from CAPPALT on the Viability of Endospores

This CAPPLAT also had sporocidal property. We could inactivate spores successfully, the process and the mechanism of spore inactivation have already explained in Chapter 4. The number of viable CFUs was plotted as the function of the time of plasma discharge exposure (Figure 5.1). The decimal reduction time because of plasma exposure (D_P value), and the time required to kill the whole population of spores (F_P) at SATP (Standard Ambient Temperature and Pressure which refers to 25°C (298.15 K) and pressure of 101kPa were calculated.

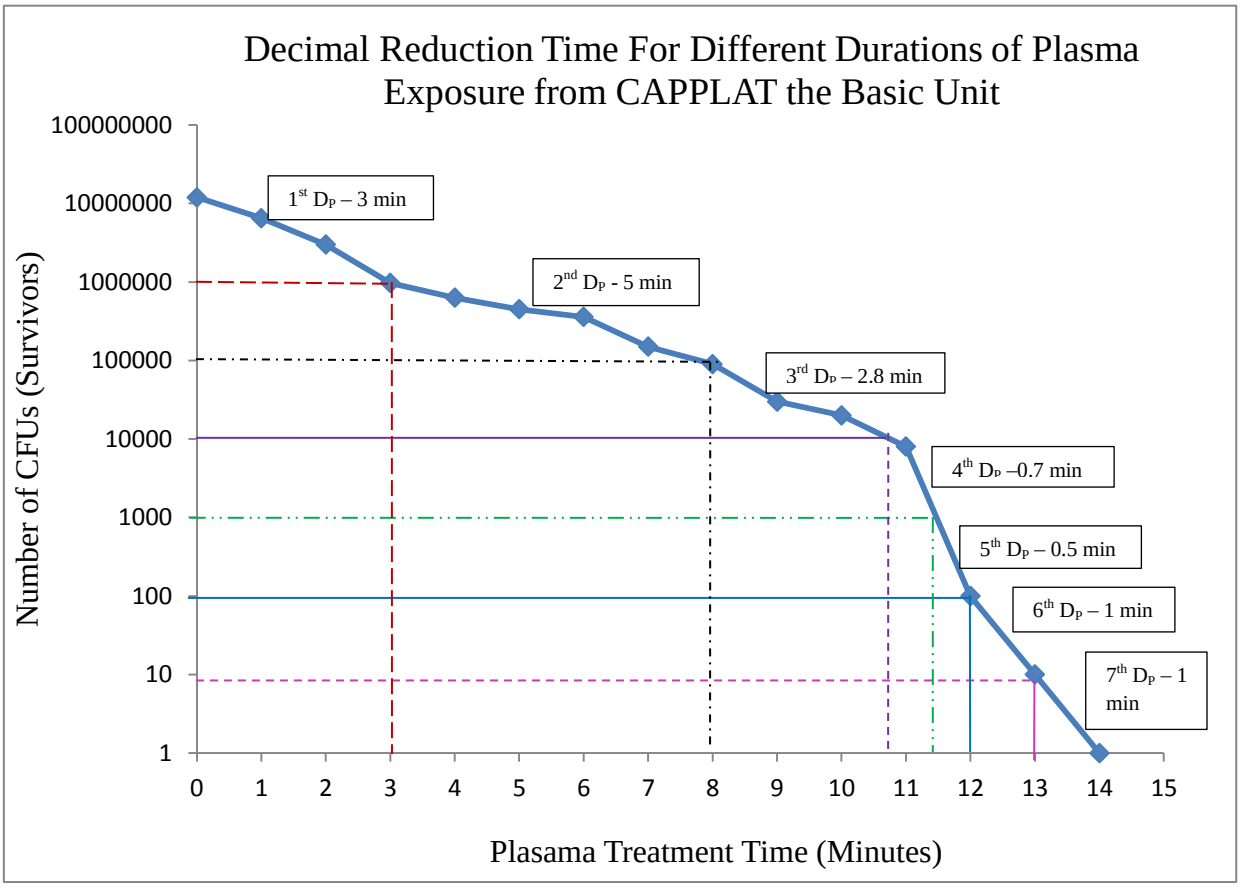

Figure 5.1 The number of viable CFUs as the function of the time of plasma discharge exposure. The biphasic survival curve of Bacillus endospores showing the time in minutes taken by each decimal reduction due to plasma exposure (D_p). The samples were exposed to the plasma (Ar 10 slm, N_2 100 sccm) for different durations.

According to the Figure 5.1, for the total inactivation of the endospores we needed 7 D_Ps (1st D_P - 3 min, 2nd D_P - 5 min, 3rd D_P – 2.8 min, 4th D_P -0.7 min, 5th D_P - 0.5 min, 6th D_P -1 min and 7th D_P - 1 min). The time required for the complete sterilization (F_p) was about 14 minutes. The

inactivation was a biphasic inactivation. Although the first phase of inactivation had several linear segment but there was a striking difference between the first and the second phase of inactivation. The second phase of inactivation or the tailing deviation was due to super dormant endospores or due to the spores buried in cellular debris due to spore inactivation in previous phases. The population represented these stubborn super dormant endospores was less than 0.1% of the whole population. The second phase of inactivation was much shorter than the first phase. The first phase took 11 minutes whereas the second phase took just 3 minutes. It could be possible because of the continuous cumulative effects of plasma exposure during the first phase on endospores. Other stages and the mechanism of inactivation could be explained just like the previous decimal reduction curve for CAPPLAT- 9Ne, given in Chapter 4 (See 4.3.4).

CAPPLAT is little weaker than the CAPPLAT- 9Ne although both followed the same pattern but the CAPPLAT took longer to inactivate a population of $1.0X10^7$ to $1.4X10^7$ *Bacillus subtilis* spores per ml, shown in Figure 5.2.

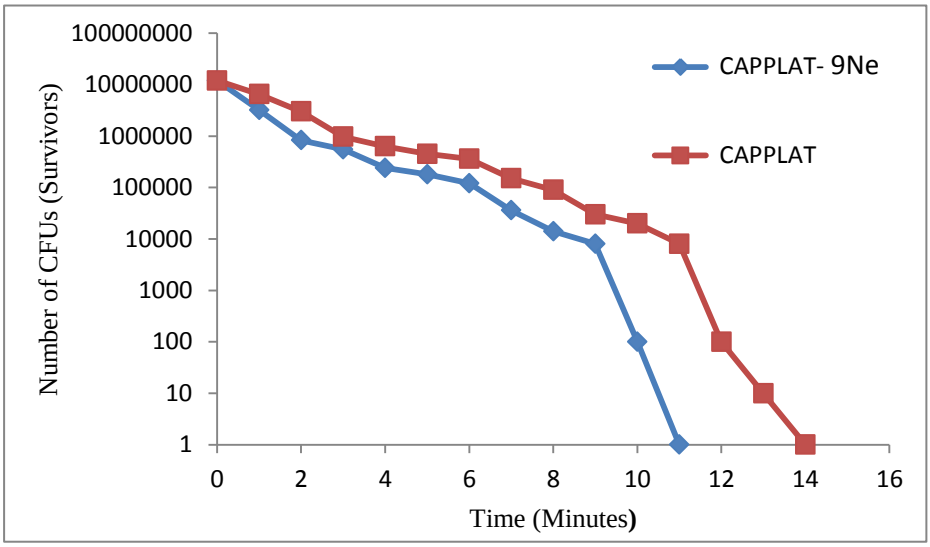

Figure 5.2 Comparison of the sporocidal property of CAPPLAT- 9 Ne (blue line) and CAPPLAT (red line); CAPPLAT- 9Ne took shorter time than CAPPLAT

As we have already discussed about the OES spectra in Chapter 2 and 3 and particularly in Chapter 4 that Ar metastables and the second positive systems of N_2 (N_2 ($C^3\prod_u$ — $B^3\prod_g$)) are

responsible for the inactivation. CAPPLAT- 9Ne worked at higher voltage (V_{pp} 20 sinusoidal voltage) than CAPPLAT (V_{pp} 16 kV square wave voltage) besides that CAPPLAT- 9Ne used less volume of N_2 for quenching, it means, plasma discharge from CAPPLAT- 9Ne , had higher density of active species than the CAPPLAT the basic unit. It was further proved by the comparison of optical emission spectra of CAPPLAT (Figure 3.11 A and 3.12 A, Chapter 3) and CAPPLAT- 9Ne (Figure 3.11 B and 3.12 B, Chapter 3). All of the spectra show that the intensity count was much higher for CAPPLAT- 9Ne than the intensity count for CAPPLAT the basic unit. That is why CAPPLAT- 9Ne caused inactivation in shorter time than the CAPPLAT the basic unit.

We also checked the amount of released DPA as shown in Figure 5.3. Method of DPA estimation has already been discussed in detail in Chapter 4. The estimation of DPA was used as an indicator to confirm the cortex and then protoplast lysis. Although the amount of DPA was not consistent as we discussed before but it followed the same pattern as it first increased and then started decreasing.

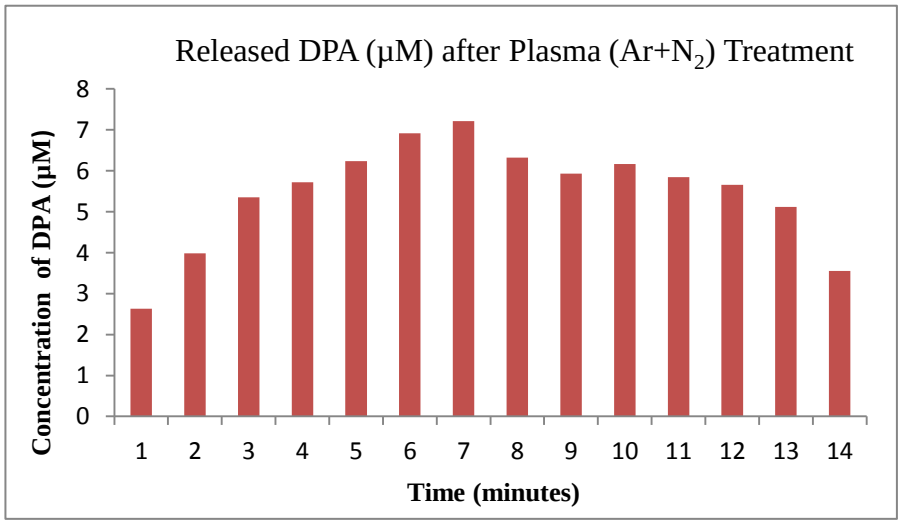

Figure 5.3 Amount of DPA (µM) released from the spores after plasma ($Ar+N_2$) exposure from 1 minute to 14 minutes. The graph of released DPA as a function of time of plasma exposure, by checking the intensity of fluorescence emission at the excitation wavelength 270 nm and emission wavelength 544 nm. The equation derived for the calibration curve (y=0.481x) was used to calculate the amount of released DPA.

5.3.4 Effects of Ar –N_2 – O_2 Plasma Jet from CAPPALT on the Viability of Endospores

To achieve this plasma jet, a mixture of Ar (10 slm) and N_2 (300 sccm) were fed into the hollow inner electrode through an inlet tube. O_2 was added in the direct injection mode through the capillary inserted in to the inner electrode as shown in Figure 3.3 (Chapter 3) to the plasma jet directly. Addition of O_2, in the mixture of Ar and N_2 was not possible because the quenching so heavy that we could have any plasma discharge. This plasma jet (Ar-N_2-O_2) also had sporocidal property. We could inactivate the spores successfully and the mechanism of spore inactivation has already been explained in Chapter 4. The number of viable CFUs was plotted as the function of the time of plasma discharge exposure (Figure 5.4).

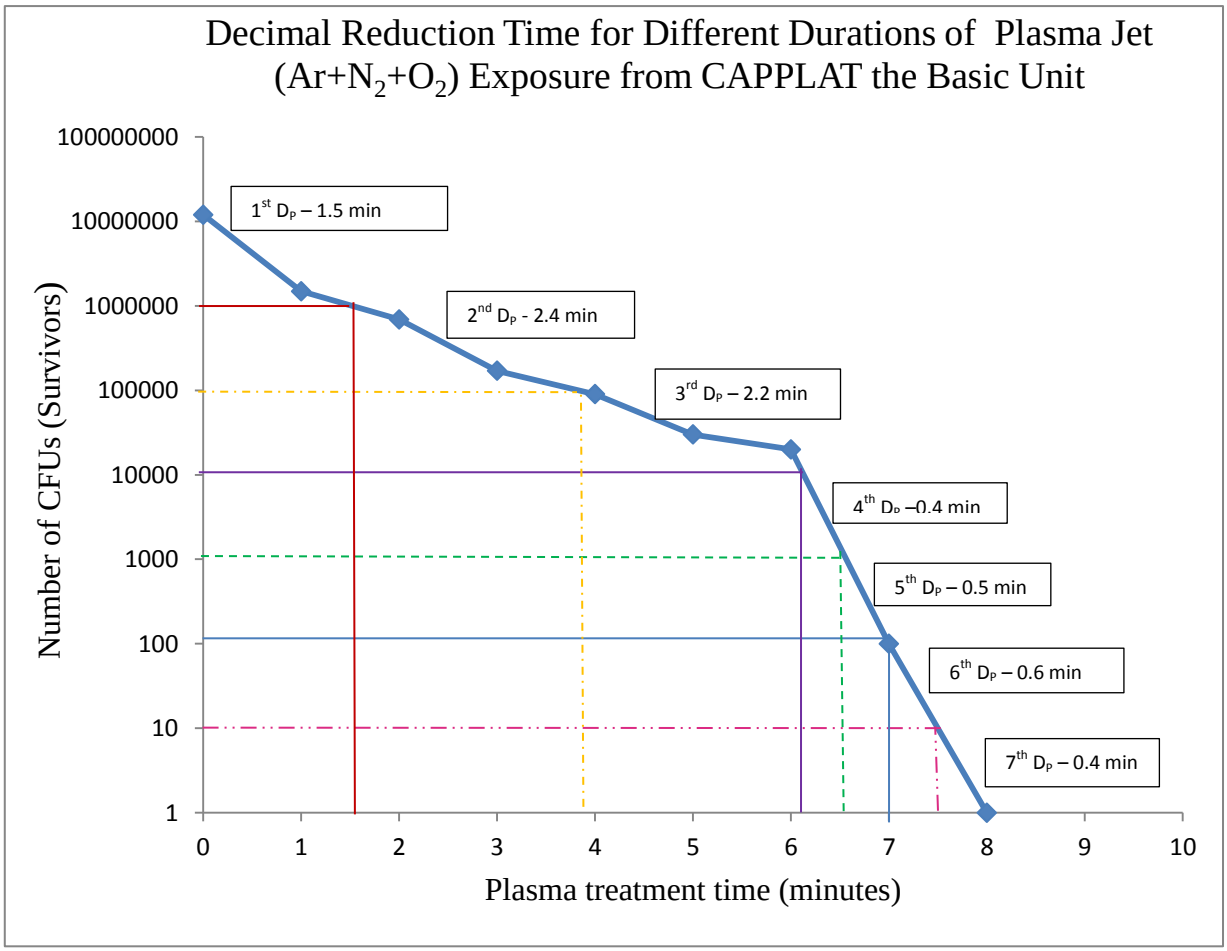

Figure 5.4 The number of viable CFUs as the function of the time of plasma discharge exposure. The biphasic survival curve of Bacillus endospores showing the time in minutes taken for each decimal reduction due to plasma exposure (D_p). The samples were exposed to the plasma (Ar 10 slm, N_2 100 sccm and O_2 500 sccm) for different durations.

The decimal reduction time because of plasma exposure (D_P value) and the time required to kill the whole population of spores (F_P) at SATP (Standard Ambient Temperature and Pressure which refers to 25°C (298.15 K) and pressure of 101kPa, were calculated. According to the Figure 5.4, for the total inactivation of the endospores we needed 7 D_Ps (1^{st} D_P – 1.5 min, 2^{nd} D_P – 2.4 min, 3^{rd} D_P – 2.2 min, 4^{th} D_P -0.4 min, 5^{th} D_P - 0.5 min, 6^{th} D_P -0.6 min and 7^{th} D_P – 0.4 min). The time required for the complete sterilization (F_p) was about 8 minutes. The inactivation was a biphasic inactivation. Although the first phase of inactivation had several linear segment but there was a striking difference between the first and the second phase of inactivation. The second phase of inactivation was due to super dormant endospores or the spores stuck in cellular debris. The population represents these stubborn super dormant endospores or inactivated spores, was less than 0.1% of the whole population. The second phase of inactivation was much shorter than the first phase. The first phase took 6 minutes whereas the second phase took just 2 minutes. Although the mechanism of inactivation has already been explained in Chapter 4 but with the addition of O_2, Fp (time for total inactivation) was further decreased.

In Chapter 3, we talked about the OES spectra for the addition of O_2 (Figure 3.14). It has already been discussed that Ar metastables and the second positive systems of N_2 (N_2 ($C^3\prod_u$ — $B^3\prod_g$) are responsible for the inactivation. Besides that because of the addition of O_2 gas, some active species because of O_2 should also be there. Although the addition of O_2 enhanced the sporocidal effect of the plasma jet but we couldn't find any peaks related to the O_2 or O atoms (Figure 3.4). It seems like the O active species are very reactive and short lived. It was reported that the most probable channel for the formation of O atoms was through collisions between the oxygen molecular ions (O_2^+) and electrons [1]. Oxygen molecular ions (O_2^+) formation is not possible because it needs higher energy (E ≈ 18.2 eV) for penning ionization which is higher than the energy of Ar metastables' energy (E ≈ 11.5 eV [2]. However oxygen atoms can probably be generated through the following channels in Ar discharge [2, 3-5]:

$$Ar^* + O_2 (X^3\Sigma^-_g) \rightarrow O (^1D) + O (^3P) + Ar^0 \qquad (1)$$

$$e^* + O_2 (X^3\Sigma^-_g) \rightarrow e + [O (^1D) \text{ or } O (^1S)] + O (^3P) \quad (2)$$

$$e^* + O_2 (X^3\Sigma^-_g) \rightarrow 2e + O_2^+ (b^4\Sigma^-_g) \quad (3)$$

$$e^* + O_2^+ (b^4\Sigma^-_g) \rightarrow 2O (^3P) \quad (4)$$

Considering the electron density and the electron energy, reaction (1) is the only channel for the generation of O atoms in CAPPLAT Ar plasma jet which can combine with other molecules or can make O_3 very easily.

$$O + O_2 + M \longrightarrow O_3 + M$$

Where *M* could be O, O_2, or O_3, M is the third collision partner.

The second positive system of nitrogen N_2^* can also lead to the formation of oxygen atoms by the following reactions [6].

$$N_2^* + O_2 \longrightarrow N_2 + 2O$$

$$N_2^* + O_2 \longrightarrow N_2O + O$$

$$O + O_2 + M \longrightarrow O_3 + M$$

According to several authors, reactive neutral species (such as O, O_2*, O_3, OH•, NO and NO_2) can make a significant contribution to the plasma sterilization process, especially at high pressures [7, 8, and 9]. Several authors have also experimentally shown that discharges containing oxygen provide a strong germicidal effect [10, 11, and 12].

It is believed that the oxygen species attribute to the sterilization process due to their strong oxidative effects on the outer structures of cells [7]. Moreover, discharges containing oxygen also generate ozone (O_3) which interferes with the cellular respiration system and is known to have a strong bactericidal effect [8].

We also checked the amount of released DPA as shown in Figure 5.5. Although the amount of DPA was not consistent as we discussed before but it followed the same pattern as it first increased and then started decreasing. Around 11 and 12 minutes, there is a clear increase in the amount of DPA. It means there was more production of DPA by O_2 than the destruction of DPA by plasma because of oxidative effect of oxygen species on decaying spores.

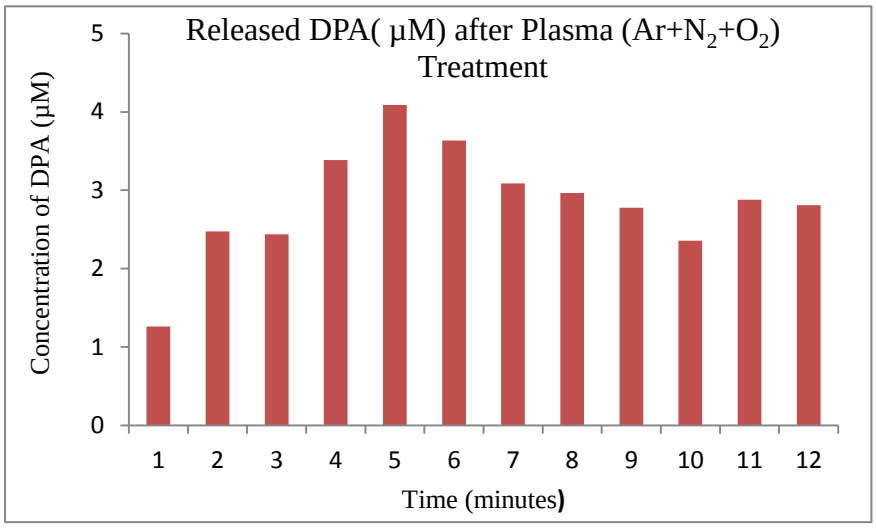

Figure 5.5 Amount of DPA (µM) released due to plasma ($Ar+N_2+O_2$) exposure from 1 minute to 12 minutes. The graph of released DPA as a function of time of plasma exposure, by checking the intensity of fluorescence emission at the excitation wavelength 270 nm and emission wavelength 544 nm. The equation derived for the calibration curve (y=0.481x) was used to calculate the amount of released DPA.

5.3.5 Effects of Ar –N_2 – H_2O_2 Plasma Jet from CAPPALT on the Viability of Endospores

To achieve this plasma jet a mixture of Ar (10 slm) and N_2 (300 sccm) were fed into the hollow inner electrode through an inlet tube. H_2O_2 was added in the direct injection mode through the capillary inserted in to the inner electrode. For H_2O_2 injection, it was carried by Ar with the flow rate of 150 sccm to the plasma jet through the bubbling process, as shown in Figure 3.4 (Chapter 3).This plasma jet also had sporocidal property. We could inactivate *Bacillus* spores successfully, the mechanism of spore inactivation has already explained in Chapter 3. The number of viable CFUs was plotted as the function of the time of plasma discharge exposure to the spores to get the survival curve (Figure 5.6).

The decimal reduction time because of plasma exposure (D_P value), and the time required to kill the whole population of spores (F_P) at SATP (Standard Ambient Temperature and Pressure which refers to 25°C (298.15 K) and pressure of 101kPa were calculated. According to the Figure 5.6, for the total inactivation of the endospores we needed, 7 D_Ps (1^{st} D_P – 1 min, 2^{nd} D_P – 2.2 min, 3^{rd} D_P – 1.8 min, 4^{th} D_P -0.5 min, 5^{th} D_P - 0.5 min, 6^{th} D_P -0.5 min and 7^{th} D_P – 0.5 min). The time

required for the complete sterilization was about 8 minutes. The inactivation was a biphasic inactivation. Just like previous survival curves, first phase was much longer than the second phase. It indicates the similar mechanism of inactivation but much intensified.

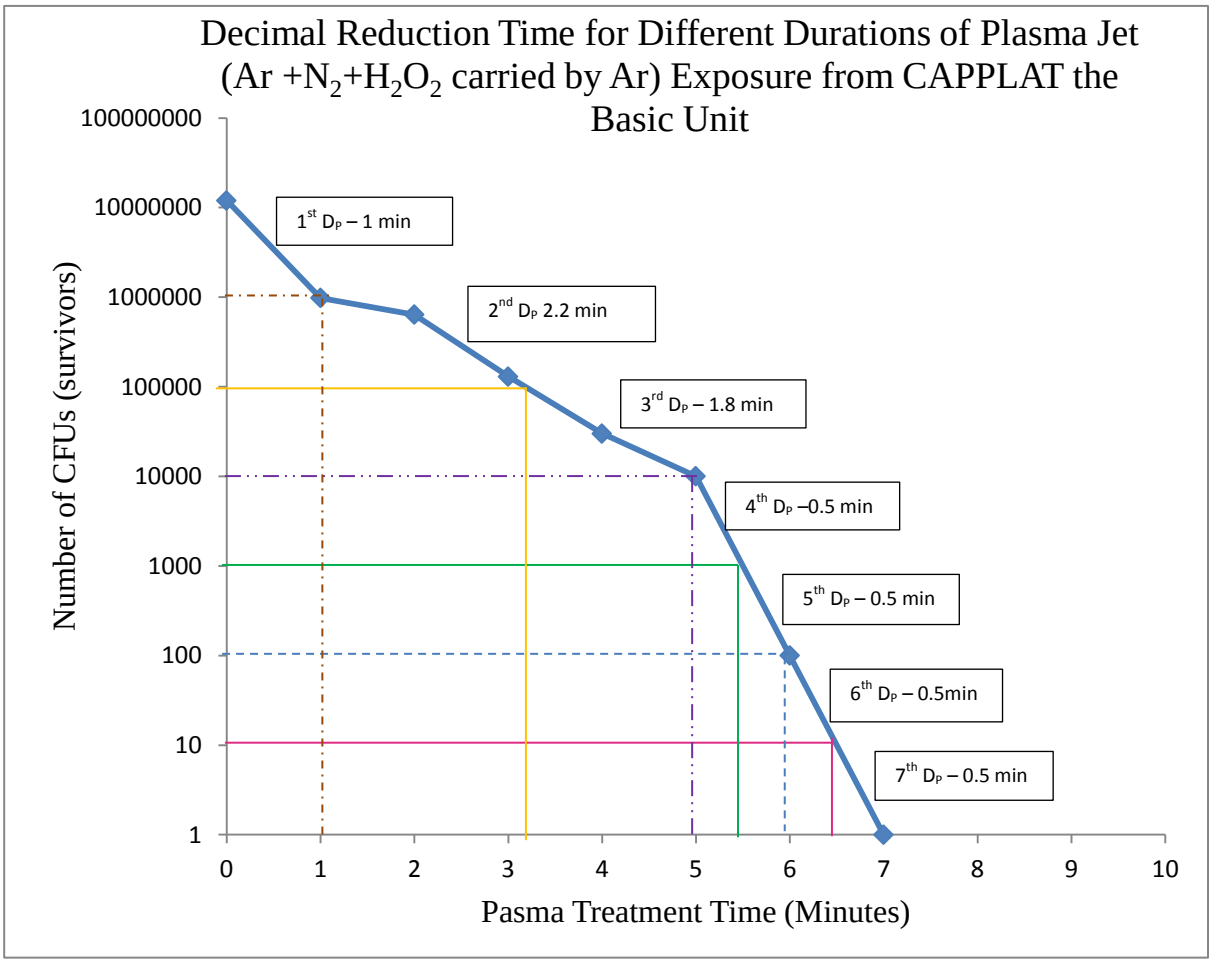

Figure 5.6 The number of viable CFUs as the function of the time of plasma discharge exposure. The biphasic survival curve of Bacillus endospores showing the time in minutes taken by each decimal reduction due to plasma exposure (D_p). The samples were exposed to the plasma (Ar 10 slm, N_2 100 sccm and H_2O_2 carried by 150sccm of Ar) for different durations.

The population represented second phase was less than 0.1% of the whole population. The second phase of inactivation was much shorter than the first phase. The first phase took 5 minutes whereas the second phase took just 2 minutes. It could be possible because of the continuous cumulative effects of plasma exposure during the first phase on endospores. Other stages could be explained just like the previous decimal reduction curve for CAPPLAT 9 Ne, given in Chapter 3.

Addition of H_2O_2 further enhanced the sporocidal effects of the plasma jet (Figure 5.8) but we couldn't find any peaks related to the O_2 or O atoms (Figure 3.14 and 3.15). As OES spectra show that there are Ar metastables and the second positive systems of N_2 (N_2 ($C^3\prod_u$ — $B^3\prod_g$)) which are responsible for the inactivation but this jet was stronger than Ar- N_2 jet and Ar-N_2- O_2 jet. It means after addition of H_2O_2, there were some other active species which our OES couldn't detect. H_2O_2 is a very strong oxidizing agent and it disintegrates very quickly.

$$2H_2O_2 \longrightarrow 2\,H_2O + O_2 \quad \text{(ionization energy of -O-O- is 1.95 eV)}$$

$$2H_2O_2 + \text{e Impact} \longrightarrow OH^* + OH^* \quad \text{(Ionization energy is 2.2 eV)}$$

$$OH^* \longrightarrow O^* + H^* \quad \text{(Ionization energy is 4.4 eV)}$$

As above mentioned reactions show that the low ionization energy is needed, this energy can be supplied by Ar metastables (E ≈ 11.5 eV) [2], second positive systems of N_2 (E ≈ 11.8 eV) or some highly energetic electrons. In Case of H_2O_2, we get oxygen which can act as we mentioned in the previous section (3.3) but we have additional water molecules which will also affect the sterilization. After experimenting with different gas mixtures, Kuzmichev et al. concluded that the best bactericidal effects were achieved in moistened oxygen and air. In the presence of moisture, hydroxyl (OH) radicals are generated in the plasma, which play a significant role by chemically attacking the outer structures of bacterial cells. In the case of air, the production of NO and NO_2 adds to the lethality of the process [13]. Penning ionization of water is not possible because it requires high energies (16.95 to 26.80 eV), which can't be supplied by Ar metastables or second positive system of nitrogen molecules.

$$H_2O + e^* \longrightarrow H^+ + OH^- + 2e \text{ (ionization energy is 16.95eV) – not possible)}$$

Water molecules' excitation energy is 7.5 eV. With the energy of by Ar metastables or second positive system of nitrogen molecules, lots of dissociative reactions are possible.

$$H_2O^* + H_2O^* \longrightarrow H_2O_2 + H_2 \quad \text{(E= 3.2 eV)}$$

$$H_2O^* + H \longrightarrow H_2 + OH \quad (E=0.9eV)$$

$$H_2O^* + OH \longrightarrow H_2O_2 + H_2 \quad (E=3.6\ eV)$$

$$H_2O + e \longrightarrow H^* + OH^* \text{ (dissociation energy is 5.1 eV)}$$

We had O_3 molecules in Ar-N_2-O_2 Plasma. Breathing ozone is known to cause chest pain, impair respiratory function, and damage lung tissue [14]. O_3 molecules can be dissociated by the byproducts of H_2O_2 and H_2O dissociation by the following reactions [15].

$$OH^* + O_3 \longrightarrow HO_2^* + O_2$$

$$H^* + O_3 \longrightarrow OH^* + O_2$$

$$HO_2^* + O_3 \longrightarrow OH^* + 2\ O_2$$

From above reactions it's clear that addition O_3 molecules were not only disintegrated but highly reactive OH* radicles also produced were which will support further inactivation. From above discussion it is clear that H_2O_2 is the most effective oxidative additive as it offers a huge range of active species and all of them are highly potent to kill the microorganisms.

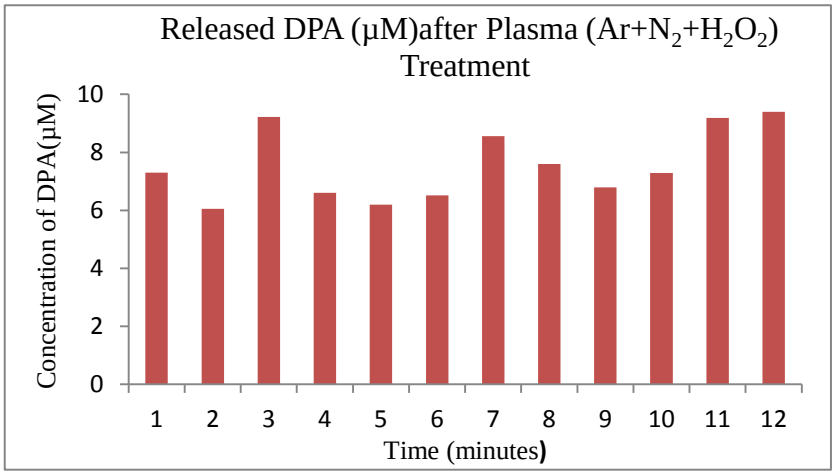

Figure 5.7 Amount of DPA (µM) released after plasma (Ar+N_2+H_2O_2) exposure from 1 minute to 12 minutes. The graph of released DPA as a function of time of plasma exposure, by checking the intensity of fluorescence emission at the excitation wavelength 270 nm and emission wavelength 544 nm. The equation derived for the calibration curve (y=0.481x) was used to calculate the amount of released DPA.

We also checked the amount of released DPA as shown in Figure 5.7. Method of DPA estimation has already discussed in detail in Chapter 3. The estimation of DPA we used it as an indicator to confirm the breakage of cortex and leakage of protoplast. The amount of DPA was not consistent as we discussed before and it even didn‘t follow the pattern as we observed in previous cases. Most probable it is because of a huge range of byproducts. Not only above mentioned byproducts, there are so many permutation and combinations are possible.

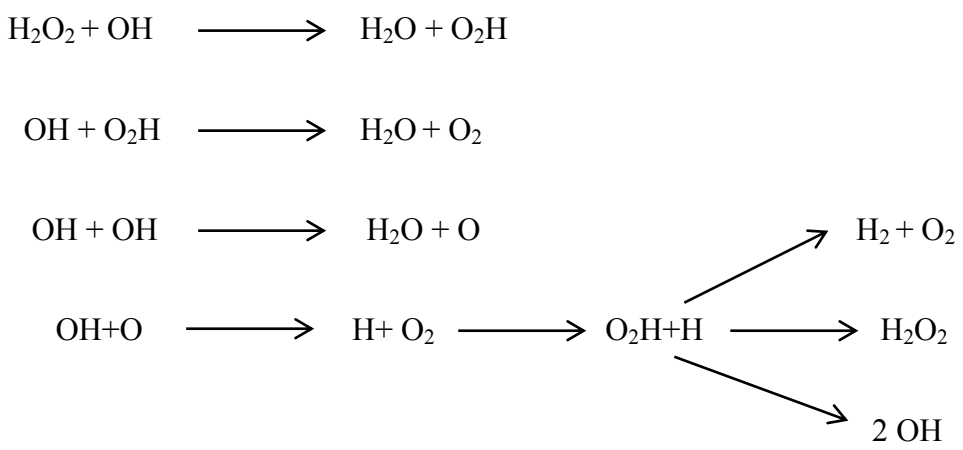

I think, this huge variety of products make a particular reaction and its affect among so many reactions, unpredictable. I think because of collective effects of so many possible reactions make, DPA emission peaks, so inconsistent. If we compare, all of the DPA peaks, we can clearly see, that Ar-N_2 had the most consistent peaks it was followed by Ar-N_2-O_2 and then by most inconsistent peaks for Ar-N_2-H_2O_2 which had the maximum variety of byproducts or the most complex reaction system, which also helped it to have the strongest effects on sterilization (Figure 5.8). DPA peaks show that the release of DPA or inactivation follows the higher order of kinetics because of complex reaction system. With the addition of oxidants, this complexity increased and with increasing complexity, inconsistency in the amount of released DPA also increased. We can assume that lots of inactivation processes take place in a parallel fashion. It might possible that some spores started their course of inactivation with etching and some with oxidation. There might be some other possible parallel inactivation processes too. All of these inactivation processes have different rates of reactions. Even if a spore is etched and dead, it still has DPA in its cellular debris.

Particularly OH* radicles affect the rate of the liberation of DPA from the partially disintegrated spores at different rates. So, there is a kind of induction time before the release of the DPA. We couldn't observe any additional emission peaks and changes in electrical characteristics but this higher order of kinetics proves the involvement of lots of additional reactants.

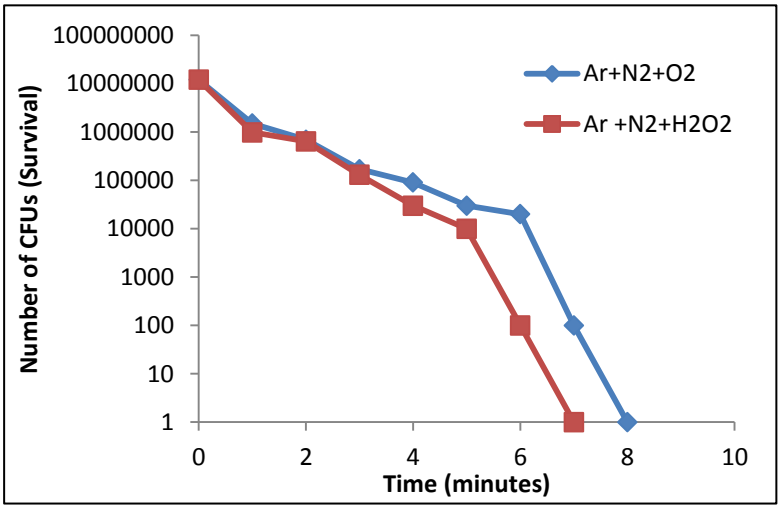

Figure 5.8 Comparison of the sporocidal property of Ar-N_2-O_2 plasma jet (blue line) and Ar-N_2-H_2O_2 (red line)

5.4 Conclusion:

To inactivate endospores high voltage is preferable. Although we couldn't identify the active species because of O_2 but there was a visible impact on the number of CFUs. We could inactivate bacteria with Ar and N_2, but the addition of O_2 and H_2O_2 was really helpful. Particularly, addition of H_2O_2 enhanced the bactericidal property the most as shown in Figure 5.9.

According to Figure 5.9, all of the inactivation followed almost the same trend. All of them were biphasic. The first phase was much longer than the second phase. The second phase was much shorter and representing extremely small part of the population. The mechanism of inactivation followed a higher order of kinetics. Ar+N_2 plasma jet from CAPPLAT the basic unit took 14 minutes, Ar+N_2 plasma jet from CAPPLAT-9Ne took 11 minutes, Ar+N_2+O_2 plasma jet from CAPPLAT the basic unit took 8 minutes and Ar+N_2+H_2O_2 plasma jet from CAPPLAT the basic unit took 7 minutes to inactivate the same population of *Bacillus subtilis* endospores. Figure 5.9,

clearly indicates that for higher level of bacterial inactivation or sterilization, we need higher voltage or more energetic plasma discharge and addition of more oxidants.

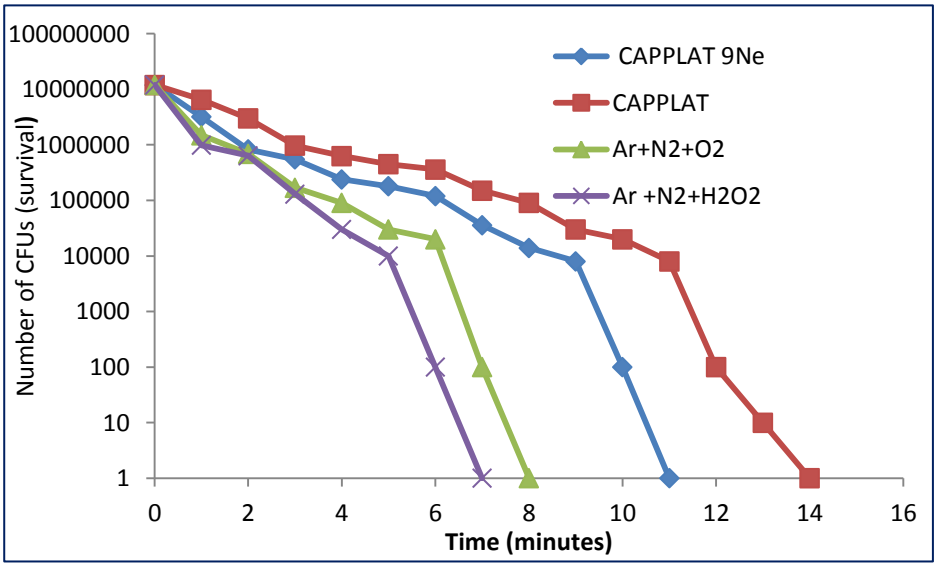

Figure 5.9 Comparison of the sporocidal property of Ar-N_2-O_2 plasma jet (green line) and Ar-N_2-H_2O_2 (purple line); CAPPLAT 9Ne (blue line); CAPPLAT (red line)

H_2O_2 addition is the most preferable. It doesn't leave any harmful byproduct and at the same time, it retards the formation of O_3 which could be a little bit hazardous to the health and of course, it has the most powerful sterilization properties.

5.5 References

[1] Léveillé V and Coulombe S. Plasma Process. Polym. 3, 587, 2006.

[2] Yu Q S, Yasud H K. Plasma Chem. Plasma Process, 18, 461, 1998.

[3] Lee C, Graves D B, Lieberman M N, and Hess D W. J. Electrochem. Soc. 141, 1546, 1994.

[4] Eliasson B, and Kogelschatz U. Basic Data for Modeling of Electrical Discharge in Gases: Oxygen. Research, Asea Brown Boveri Corporate, KLR-11C CH5405, 1986.

[5] Lee D J, Park S H, and Hong Y Kim. IEEE Trans. Plasma Sci., 33, 949, 2005.

[6] Ahn H S, Hayashi N, Ihara S, and Yamabe C. Ozone generation characteristics by superimposed discharge in oxygen-fed ozonizer, Jpn.J. Appl. Phys.42-6578-6583, 2003 .

[7] Fridman A. Plasma Biology and Plasma Medicine. *Plasma Chemistry.* New York: Cambridge University Press, 2008.

[8] Laroussi M. Nonthermal decontamination of biological media by atmospheric pressure plasmas: Review, analysis, and prospects. IEEE Transactions on Plasma Science, 30, 1409-1415, 2002.

[9] Laroussi M. Low temperature plasma-based sterilization: Overview and state-ofthe- art. Plasma Processes and Polymers, 2, 391-400, 2005.

[10] Herrmann H W, Henins I, Park J, and Selwyn G S. Decontamination of chemical and biological warfare, (CBW) agents using an atmospheric pressure plasma jet (APPJ). Physics of Plasmas, 6, 2284-2289, 1999.

[11] Moreau S, Moisan M, Tabrizian M, Barbeau J, Pelletier J, Ricard A and Yahia L. Using the flowing afterglow of a plasma to inactivate Bacillus subtilis spores: Influence of the operating conditions. Journal of Applied Physics, 88, 1166-1174, 2000.

[12] Richardson J P, Dyer F F, Dobbs F C, Alexeff I, and Laroussi M. Year. On the use of the resistive barrier discharge to kill bacteria: Recent results. In: 27th IEEE International Conference on Plasma Science - ICOPS2000, 2000 2000 New Orleans (USA). 109-109.

[13] Kuzmichev A I, Soloshenko I A, Tsiolko V V, Kryzhanovsky V I, Bazhenov V Y, Mikhno I L, and Khomich V A. Year. Feature of sterilization by different type of atmopsheric pressure discharges. *In:* 7th International Symposium on High Pressure Low Temperature Plasma Chemistry - Hakone VII, 2001 2000 Greifswald (Germany). 402-406.

[14] Sung Kil Kang, Myeong Yeol Choi, Il Gyo Koo, Paul Y Kim, Yoonsun Kim, Gon Jun Kim, Abdel-Aleam H Mohamed, George J Collins, and Jae Koo Lee1. Applied Physics Letters **98**, 143702, 2011.

[15] Soloshenko I A, Tsiolko V V, Khomich V A, Bazhenov Yu. V, Ryabtsev A V, Schedrin, A I, and Mikhno I L. IEEE Trans. Plasma Sci. **30**, 1440, 2011.

Chapter 6 - Summary

Plasma is an ionized gas. Although it is considered neutral in nature (quasi-neutral) but chemically and physically, it is very active because of free electrons, ions, radicles, and highly excited neutral and charged species in it. In order to ionize an inert gas, energy which must be more than its ionization energy is provided. Plasmas can be divided into two broad categories – Local Thermodynamic Equilibrium Plasma (LTE plasma) or thermal plasma and Non-Local Thermodynamic Equilibrium Plasma (Non-LTE plasma) or cold plasma. Normally, at atmospheric pressure, the plasmas are thermal plasmas whereas to achieve low temperature plasmas, low pressure is required which limits its applications. To solve this problem, cold plasmas at atmospheric pressure were developed. For the same purpose, Cold Atmospheric Pressure Plasma torch was developed and used for this research which has also been commercialized under the name of CAPPLAT by Cresur Corporation of Japan.

Actually, we used two different types of CAPPLATs - CAPPLAT-9Ne the commercial unit and CAPPLAT the basic unit. We did electrical and optical characterizations and compared both CAPPLATs. The CAPPLAT-9Ne, had high voltage AC power source whereas CAPPLAT the basic unit used a high voltage pulsed power source. CAPPLAT-9Ne had a sinusoidal voltage of 20 kV whereas CAPPLAT the basic unit worked on an invariable voltage of 16 kV with square wave amplitude at a 50% duty cycle. The frequency for both, CAPPLAT-9Ne and CAPPLAT the basic unit was 20 kHz. The CAPPLAT-9Ne produced filamentary glow discharge and the CAPPLAT the basic unit produced the diffuse glow discharge. For both CAPPLATs, Ar gas was used as the working gas (primary gas) and N_2 gas (secondary gas) was admixed to achieve glow discharge as N_2 molecules quenched additional Ar metastables. The Optical emission spectra for both CAPPLATs showed similar emission peaks but the intensity of emission peaks for CAPPLAT–9Ne

was much stronger than the CAPPLAT the basic unit which indicated similar mechanism with different intensities. The main transition process for the excited Ar atoms was 4p-4s transition. Whereas the main transition process for active N_2 molecules was $C^3\prod_u \rightarrow B^3\prod_g$. Addition of N_2 gas, made the emission peaks for second positive system of the nitrogen molecules (N_2 $C^3\prod_u \rightarrow B^3\prod_g$) stronger and emission peaks for Ar weaker which suggested that the addition of N_2 gas into Ar gas caused the quenching of Ar metastables with the formation of the second positive system of the nitrogen molecules (N_2 $C^3\prod_u \rightarrow B^3\prod_g$). In this quenching process the second positive systems of the nitrogen molecules (N_2 $C^3\prod_u \rightarrow B^3\prod_g$) were the main energy transferring agents. We added less amount (100 sccm) of N_2 gas to Ar gas with CAPPLAT–9 Ne than the amount of N_2 gas (300 sccm), we added to Ar gas with CAPPLAT the basic unit to achieve stabilized glow discharges because of different types of glow discharges. The CAPPLAT-9Ne has been explained in detail in Chapter 2 and CAPPLAT the basic unit has also been explained in detail in Chapter 3.

CAPPLAT-9Ne has never been used for any research purposes. Although CAPPLAT the basic unit had already been used for chemical vapour deposition and polymer surface treatment but it was never tried to use for any bio-applications. We could successfully inactivate a population of $1.0X10^7$ to $4.0X10^7$ *Bacillus subtilis* endospores/ml with both CAPPLATs. To see the pattern of inactivation, we drew the survival curves with decimal reduction time due to plasma exposure (D_p value) and the total time taken for the complete inactivation due to plasma (F_p value) were also calculated. In all of the cases, the survival curves were biphasic. The first phase of the survival curve had lots of linear segments but overall it was much longer than the second phase which represented a very small part (0.1%) of the whole population. To ensure the inactivation of the spores DPA *(Dipicolinic acid or Pyridine-2, 6- dicarboxylic acid)* which is found only in the protoplast of the spores was also measured for different plasma exposure conditions. For the fluorimetric quantification of DPA, the enhanced photoluminescence emission of DPA as a $[Tb(DPA)(H_2O)_6]^+$ complex was used, which is obtained by allowing the binding of DPA with terbium ions (Tb^{3+}) from $TbCl_3.6H_2O$. The excitation wave length was 270 nm. The emission

spectra were recorded from 475 nm to 600 nm wave length range. On the basis of above experiments, we postulated an inactivation mechanism which is very well explained in Chapter 4.

It was observed that CAPPLAT-9Ne is more effective than the CAPPLAT the basic unit as CAPPLAT-9Ne took about 11 minutes whereas CAPPLAT the basic unit took about 14 minutes to inactivate the same population. We tried to enhance the sterilization power of the CAPPLAT. To do so, O_2 and H_2O_2 were added to the plasma discharges directly (direct injection mode) through the capillary inside the hollow copper electrode. O_2 was added directly and H_2O_2 was entrained in Ar gas to feed to the plasma jet. In both cases Current and voltage waveforms didn't show any changes because O_2 and H_2O_2 were added to the remote plasma or afterglow discharge not to the active plasma. Although the addition of O_2 and H_2O_2 didn't change the optical spectra at all but there were drastic changes on bacterial survival because there were a huge range of byproducts which were lethal to the endospores. All of the possible reactions are explained in detail in Chapter 3.

All of the different types of plasma jets ($Ar+N_2$ plasma jet, $Ar+N_2+O_2$ plasma jet and $Ar+N_2+H_2O_2$ plasma jet) obtained from the CAPPLAT the basic unit were used to inactivate the endospores of *Bacillus subtilis*, just like we did with CAPPLAT-9Ne. It was observed that the addition of the oxidants (O_2 and H_2O_2) enhanced the efficiency of the sterilization and particularly H_2O_2 was found more effective than O_2. $Ar+N_2+ O_2$ plasma discharge took 8 minutes to inactivate the whole population whereas $Ar+N_2+ H_2O_2$ plasma discharge took just 7 Minutes. Both times were much less than the time taken by $Ar+N_2$ plasma discharge which was 14 minutes. Inactivation followed a higher order of kinetics because of complex reaction system which is explained in Chapter 5.

We could characterize and compare both CAPPLATs. We could understand the mechanism of plasma discharges. We could inactivate *Bacillus subtilis* endospores completely. We could further enhance the sterilization efficiency of the CAPPLAT the basic unit. We could postulate a mechanism for bacterial inactivation too.

List of Publications

1. Electrical and Optical Characterization of Cold Atmospheric Pressure Plasma Jet and the Effects of N_2 Gas on Argon Plasma Discharge

   Vinita Sharma[1, a], Katsuhiko Hosoi[2, b], Tamio Mori[2, c] and Shin-ichi Kuroda[1, d]

   This paper has been published.

   Applied Mechanics and Materials Vols. 268-270 (2013) pp 522-528
   © (2013) Trans Tech Publications, Switzerland
   doi:10.4028/www.scientific.net/AMM.268-270.522

   (Related to Chapter 2)

2. Effects of Cold Atmospheric Pressure Plasma Jet on the Viability of *Bacillus subtilis* Endospores

   Vinita Sharma[1, a], Katsuhiko Hosoi[2, b], Tamio Mori[2, c] and Shin-ichi Kuroda[1, d]

   This paper has also been published.

   Advanced Materials Research Vol. 647 (2013) pp 524-531
   Online available since 2013/Jan/11 at www.scientific.net
   © (2013) Trans Tech Publications, Switzerland
   doi:10.4028/www.scientific.net/AMR.647.524.

   (Related to Chapter 4)

ACKNOWLEDGEMENTS

First and foremost, I would like to express my sincere and the deepest gratitude to my supervisor Professor Shin-ichi Kuroda for his invaluable guidance, enduring support and continuous encouragement to complete this dissertation successfully.

I would like to express my deep appreciation to the members of my advisory committee including Professor Takayuki Oshima, Professor Akio Matsuoka, Professor Masaru Hakoda, and Professor Tomohide Watanabe for their critical and constructive comments to improve this thesis. I would like to extend my deep appreciation to Dr. Takanori Tanino for his invaluable support with my microbiological experiments. I deeply appreciate Professor Takahiko Kawai for his continuous encouragement and invaluable advices. I would like to express my heartfelt thanks to Dr. Shraddha Sharma for all of the long and fruitful discussions about different topics of microbiology. I am really grateful to Dr. Tadashi Hashizume for his earnest support throughout my studies.

I'm grateful to all of my colleagues and friends at Kuroda lab and Oshima lab. I really appreciate Dr. Katsuhiko Hosoi for his constant support with several aspects of my studies, particularly about plasma, throughout my doctoral studies. I really appreciate Dr. Xiaomeng Fei also for the insights about plasma, he shared with me. I'm really thankful to Mr. Masatoshi Sekiguchi for his great assistance with my microbiological experiments. I have been very privileged to have befriended you all.

Last but by not least; I'm indebted to my parents, Dr. J.P. Sharma and Mrs. Veer Bala Sharma, for their inexhaustible blessings and support. I owe my success to my husband Mr. Sunil Sharma, my son Arjun Sharma and my daughter Arushi Sharma for their incredibly huge support, dedication and immense patience at all times. I'm deeply thankful to my parents in law Mr. Vijendra Sharma and Mrs. Mamila Sharma, my brother Dr. Vinay Sharma, my sisters Dr. Shraddha Sharma & Dr. Sujata Sharma and my brother-in-law Mr. Abhay Sharma for their moral support.

I would like to share the credit of my work with all of the people around me. For any errors or inadequacies that may remain in this work, of course, the responsibility is entirely my own.